



2013

EFFICIENT ELECTROCHEMICAL FUNCTIONALIZATION OF CARBON NANOTUBES AND CARBON NANOTUBE MEMBRANES FOR ENERGY, DRUG DELIVERY AND POTENTIAL CATALYSIS APPLICATIONS

Xin Zhan

University of Kentucky, xinsimba@gmail.com

[Right click to open a feedback form in a new tab to let us know how this document benefits you.](#)

Recommended Citation

Zhan, Xin, "EFFICIENT ELECTROCHEMICAL FUNCTIONALIZATION OF CARBON NANOTUBES AND CARBON NANOTUBE MEMBRANES FOR ENERGY, DRUG DELIVERY AND POTENTIAL CATALYSIS APPLICATIONS" (2013). *Theses and Dissertations--Chemistry*. 15.
https://uknowledge.uky.edu/chemistry_etds/15

This Doctoral Dissertation is brought to you for free and open access by the Chemistry at UKnowledge. It has been accepted for inclusion in Theses and Dissertations--Chemistry by an authorized administrator of UKnowledge. For more information, please contact UKnowledge@lsv.uky.edu.

STUDENT AGREEMENT:

I represent that my thesis or dissertation and abstract are my original work. Proper attribution has been given to all outside sources. I understand that I am solely responsible for obtaining any needed copyright permissions. I have obtained and attached hereto needed written permission statements(s) from the owner(s) of each third-party copyrighted matter to be included in my work, allowing electronic distribution (if such use is not permitted by the fair use doctrine).

I hereby grant to The University of Kentucky and its agents the non-exclusive license to archive and make accessible my work in whole or in part in all forms of media, now or hereafter known. I agree that the document mentioned above may be made available immediately for worldwide access unless a preapproved embargo applies.

I retain all other ownership rights to the copyright of my work. I also retain the right to use in future works (such as articles or books) all or part of my work. I understand that I am free to register the copyright to my work.

REVIEW, APPROVAL AND ACCEPTANCE

The document mentioned above has been reviewed and accepted by the student's advisor, on behalf of the advisory committee, and by the Director of Graduate Studies (DGS), on behalf of the program; we verify that this is the final, approved version of the student's dissertation including all changes required by the advisory committee. The undersigned agree to abide by the statements above.

Xin Zhan, Student

Dr. Bruce Hinds, Major Professor

Dr. John Anthony, Director of Graduate Studies

EFFICIENT ELECTROCHEMICAL FUNCTIONALIZATION OF CARBON
NANOTUBES AND CARBON NANOTUBE MEMBRANES FOR ENERGY, DRUG
DELIVERY AND POTENTIAL CATALYSIS APPLICATIONS

DISSERTATION

A dissertation submitted in partial fulfillment of the requirements for the degree of
Doctor of Philosophy in the College of Medicine at the University of Kentucky

By
Xin Zhan

Lexington, Kentucky

Director: Dr. Bruce J. Hinds, Professor of Chemistry and Chemical and Materials
Engineering
Lexington, Kentucky

2013

Copyright © Xin Zhan 2013

ABSTRACT OF DISSERTATION

EFFICIENT ELECTROCHEMICAL FUNCTIONALIZATION OF CARBON NANOTUBES AND CARBON NANOTUBE MEMBRANES FOR ENERGY, DRUG DELIVERY AND POTENTIAL CATALYSIS APPLICATIONS

Electrochemical diazonium grafting offers versatile functionalization of chemically inert graphite under mild condition, which is particularly suitable for CNT composite modification. Tetrafluorinated carboxylphenyl diazonium grafting provides the most controllable functionalization chemistry allowing near monolayer levels of functionality on carbon nanotubes. The functional density was successfully quantified by anion selective dye-assay and X-ray photoelectron spectroscopy (XPS) of thiol-Au self-assembled monolayers (SAM) as a calibration reference. This technique enables monolayer functionality at the tips of carbon nanotube membranes for biomimetic pumps and valves as well as thin conductive layers for CNT-based high area electrochemical support electrodes.

Double-walled carbon nanotube (DWCNT) membranes were functionalized with sterically bulky dye molecules with amine termination in a single step functionalization process. Non-faradic (EIS) spectra indicated that the functionalized gatekeeper by single-step modification can be actuated to mimic protein channel under bias. This functional chemistry on membranes resulted in rectification factors of up to 14.4 with potassium ferricyanide in trans-membrane electrochemical measurements. One step functionalization by electrooxidation of amines provides simple and promising functionalization chemistry for the application of CNT membranes.

Carbon nanotubes (CNTs) are considered a promising catalyst support due to high surface area, conductivity and stability. But very few cases of asymmetric catalysis have been reported using CNTs as support. Three noncovalent functionalization approaches have been carried out to immobilize Rh-Josiphos complex on CNTs for asymmetric hydrogenation of dimethyl itaconate. Coordinated Rh catalyst on CNTs exhibited excellent activity and reuse ability even after seventh run in hydrogenation but no enantiomeric excess as expected for lacking a chiral directing ligand. The catalyst using pyrene absorption gave 100% yield and excellent enantiomer excess (>90%) but suffered from leaching into solution. The phosphotungstic acid (PTA) anchored catalyst gave 100% yield and higher ee (99%) and better reusability over pyrene absorbed catalyst but

had significant leaching after the second run. At this point it remains a significant challenge to utilize CNTs as a chiral catalyst support.

Keywords: Carbon nanotube, carbon nanotube membranes, electrochemical diazonium grafting, electrooxidation of amine.

Xin Zhan

03-22-2013

EFFICIENT ELECTROCHEMICAL FUNCTIONALIZATION OF CARBON
NANOTUBES AND CARBON NANOTUBE MEMBRANES FOR ENERGY, DRUG
DELIVERY AND POTENTIAL CATALYSIS APPLICATIONS

By

Xin Zhan

Dr. Bruce Hinds

Director of Dissertation

Dr. John Anthony

Director of Graduate Studies

03-22-2013

DEDICATION

To Chunxia, family, and friends

ACKNOWLEDGEMENTS

First and foremost I would like to express my greatest gratitude to my mentor, Dr. Bruce Hinds, for taking me as a graduate student and opening the nano world for me. I learned how to critically thinking and have been gradually educated to work independently.

I would like to thank my committee members, Dr. Folami Ladipo, Dr. Mark Watson, Dr. Stephen Rankin, Dr. Doo Young Kim for encouraging me, challenging me, analyzing my projects and providing very useful suggestions about my research. In addition, I would like to thank Dr. Vander Kooi, my outside examiner, for his helpful comments.

I would like to thank all of our group members in the Hinds lab. Most especially, I want to thank Dr. Ji Wu, Dr. Xin Su, and Dr. Mainak Majumder who gave me a lot of help during my study. Dr. Ji Wu taught me many experiment techniques and gave me lots of constructive suggestions in my research. I learned CNT Buckypaper from Dr. Xin Su. The first experiment of carbon nanotube membranes was taught by Mainak. I learned a lot of carobon nanotube membrane from him. I would also thank Dr.Bing Hu, Dr.Xinhua Sun, Jingyuan Yao, Zhiqiang Chen for their great supports all the time.

I would like to thank Phillip Swartzentruber in Balk Lab. He is extremely patient to teach me operate X-ray photoelectron spectroscopy. At the beginning, I didn't know much about this instrument. I would like to thank Dr. Selegue and Dr.Holms, for their great help for the chiral synthesis when I knew nothing in this area at the beginning. I would also like to thank the chemistry staff for their great support, especially, John

Laton, Jeff Babbitts and Art Sebesta. I learned how to operate NMR from John. Jeff made great glassware for my experiments. Art did great job on repairing the drybox.

Finally, I'd like to acknowledge my family, my father, my mother and my two sisters, for their endless love and support. I would especially like to thank my wife, Dr. Chunxia Zhao. She gave me tremendous support on my life and research. She is the first reader of my writing and gives great suggestions. Without her gracious support I would not be at this point in my career.

TABLE OF CONTENTS

ACKNOWLEDGEMENTS	III
LIST OF TABLES	IX
LIST OF FIGURES	X
LIST OF SCHEMES.....	XV
Chapter 1 Introduction	1
1.1 Extraordinary properties of carbon nanotubes	1
1.2 Significance of Functional chemistry of carbon nanotubes	2
1.3 Covalent functionalization of carbon nanotubes.....	2
1.4 Non-covalent functionalization of carbon nanotubes.....	5
1.5 Applications of functionalized carbon nanotubes	6
1.5.1 Medicine	6
1.5.2 Catalysis.....	9
1.6 Carbon nanotube membranes: a robust fast fluid platform.....	11
1.7 Exciting application of carbon nanotube membranes in chemical separation and drug delivery	13
1.8 Immobilization of chiral catalysts for asymmetric catalysis.....	17
1.8.1 Significance of asymmetric catalysis	17
1.8.2 Covalent immobilization of chiral catalysts	18
1.8.3 Non-covalent immobilization of chiral catalysts.....	20

1.8.4 Theoretical study of immobilization of chiral catalysts	20
1.8.5 CNTs and CNT membrane as promising catalytic platform	22
1.9 Goals and summary of dissertation	23
Chapter 2 Near monolayer functionality produced by electrochemical diazonium grafting on carbon nanotubes	50
2.1 Introduction	50
2.2 Experimental methods.....	52
2.2.1 Reagents.....	52
2.2.2 Synthesis of 4-carboxylphenyl diazonium tetrafluoroborate.....	53
2.2.3 Synthesis of tetrafluorinated 4-carboxylphenyl diazonium tetrafluoroborate ..	53
2.2.4 Electrochemical reduction of diazonium salts on glassy Carbon.	54
2.2.5 Electrochemical reduction of diazonium salts on Au substrate.....	54
2.2.6 Preparation of self-assembly monolayer (SAM) on Au substrate.....	55
2.2.7 Electrochemical grafting of diazonium salts on carbon nanotube (CNT) buckypaper.....	55
2.2.8 Modification of CNT Buckypaper with pyrenebutyric acid.....	55
2.2.9 Quantification of carboxyl density using Dye-Assay.	56
2.2.10 X-ray Photoelectron Spectroscopy (XPS).	56
2.3 Results and discussions	57
2.4 Conclusions	62

Chapter 3 Single-step electrochemical functionalization of double-walled carbon nanotube (DWCNT) membranes and the demonstration of ionic rectification	76
3.1 Introduction	76
3.2 Experimental methods.....	79
3.2.1 Fabrication of double-walled carbon nanotube membranes.....	79
3.2.2 Modification of DWCNT membranes	79
3.2.3 Rectification experimental setup	80
3.2.4 Dye assay quantification of carboxyl and sulfonate density on glassy carbon	81
3.3 Results and discussions	81
3.4 Conclusions	87
Chapter 4 Covalent and noncovalent immobilization of chiral ferrocenyldiphosphine ligand on carbon nanotubes for asymmetric Rh catalyzed hydrogenation	107
4.1 Introduction	107
4.2 Experimental methods.....	111
4.2.1 Chemicals	111
4.2.2 Synthesis of chiral ligand precursor:(R)-[3-(N, N-Dimethylamino) ethyl] ferrocene	111
4.2.3 Synthesis of chiral tethered Josiphos ligand: (R)-1[(S)-2(Diphenylphosphino)-1'-(dimethyl-3'aminopropylsilyl)-ferrocenyl] ethyldicyclohexylphosphine	112
4.2.4 General procedure of homogenous and heterogeneous hydrogenation of dimethyl itaconate.....	114

4.2.5 Quantification of enantiomeric excess by chiral NMR	115
4.2.6 Fabrication and oxidation of multiwalled CNTs	115
4.2.7 Covalent immobilization of chiral catalyst.....	116
4.2.8 Non-covalent immobilization of chiral catalyst	117
4.3 Results and discussions	117
4.3.1 Covalent immobilization of tethered Rh-josiphos ligand complex on CNT ..	118
4.3.2 Three non-covalent immobilizations of Rh-Josiphos on carbon nanotubes...	120
4.4 Conclusions	123
Chapter 5 Conclusions and future research direction	138
5.1. Electrochemical diazonium grafting and quantification of its surface functional density.	139
5.2 Single-step electrochemical oxidation of amine on double-walled carbon nanotube (DWCNT) membranes and the demonstration of ionic rectification.....	140
5.3 Synthesis and immobilization of chiral ferrocenyldiphosphine ligand on carbon nanotubes for asymmetric hydrogenation.	141
LIST OF ABBREVIATIONS	144
REFERENCES	145
VITA	157

LIST OF TABLES

Table 2 1 Comparison of XPS and dye-assay quantification.	63
Table 2 2 Enhanced grafting efficiency of CNT buckypaper on glassy carbon	64
Table 3 1 Comparison of ionic current rectification factor (Rf) in K ₃ Fe(CN) ₆ solution..	89
Table 3 2 Summary of ionic rectification factor on single-step modified DWCNT-dye membrane.....	90
Table 3 3 Summary of ionic rectification factor on DWCNT membrane after water plasma oxidation to remove gatekeepers.	91
Table 3 4 Quantification of carboxyl and sulfonate density using dye-assay.....	92
Table 4 1 Asymmetric homogeneous hydrogenation of dimethyl itaconate with Rh-Josiphos ligand.....	124
Table 4 2 Heterogeneous hydrogenation with the covalent immobilized Josiphos ligand-Rh complex on polystyrene..	125
Table 4 3 Heterogeneous hydrogenation with the covalent immobilized Josihpis ligand-Rh complex on polystyrene..	125
Table 4 4 Heterogeneous hydrogenation with coordinated [Rh(nbd) ₂] ⁺ BF ₄ ⁻ on CNTs	126
Table 4 5 Heterogeneous hydrogenation with immobilized pyrene modified chiral catalysts on CNTs	127
Table 4 6 Heterogeneous hydrogenation with immobilized Rh-Josiphos ligand complex using phosphotungstic acid.....	127

LIST OF FIGURES

Figure1 1 Structural varieties of carbon nanotubes (CNTs)	26
Figure1 2 Covalent surface chemistry of CNTs.	27
Figure1 3 Schematic of chemical modification of CNTs by acid treatment and coupling with octadecylamine (ODA) using thionyl chloride.....	28
Figure1 4 (a). Schematic of chemical modification of nanotube end with carbodiimide coupling reaction. (b). Functionalized probe to sense specific interaction with functional group (X) of a substrate.	29
Figure1 5 Schematic mechanism of multilayer growth in diazonium grafting.	30
Figure1 6 Amide coupling of protein with the irreversibly adsorbed pyrene succinimidyl ester onto sidewall of SWNT via π -stacking.	31
Figure1 7 How surfactants may adsorb onto the nanotube surface.	32
Figure1 8 NIR fluorescence images of (a) Raji cells (B-cell lymphoma), (b) CEM cells (T-cell lymphoma) treated with the SWNT-Rituxan conjugate. (c) Schematic of NIR photoluminescence (PL) detection of SWNT-Rituxan conjugate selectively bound to CD20 cell surface receptors on B-cell lymphoma (left).	33
Figure1 9 Carbon nanotubes as multifunctional biological transporters and near-infrared agents for selective cancer cell destruction.....	34
Figure1 10 Carbon nanotube for PTX delivery.	35
Figure1 11 (a) Schematic diagram showing ethanol production from syngas inside Rh-loaded Carbon nanotubes. (b)TEM image of Rh, Mn-in-CNTs catalyst. (c)TEM image of Rh, Mn-out-CNT catalyst. (d) C ₂ oxegenate formation activities as a function of time on stream.....	37

Figure1 12 Schematic illustration of the fabrication procedure for Pt monolayer coating onto MWCNT mattes. [59].....	38
Figure1 13 (a) SEM image, (b) TEM image in bright field and (c) STEM image in dark field of the Pt monolayer coated on MWCNTs. (d) Cyclic voltammogram of Pt monolayer and film coated on MWCNTs of buckypaper.....	39
Figure1 14 Natural ion channel inspired biomimetic nanopores and nanochannels.	40
Figure1 15 Schematic fabrication process of CNT membrane. Reproduced from reference.[68].....	41
Figure1 16 (a) An as-grown aligned multiwalled CNT array produced by Fe-catalyzed chemical vapor deposition (b) Idealized membrane with aligned CNT array passing across a solid polymer film. (c) Cross-sectional SEM image of CNT-polystyrene membrane. Reproduced from reference.....	42
Figure1 17 (a) Apparatus for static grafting (SG). (b) Apparatus for flow grafting (FG). <i>H</i> determines the height of the liquid column and hence the high flow velocity through the membrane, forcing preferential reaction at the CNT tips. Yellow section represents functionalized site. . Reproduced from reference.	43
Figure1 18 (a) Anionic dye molecule as gatekeeper on CNT membrane; (b) Change in separation co-efficient with voltage applied to the CNT- FG-spacer (polypeptide)-dye membrane. (c) Fluxes of the two permeates at applied voltages across CNT-FG membrane.....	44
Figure1 19 (a) Schematic of highly efficient electro-osmotic pumping of caffeine using various cations (b) TEM image of SWCNTs with ~2 nm inner diameter; (c) 3-dimensional model of Ru(bpy) ₃ ²⁺ moving in a (12,12) SWCNT.	45

Figure1 20 (a) Ionic rectification curves of H ₂ O plasma etched, diazonium grafted and dye modified SWCNT membranes (b) Ionic rectification curve when feed side of the U-shape tube is filled with 0.1 M LiCl, KCl, ZnSO ₄ , or BaCl ₂ and permeate side is filled with deionized (DI) water. (c) Visualization of different rectification mechanisms of water plasma etched, diazonium grafted and dye modified SWCNT membranes	46
Figure1 21 The principle of asymmetric catalysis.....	47
Figure1 22 Difference in the Gibbs free energy change for the R and S transition states	48
Figure1 23 Simulation of water-methanol flux through Pt catalytic CNT membrane (Pt coated on CNT tip).....	49
Figure 2 1 (a) The mechanism of multilayer formation by electrochemical reduction of 4-carboxylphenyl diazonium grafting. (b) Hindrance of multilayer growth by C-F bond on aryl ring	65
Figure 2 2 Schematic illustration of quantification of carboxylic density on surface of glassy carbon by pH dependent adsorption/desorption of charged dye molecule.....	66
Figure 2 3 4-carboxyl phenyl diazonium and tetrafluorinated 4-carboxyl phenyl diazonium grafting density on glassy carbon as measured by TBO dye assay.	67
Figure 2 4 XPS spectra of Self-Assembled Monolayers (SAMs) and diazonium modified Au surface (a) XPS survey scan for 12-mercaptododecanoic acid SAM on Au	68
Figure 2 5 Schematic of fabrication and grafting of CNT buckypaper on Teflon membrane.....	72
Figure 2 6 Grafting time vs carboxyl density on CNT buckypaper on Teflon membrane. As measured by dye-assay method.	73

Figure 2 7 Enhanced grafting efficiency of CNT buckypaper on glassy carbon. 4-carboxyl phenyl diazonium and tetrafluorinated 4-carboxyl phenyl diazonium grafting of CNT buckypaper on glassy carbon (GCE) as substrate.....	74
Figure 2 8 Schematic of making non-covalent functionalized CNT with pyrenebutyric acid	75
Figure 3 1 (a) TEM image of DWCNTs (purchased from Sigma-Aldrich). (b) SEM image of as-made DWCNT membrane in the cross-sectional view. (c) Schematic diagram of the functionalized anionic dye on CNT tip playing as gatekeeper.	93
Figure 3 2 Schematic illustration of two step functionalization. (a) Electrochemical grafting or chemical grafting of 4-carboxyl phenyl diazonium. (b) Carbodiimide coupling of Direct Blue 71 dye.....	94
Figure 3 3 (a) Schematic mechanism of electrochemical oxidation of primary amine on conductive surface. (b) Schematic illustration of one step functionalization of Direct Blue 71 via electrooxidation of amine.....	95
Figure 3 4 (a) Schematic mechanism of ionic rectification on DWCNT-dye membrane. (b) Schematic rectification setup..	97
Figure 3 5 Nyquist plots of dye modified membrane	99
Figure 3 6 Ionic rectification curves on (a) as-made and (b) modified DWCNT membrane (electrochemical oxidation of amine) with potassium ferricyanide. (c) in 10 mM potassium ferricyanide and (d) in 100 mM potassium ferricyanide	101
Figure 3 7 Control experiments on DWNT membrane to rule out redox current.....	102
Figure 3 8 Control experiments on glassy carbon to rule out redox current.....	104
Figure 3 9 Schematic illustration of Dye-Assay quantification.....	105

Figure 3 10 Quantification of sulfonate density as a function of grafting time using dye- assay.....	106
Figure 4 1 Quantification of enantiomer excess (<i>ee</i> %) by ¹ NMR with lanthanide shift reagent.....	137

LIST OF SCHEMES

Scheme 4 1 Synthesis of chiral ligand precursor: (R)-[3-(N, N-Dimethylamino) ethyl] ferrocene.	128
Scheme 4 2 Synthesis of tethered Josiphos ligand: (R)-1[(S)-2(Diphenylphosphino)-1'-(dimethyl-3'aminopropylsilyl)-ferrocenyl] ethyldicyclohexylphosphine.	129
Scheme 4 3 Asymmetric hydrogenation of dimethyl itaconate.	130
Scheme 4 4 Covalent immobilization of chiral tethered ligand on three different solid supports: Amberlite IRC-50 resin, carboxylated polystyrene and carboxylated CNT, respectively.	131
Scheme 4 5 Covalent immobilization of chiral tethered ligand on Polystyrene-NH ₂	132
Scheme 4 6 Coordination of Rh–ligand complex with carboxylate on CNT.	133
Scheme 4 7 Pyrene modified chiral catalysts on CNTs via π - π stacking interaction.	134
Scheme 4 8 Rh-chiral ligand anchoring on CNT using phosphotungstic acid.	135

Chapter 1 Introduction

1.1 Extraordinary properties of carbon nanotubes

The progress of nanotechnology has profound impact on our society. The global business incorporating nanotechnology increased up to \$254 billion in 2009.[1] The inventions of new functional material and device have greatly changed our life and future. Nanotechnology does not only control the synthesis and fabrication at the size less than 100nm, but also turn the production towards in more efficient and sustainable way. Carbon nanotubes (CNTs) were one of the greatest discoveries by Ijima in 1991.[2] CNTs belong to the allotrope of carbon, besides diamond and graphite. They are considered as high aspect ratio fullerene by rolling up graphene sheets into tubular shape. Depending on the number of graphite layers in their sidewall, CNTs can be classified as single-walled (SWCNT), double-walled (DWCNT) and multi-walled carbon nanotubes (MWCNT). Figure 1.1 shows the structure of carbon nanotubes.

CNTs have been prepared in various methods including arc discharge, chemical vapor deposition (CVD), high pressure carbon monoxide (HiPco) and laser ablation.[3,4] Carbon nanotubes exhibit extraordinary mechanic, thermal and electrical properties. The modulus of elasticity of SWCNT is about 1000Gpa (1TPa), which is 5 times higher than the strength of carbon steel.[5] The theoretically thermal conductivity is up to 6600W/ (m K), more than 5 times higher than that of diamonds. Due to elimination of electron scattering, CNTs are ballistic conductors. They have the highest current density as $10^9\text{A}/\text{cm}^2$ in record, which is 100 times greater than copper wires.[6] The high aspect ratio (up to 1.36×10^8) and surface area (up to $1315\text{m}^2/\text{g}$) provide highly active area for

functional molecules.[7,8] CNTs also possess good chemical and thermal stability as promising platform for functional molecules due to inert graphite layer of CNTs.

1.2 Significance of Functional chemistry of carbon nanotubes

The unique properties of carbon nanotubes have attracted worldwide attentions to explore their applications. However, the pristine carbon nanotubes are insoluble in aqueous and organic solvents because they are easy to aggregate into bundles due to van der Waals force. This makes difficult for the applications of CNTs. Functional chemistry of CNTs is critical for their applications. The functionalization does not only remove the impurities from CNTs, but also enhances the solubility of carbon nanotubes in solution and composite. Most importantly, functionalization generates anchoring sites for functional molecules on CNTs. Many exciting applications of functionalized CNTs have been exploited, such as nano-composites, electronics, medicine, catalysis and membranes.[3,4,5,6,9,10,11,12] It opens the door to build the nature-mimicking material and device at nano-scale, moving forward their applications in industry.

1.3 Covalent functionalization of carbon nanotubes

CNTs can be functionalized using versatile modifications. The covalent functionalization includes oxidation, halogenations, addition and etc, which are highlighted in Figure 1.2. These conventional chemical treatments require aggressive treatment on chemical inert graphite wall, which creates defects on CNT surface.[13]

The most popular approach of CNT covalent functionalization is the treatment of CNTs by strong oxidizing agents. 3:1 concentrated $\text{H}_2\text{SO}_4:\text{HNO}_3$ is used to remove the carbonaceous impurities and catalyst, and creates oxygen moiety such as carboxyl group at the open ends of CNTs.[14] The carboxylated CNTs can be further formed covalent

amide bond with molecules containing amine moiety. Haddon group first functionalized the carboxyl group on CNTs with octadecylamine after acylation with thionyl chloride in dimethylformamide at 70°C for 24 hours (Figure 1.3).[15] The functionalized CNTs are soluble in a few organic solvents including chloroform, dichloromethane, aromatic solvents and CS₂. Liber et al. covalently linked the primary amine to carboxylated end of nanotube using carbodiimide chemistry. [16] The modified CNT tip enables to probe the intermolecular interaction in chemical or biological systems at nanoscale, as shown in Figure 1.4. Moreover, this method can be carried out in aqueous solution and room temperature, which provides functionalization of biomolecules and catalysts on CNTs under mild condition.

However, the traditional covalent modification cut CNTs in short and creates defects on surface in harsh treatment. It is also difficult to control the variation of functionality. Electrografting offered a powerful method for surface modification in both oxidative and reductive manner.[17] Although the functional moiety can be attached by the electrochemical oxidation of amine, carboxylates, alcohols and Grignard reagents, electrochemical reduction of diazonium has attracted great attentions.

Diazonium was found 100 years ago. Pinson et al. first reported the electrochemical grafting of 4-nitrophenyl diazonium grafting on glassy carbon in 1992.[18] Compared to other surface modification, diazonium grafting offers several advantages in surface functionalization.[17,19] First, it offers versatile functionality (-NO₂, -COOH, -SO₃H, etc) since large variety of aryl diazonium can be simply synthesized or prepared in situ from commercial available aniline [20,21]. Even the enzyme can be simply synthesized as diazonium adduct in situ and immobilized on surface for biosensing.[22,23] Secondly, it

can modify many conductive substrates (carbon, metal, polymers, semiconductor and etc). Third, the modified layer on substrate shows stronger stability compared to thiol derived layer due to its covalent modification.[24,25] However, it is hard to precisely control the surface functionality. The diazonium grafting was initially considered as monolayer modification,[18,26,27] but the study of mechanism and characterizations indicated that multilayer can be formed on substrates.[28,29,30,31,32,33] Figure 1.5 shows the mechanism of multilayer growth. The highly aggressive aryl radicals are first bounded to surface, and then continually attached to the first grafting layer on substrates. Laforgue et, al. studied the growth of nitrobenzene film on gold by electrochemical quartz crystal microbalance (EQCM) during electrochemical deposition.[34] The formation of multilayer by diazonium grafting on carbon substrate was also characterized by X-ray Photoelectron Spectroscopy (XPS), Raman, Atomic force microscopy (AFM), Infrared-Reflection-Absorption Spectroscopy (IRRAS) and electrochemistry study. [24,28,29,30] Although the surface functionality was characterized by various methods, systematical quantification has been rarely reported. The reported functionality varies in 1.6 to 28×10^{-10} mol/cm² in different quantification methods.[26] In fact the surface functionality can be greatly fluctuated under different grafting conditions such as substrate, diazonium salt, potential and etc.[35] Therefore, it is important to develop the controllable diazonium grafting and accurate quantification method.

The inert graphite surface of CNT requires aggressive chemical treatment that may disturb the properties of CNTs. The primary advantage of diazonium grafting is that CNT can be covalently modified under mild condition. Particularly, it won't damage the surface and structure of CNTs and CNT composites. Tour's group first studied the

electrochemical diazonium grafting on CNTs buckypaper electrode in 2001.[36] The grafted organic layer is characterized by thermogravimetric analysis and Raman spectra. However, the multilayer growth was also found on CNT that was characterized by XPS and micro-Raman spectroscopy. [28] The polymerization of diazonium grafting insulated Pt layer with CNT, thereby reducing current density.[37] Moreover, the thick layer on CNTs tip can block carbon nanotube membrane and dramatically reduce the fast fluid (Discussed in Section 1.7). Thus, it is fundamentally important to develop controllable functional chemistry and quantify the functional density for applications of carbon nanotubes.

1.4 Non-covalent functionalization of carbon nanotubes

CNT can be simply modified by non-covalent functionalization with aromatic molecules and surfactants. The non-covalent interaction includes π - π stacking, van der Waals force, hydrogen bonding, electrostatic forces and wrapping interaction.[38,39,40] Covalent functionalization may deteriorate the electronic property of CNT due to generating of defects on CNTs, while non-covalent functionalization offers an attractive modification for CNTs because it will not disrupt the structure of CNTs.

Chen et al. first reported that pyrene moiety attachment on CNTs via π - π stacking.[41] Figure 1.6 shows schematic illustration of anchoring proteins with adsorbed pyrene onto single walled carbon nanotubes. The non-covalent functionalization is attributed to the strong π - π stacking interaction between aromatic pyrene and basal plane of graphite. This method offers simple immobilization strategy for proteins, nano-particles and metal-complex. [42]

The insoluble CNTs can be dispersed in aqueous solution of surfactants. Islam et al. found CNTs are highly dispersed in sulfonate solution including sodium dodecylbenzene, triton X-100 and sodium dodecylbenzene sulfonate (Figure 1.7).[43] AFM measurement found that ~ 63% CNT bundles exfoliated into single tubes at even 20 mg/ml. Aromatic ring or alkyl chain tangled on CNT wall, as well as charge repulsion contributes the breakage of the bundles. Non-covalent modification of CNT using surfactant does not only improve the solubility of CNT in solution, but also stabilize the dispersion of CNT in polymer, which is essential in the application of CNT-polymer composites.[44] CNTs can be wrapped by polymers and biomolecules due to its high affinity.[45] By using DNA as template, the single stranded DNA is self-assembled to CNT, which allows separation of metallic and semiconducting CNTs with specific diameter size using ionic exchange chromatography.[46] This method is used to obtain uniform sized CNTs for the application of nano-electronics. Non-covalent functionalization enables carbon nanotubes assembled with aromatic compounds, surfactant, polymer and biomacromolecules without disturbing intrinsic properties. It is particular useful for CNT applications in electronics, biomedication and catalysis.

1.5 Applications of functionalized carbon nanotubes

1.5.1 Medicine

Carbon nanotubes were considered as promising nano-carrier that can penetrate cell membranes for diagnostic and drug delivery.[9] However, the pristine CNTs are insoluble in aqueous solution. Recent progress of functionalization chemistry of CNTs enhances the CNTs solubility and improves the biocompatibility of CNTs, which make CNT readily loaded with drug, sensing and imaging agents for drug delivery in *in vitro* and *in vivo* biological system.[13,47] Owing to the remarkable physical and chemical

property, CNT has been intensively explored for a variety of biomedical applications in the past few years.

Dai et al developed antibody conjugated SWCNTs as near-infrared (NIR) fluorescent tags for selective probing of cell surface receptors and cell imaging.[48] The advantage of this method is in use of high contrast photoluminescence of SWCNTs compared with negligible background signal of cell in NIR region. Rituxan, an antibody specific to CD₂₀ cell surface receptor on B-cell lymphomas, was functionalized on SWCNTs with the phospholipid-polyethyleneglycol tether (PL-PEG-Rituxan). NIR fluorescence images in Figure 1.8 showed the selective binding between B-cell lymphoma and SWCNT-Rituxan, while T-cell lymphoma was not recognized by the SWCNT-Rituxan tag. This technique enables the sensitive and selective probing and imaging of cell *in vitro* and potentially *in vivo*.

The near-infrared (NIR) light absorption property of carbon nanotube has been used to destruct cancer cells *in vitro*.[49] Biological systems are highly transparent in NIR wavelength ($\sim 0.8 - 2 \mu\text{m}$). However, SWCNTs have strong optical absorbance and the intrinsic band gap photoluminescence in the NIR region, which can be utilized for therapeutic agents. Figure 1.9 showed that the functionalized SWCNTs with DNA can target the tumor and selectively kill the tumor without destructing receptor free normal cell in NIR light. SWCNTs functionalized by Cy3-labeled single-stranded DNA (Cy3-DNA-SWCNT) were incubated with HeLa cells at 37°C. Normal cells without binding to DNA-SWCNT can retain normal morphology under continuous laser radiation at $3.5\text{W}/\text{cm}^2$ ($\lambda = 808 \text{ nm}$) for 5min. No cell death was observed. However, DNA-SWCNT can selectively internalize with cell labeled with folate receptor tumor marker. After

continuously radiated by a 1.4 W/cm^2 ($\lambda = 808 \text{ nm}$) laser for 2 min, extensive cell death was observed since the continuous NIR absorption of SWCNTs causes extensive local heating of SWCNT inside living cells. CNTs as selective targeting agents in NIR region offer powerful method for drug delivery and cancer therapy.

Liposomes, emulsions, cationic polymers, micro and nanoparticles are the most commonly studied vehicles for drug delivery. The functionalized CNT has been used for delivery of small drug molecules and biomacromolecules, such as proteins, DNA and small interfering RNA in *in vitro* and *in vivo*. [50] The pioneer work in this field was the use of carbon nanotubes as drug delivery vehicles *in vivo* cancer therapy in 2008.[51] Figure 1.10 showed single walled carbon nanotube (SWCNT) delivery of paclitaxel (PTX) for suppression of tumors growth in 4T1 breast cancer mice model. Paclitaxel (PTX), a widely used cancer chemotherapy drug, was conjugated to the terminal amine group of the branched polyethylene glycol (PEG) chains on PEGylated SWCNTs. The clinical drug formulation Taxol or SWCNT-PTX was injected into tumor-bearing female BALB/c mice. The mice were observed daily and the tumor volume was measured every other day. In comparison to Taxol, which showed 27.7% tumor growth inhibition (TGI) on day 22, SWCNT-PTX showed a high tumor suppression efficacy with a TGI of 59.4%. Nontoxicity was found in SWCNT-PTX treated mice *in vivo* monitored over many months (ref). The strong therapeutic efficacy of SWCNT-PTX to tumor tissue, plus no obvious toxic side-effects to normal organs makes nanotube drug delivery is a promising technology for future cancer therapy.

Carbon nanotubes have been successfully applied *in vitro* and *in vivo* diagnostic and drug delivery for cancer treatment. It is important to mention that CNTs toxicity can limit

their applications in biology and medicine though it is still in controversy. Recent progress of CNT toxicity indicated that the accumulation of CNT in body varies with the size and functionalization.[50] The highly soluble and stable functionalized CNTs are more biocompatible and nontoxic which allow CNTs to excrete through biliary pathway in feces. Therefore, it is critical to develop the desired functional chemistry of CNTs for biomedical applications.

1.5.2 Catalysis

Carbon nanotubes are considered as promising catalyst support due to their unique geometry, high surface area, electric conductivity and stability.[3,4,6] The development of CNT functionalization improves the building of CNTs-nanocrystal heterostructure in both covalent and noncovalent approach.[52,53,54] CNTs are very attractive as catalyst supports for organic synthesis and fuel cell. The enhancements of catalytic activity and selectivity have been reported.[54] However, it is a challenge to control the morphology of noble catalyst on CNTs, which is essential to obtain its high activity with longer life time. The mechanism of heterogeneous catalysis on CNTs is still under investigation.

In 1994, Ajayan et al. reported the first application of CNTs as support in heterogeneous catalysis.[55] The Ru deposited on CNTs displayed higher selectivity (90%) for cinnamylalcohol than that of on alumina support (20-30%) in cinnamaldehyde hydrogenation. The author claimed that high selectivity is attributed to interaction between metal and CNTs though the mechanism is unclear. Similar work was also reported from Tessonnier and coworkers.[56] The Pd nanoparticles were encapsulated inside the CNTs with capillary force during impregnation. The high selectivity for hydrocinnamaldehyde was obtained more than 80% with Pd-CNTs. No selectivity of

hydrocinnamaldehyde over phenyl propanol was found on Pd-active carbon. The high selectivity of Pd-CNT is possibly ascribed to low concentration of oxygenate density and peculiar morphology of CNT, which may greatly influence the adsorption mode of reactant. Pan et al. found that the activity of Rh inside the nanotube ($30.0 \text{ mol mol}^{-1} \text{ Rh h}^{-1}$) was enhanced ~ 10 times than that outside the tube in the ethanol production from CO and H₂ (Figure 1.11).[57] Raman spectroscopy indicates the strong interaction of Mn-CO inside the CNT while no or very weak adsorption of Mn-CO occurs outside the CNT. The oxophilic Mn inside CNTs could attract O of CO with C binding to the adjacent Rh. The adsorption of CO bridging Rh and Mn facilitates CO dissociation and enhances the ethanol production. Temperature programmed desorption experiment also confirmed that the higher hydrogen concentration was maintained inside the CNT. Rh-Mn inside the CNTs exhibited enhanced activity since CNT played as nano-reactor that confined local high concentration of hydrogen. CNTs are promising catalyst support for organic synthesis. However, it required more investigations on the unclear mechanism of the enhanced selectivity and activity. The future direction is to immobilize more expensive chiral ligand complex on CNT, which allowed reusing multiple times and easy separation of products.

Methanol fuel cell containing Pt catalyst offers safe and clean energy as mobile power. However, the cost and stability of Pt catalyst limit its application.[11,58] Electrochemical deposition of Pt on CNTs requires organic layer modification to provide binding sites for catalysts. The common problem is that thick organic layer causes the insulation of deposited Pt from conductive CNT surface and greatly reduces the current density. We developed electrochemical grafting of fluorinated benzoic acid layer, which is critical to

provide near monolayer binding sites for Cu monolayer deposition since strong C-F bonds are resistant to polymerization (Figure 1.12).[59] The Pt was coated on CNT by replacing Cu. No thick Pt coating or isolated Pt nanoparticles was found in the scanning electron microscope (SEM) image of Figure 1.13a. High resolution transmission electron microscopy (TEM) image of Figure 1.13 b and Figure 1.13c indicated the likely presence of Pt monolayer, which is consistent with XPS and Inductively coupled plasma atomic emission spectroscopy (ICP-AES) measurements. Hence, the monolayer deposition improved the conductivity and electrochemical activity. The mass activity of deposited monolayer Pt on CNTs reached highest record as 2711 A g^{-1} in methanol oxidation, as shown in Figure 1.13d. It is about 13 times higher than that of $\sim 10 \text{ nm}$ thick Pt film coated on MWCNT, and 6 times higher than those of other reported Pt/Carbon electrode.[59] CNTs provide a conductive and robust catalyst platform. More controllable functional chemistry can reduce the amount of noble metal catalyst and improve its electrochemical activity.

1.6 Carbon nanotube membranes: a robust fast fluid platform

Cell membranes have high selective permeability because embedded proteins in phospholipid bilayer can act as pump and channels allowing the transportation of nutrient and wastes.[60] X-ray structure indicates that conformation of ion channels can be controlled under voltage, which can open and close the gate of channel. Therefore it can regulate ion permeation through cell membrane.[61,62,63] Recent nanotechnology developed artificial biomimicking materials and devices for the application in sensing and separation. Figure 1.14 demonstrates the biomimetic smart nanopores and nanochannels. The gating molecules can regulate ionic flowing with the ambient stimuli such as pH, temperature, light and ions in nanopores or nanochannels. [64]

CNTs structure is some similar to that of protein channel due to the nano-cylinder shape and hydrophobic inner graphite wall, which enable CNTs to mimick its function. Hummer's molecular dynamics simulation suggested the formation of ordered water molecule chain through the hydrophobic channel of carbon nanotube.[65] The pulse transmission of water allows fast fluid flow though slipper graphite inner wall without hindered interaction. Crooks et al. reported the single carbon nanotube membrane with 150 nm diameter and measured mass transport of polystyrene particles, but no enhanced transport was observed due to large inner diameter size.[66] Hinds and coworkers first reported the aligned multiwalled carbon nanotube membrane with well ordered nanoporous structure in 2004.[67] Figure 1.15 shows the schematic fabrication procedure of CNT membranes.[68] The array of vertically aligned CNTs (Figure 1.16a) was first grown on quartz substrate by chemical vapor deposition (CVD) method. Then it was embedded in the polystyrene film. The idealized membrane structure and cross-sectional SEM image of CNT-polystyrene membrane were shown in Figure 1.16 b and c, respectively. Water plasma treatment removed the excess of polymer and Fe catalysts on the film top and opened the pores of CNTs. It also created carboxyl group on CNT tips that can be covalently functionalized with biotin using carbodiimide chemistry. After biotin tether modification, the $\text{Ru}(\text{NH}_3)_6^{3+}$ flux went down by a factor of 5.5. The following binding with streptavidin reduced the $\text{Ru}(\text{NH}_3)_6^{3+}$ flux by a factor of 15. It successfully demonstrate the bulky molecules at the entrance of CNT can sterically hinder the ionic flux.[67] Majumder et al. further studied the gate keeper effect on selectivity of ion transport.[69] The anionic tethered dye molecules were attached to the carboxylated CNT tip as gate keeper. It was found that the anionic charge tether greatly

enhanced the cation transport due to electrostatic attraction. Those experiments suggested that ionic transport can be controlled by the molecular size and charge in some degree.

Hinds group found that fluid flow through CNT membranes is 4-5 orders of magnitude faster than conventional fluid in 2005.[70] The fast flow velocity is due to the large van der Waals distance and the atomically flat surface.[12] Hence, the flowing molecules inside CNTs would not scatter on the frictionless CNT graphite walls. The similar result of fast mass transport in CNT membranes was also reported by Holt group in 2006.[71] CNT membranes were fabricated by incorporating aligned CNTs (less than 2 nm diameter) in silicon nitride film. The measured gas flow through the CNT membranes exceeds more than one order of magnitude than predicted model. And the measured water flow exceeds more than three orders of magnitude faster than predicted model, which are several orders of magnitude higher than commercial polycarbonate membranes. Both Hinds group and Holt group reported the experimental measurement of fast mass transport through CNT membrane, which is consistent with Hummer's molecular dynamic simulation results.[65] The high flux carbon nanotube membranes make it possible for large scale applications in energy economical separation of gas and liquid.[72]

1.7 Exciting application of carbon nanotube membranes in chemical separation and drug delivery

Carbon nanotube (CNT) membranes offer an exciting fast fluid platform which is 10000 fold faster than conventional materials. The CNT membrane is fabricated by embedding CNTs in polymer film. So the mechanical strength is much more robust than biological membrane. Charged tethered molecules can be functionalized on the tip of CNT to act as protein mimetic pumps. The molecules at conductive CNT tip can be

regulated for gate keeping under electric field. Those features enable functionalized CNT membrane mimic protein channel for wide applications in separation, sensing and drug delivery.[12,73]

The modest regulation of the ion transportation by gatekeeper was seen on CNT membranes based on steric and electrostatic effect.[67,69] However, more efficient modulation is required to obtain higher selectivity. The concept of voltage gatekeeping effect was first demonstrated on the anionic tethered CNT membranes.[74] The negative charged tethers were placed on CNT tip via two-step functionalization chemistry. The first step is to increase the carboxyl density on CNT tip by diazonium grafting because the more effective modulation requires higher gatekeeper density. The second step is amide coupling of charged dye molecules (direct blue71) on the carboxylated CNT tips. We used electrochemical grafting of 4-carboxylphenyl diazonium to increase the carboxyl density on CNT membrane, which was confirmed by dye-assay.[75] However, electrochemical reduction of diazonium generates very reactive radical that can be attached to anywhere of CNT tips and inner core. Simulation study suggests that the hydrophilic modification inside the CNT disrupts the smoothness of graphite wall, which results in dramatically reducing the outstanding flowing rate.[76] In order to modify CNT tips only, the flowing grafting was carried out by applying 10 cm column of inert water higher than diazonium side in the U tube. The continuous flowing of inert water can prevent the reactive diazonium from entering inside of CNT. The experiment setup is shown in Figure 1.17.[74]

Figure 1.18 shows that the negative charged dye molecules play as gatekeepers to control the ionic transport under the electric field. Two different size cation methyl

viologen (MV^{2+}) and $Ru(bipy)_3^{2+}$ (0.6 nm and 1.1 nm respectively) were chosen to measure the ionic flux. The selectivity as well as separation factor between two ions was calculated by the flux ratio of $[MV^{2+} / Ru(bipy)_3^{2+}]$. At 0 V bias, the selectivity was only about 2. At positive bias, The selectivity was increased up to ~ 10 because the negative charged tethers were attracted into the pore to block the larger ion $Ru(bipy)_3^{2+}$. In the control experiment, non-dye modified membranes didn't show any increasing separation factor under positive bias. The concept of voltage gating was proved by the tunable selectivity under the applied bias. However, it couldn't effectively block the small molecules such as nicotine and clonidine for the drug delivery application. To enhance the efficiency of separation, more controllable functional chemistry and uniform pore sized CNT membranes have been developed.

Wu et al. studied CNTs membrane for switchable transdermal drug delivery of nicotine on human skin *in vitro*. [77] CNT membranes were fabricated using microtome cutting methods that is referred to Crooks et al. [66] The CNTs-Epoxy composite was prepared by mixing with epoxy, surfactant and hardener. After curing, the composites were cut into $\sim 5 \mu m$ thick membranes using microtome machine. It simplifies the previously complicated fabrication [67] and enables producing large amount of CNT membrane in one batch. The CNT membrane was functionalized with anionic dye molecules containing four sulfonate groups, which allows high efficient electrophoretic pumping nicotine into human skin *in vitro*. Wu et al. also studied highly efficient electroosmotic flow through functionalized CNT membranes. [78] Electroosmotic flow (EOF) requires high surface charge density that allows the ions flow on the opposite charged surface in the direction of applied bias, which can pump neutral solvent and solute in the flow. But

EOF is usually inefficient because it is limited within 2 nm Debye screening strength. The small size charged CNT entrance and nearly ideal slip boundary of CNT channel provides promising conditions for highly efficient EOF. Figure 1.19 showed the schematic of highly efficient electroosmotic pumping of caffeine using various cations. The negative charged carboxyl group on CNT tip can reject cations through the tube in the direction of electric field. The moving cations can efficiently pump the neutral caffeine molecules. Compared with the sulfonate modified Anodic aluminum Oxide membrane, the electroosmotic velocities were enhanced by nearly 500 fold. The power efficiencies were improved by 19 fold. More important, the electroosmotic pumping was observed at low voltages (0.3–0.6 V), which allows the potential application for portable medical devices. We observed ionic rectification by electrostatically actuated tethers on SWCNT membranes.[79] Figure 1.20 showed the ionic current rectification by anionic tether repulsion. Rectification factor was defined as ratio of maximum ionic transport current at negative bias and positive bias ($R_f = I_{\text{negative bias}} / I_{\text{positive bias}}$). The I-V curve was linear line for the plasma etched CNT membrane. After diazonium grafting, the ionic transport current at positive bias was decreased due to the carboxylate anion repulsion, which rectification factor was 2.3. The significant rectification was observed by the actuation of the bulky charged dye molecule (rectification factor up to ~18). The anionic dye molecules can be drawn close to CNT pore under positive bias, which can effectively block ionic transport, resulting in significant increase of rectification. It closely mimics the function of protein channel, which has potential application for small drug delivery.

Molecular dynamic simulation reveals the CNT membrane potential application for efficient desalination.[80] CNT (5, 5) and (6, 6) with the narrow pore (diameter ranging

from 6 to 11 Å) reject ions extremely well due to large energy barrier for ion permeation. Bakajin group studied the sub-2-nm CNT membranes for ion exclusion.[81] CNT membrane was prepared by filling aligned CNTs in silicon nitride film. CNT tips were functionalized with carboxylic group by plasma oxidation, which can reject ions by electrostatic interaction. The experimental results showed nearly 40% ion rejection of 1.0 mM potassium chloride and 91% potassium ferricyanide.

CNT membranes exhibit amazing properties such as fast transport and high selectivity as a robust biomimetic membrane. A few successful CNT membrane applications in separation and drug delivery have been discussed. Functional chemistry places gate molecules on CNT pore to enhance the selectivity, but deteriorates the remarkable fast fluid. The future direction is to develop more controllable chemistry that can ideally control the function density and distribution.

1.8 Immobilization of chiral catalysts for asymmetric catalysis

1.8.1 Significance of asymmetric catalysis

Pasteur stated that life is dominated by dissymmetrical actions about 100 years ago.[82] Molecular chirality is essential in biological system. Chiral drugs produce significant pharmacologic difference since each enantiomer interacts with receptor in asymmetric way.[83] People learned this lesson from the tragedy resulted from the racemic thalidomide in 1960s. Approximately 10,000 children were born with fetal malformations because their mother had taken racemic thalidomide. Its R-enantiomer has desirable sedative property, but S enantiomer is teratogenic. In 1992, FDA issued policy to promote the production of chiral drugs. In 2000, the chiral drug sales reached 123

billion US \$, close to one third of all drug in worldwide. In 2006, 80% of small-molecule drugs approved by FDA were chiral and 75% were single enantiomers.[84]

Asymmetric synthesis produces chiral compounds with significant higher optical purity over traditional method such as chemical transformation and chiral resolution.[85,86] Knowles et al. developed rhodium-chiral phosphine ligand as catalyst in the asymmetric hydrogenation in 1970s, which has been successfully applied in the commercial synthesis of L-dopa (anti-Parkinson drug). [87] This work was recognized in 2001 Nobel Prize. The principle of asymmetric catalysis is illustrated in Figure 1.21.[88] Coordination between prochiral substrates A and B occurs on chiral-metal complex; subsequently the formed AB chiral products are detached from catalyst complex.

Several parameters are used to describe the activity of the catalyst.[82] 1) Turnover number (TON) was defined as ratio of the converted substrate to the catalyst. The activity of catalyst is measured by turnover frequency (TOF) that is turnover number per unit time (h^{-1}); 2) enantiomer excess ($ee\%$) is referred to the excess of one enantiomer over the other.

$$ee\% = \frac{|[R] - [S]|}{|[R] + [S]|} \times 100\% \qquad (ee\%) = \left(\frac{|\alpha|_{observed}}{|\alpha|_{pure}} \right) \times 100\%$$

1.8.2 Covalent immobilization of chiral catalysts

Homogenous catalysis has been dominated in chiral drug synthesis due to its high enantioselectivity and activity. However, the homogenous chiral catalysts are expensive and hard to be separated from products, which restrict their application in industry. Recently, the immobilized chiral catalysts show promising potential in easy separation

and recycling. But the activity and enantioselectivity of heterogeneous chiral catalysts may be dramatically decreased because of the distorted structure and mass transfer limitation after immobilization. Furthermore, contamination of products by the metal leaching is costly to be purified[89]. Therefore, it is imperative to develop immobilized chiral catalysts which have promising reuse ability and maintain comparable enantioselectivity and activity as that of the homogenous catalysts.

Numerous chiral catalysts have been covalently immobilized on zeolite, alumina and silica materials[89,90,91,92]. For example, the ferrocenyl diphosphine ligand with isocyanate linker is covalently attached to the surface of silica and polystyrene. The immobilized Ir-diphosphine exhibits high TON (100,000) and TOF (20,000 h⁻¹) in asymmetric imine hydrogenation under 80 bar. The conversion is above 95% while *ee* is comparable to homogenous analogue[93]. The immobilized catalysts on solid support can be separated by simple filtration. Among them, dendrimer is a good catalyst support with well defined sites. [94,95] The *ee* of immobilized catalysts (98%) on different size of dendrimer is only slightly lower than homogenous one. It is attributed to that chiral catalysts are anchored in isolated site to prevent the formation of multinuclear species in homogenous catalysis. It is found that the immobilization of chiral catalyst in nanopore can enhance the *ee* due to confinement effects (the effects of surface and pore). Zhang H.D et al. immobilized Mn (salen) on mesoporous material (MCM-41 and SBA-15) for asymmetric epoxidation.[96,97,98] The size of nanopore can affect the *ee* of epoxidation. The immobilized chiral Mn (salen) catalysts in the nanopore showed higher *ee* than those grafting on the outside of supports. The increasing length of linker also improves *ee* of those catalysts in nanopore.

1.8.3 Non-covalent immobilization of chiral catalysts

Non-covalent immobilization of chiral catalysts has also received considerable attention.[89,91,99] It does not require the expensive tethered ligand synthesis, the weak interaction between catalyst and support simulate homogeneous environment to obtain high activity but the stability of metal catalysts is always an issue to be considered. The leaching is strongly affected by the nature of ligand, solvents and reaction time.[91,100] Chiral Rh complexes are immobilized into mesoporous material MCM-41 by ion-exchange which is simple and does not require ligand modification[101]. The Rh-ligand complex can be immobilized directly into zeolite or the immobilized Rh precursor can be chiral modified subsequently. The immobilized chiral diphosphine [Rh-Josiphos (COD)] catalysts give comparable *ee* and conversion as corresponding homogeneous catalysts after ten runs. Another promising example is that homogeneous Mn (salen) for asymmetric epoxidation of olefins is anchored on phenyl sulfonic anion of mesoporous material via ion-exchange.[96] It is surprising that the immobilized Mn (salen) give higher *ee* (78.1%) than that of homogenous counterpart (55.0%) although its yield (87.3%) is lower than homogenous catalyst (100%) due to diffusion limitation. The *ee* remains 75% after 5 runs. The enhanced *ee* is simply attributed to the nanopore confinement even though the mechanism is not well understood.

1.8.4 Theoretical study of immobilization of chiral catalysts

There is no universal principle for immobilization of chiral catalysts since the multiphase catalytic reaction is complicated. The successful immobilization examples truly depend upon the nature of ligand and immobilized system. But the kinetic study indicates that subtle difference of R and S transition energy (less than 15kJ/mol) significantly changes the *ee* (Figure1.22).[89] This energy level is close to the weak

interactions in immobilized environment including van der Waals force (0-10 kJ/mol), hydrogen bonding (10-30 kJ/mol) and physical adsorption (10-80 kJ/mol). Hence, small change of surface/pore environment of immobilized chiral catalysts dramatically changes *ee*.

The transition state and kinetics in heterogeneous chiral catalysis are greatly affected by spatial restriction, diffusion, electronic interaction and adsorption of substrates and products[89]. Increasing transition energy difference will enhance *ee* while the *ee* will go down with less transition energy difference. The heterogenizations of chiral catalysts usually decrease the activity and *ee* due to distorted structure and mass transfer limitation. But it is possible that confinement, site isolation and cooperative effect can improve the enantioselectivity and activity of immobilized asymmetric catalysts. Those studies provide theoretical and experimental clues to obtain comparable or even higher *ee* after immobilization.

Although the advantage of heterogeneous catalysis is apparently seen as easy separation and recycling of expensive chiral catalysts, homogenous catalysis has been dominated in asymmetric synthesis. The covalent immobilization offers strong stability, but usually decreases the activity and enantioselectivity of chiral catalysts due to distorted structure and mass transfer limitation in multiple-phase reaction. The cost of functionalized chiral ligand synthesis also restricts its application. Although a few promising immobilizations of chiral catalysts on polymers and zeolites have been highlighted, the successful immobilization is subtle, truly depending upon the nature of ligand, support and etc. The transition state and kinetics in heterogeneous chiral catalysis are greatly affected by

spatial restriction, diffusion, electron transfer and adsorption of substrates and products.[89]

1.8.5 CNTs and CNT membrane as promising catalytic platform

A few successful applications of CNTs as metal catalyst support for organic synthesis and fuel cell have been discussed in section 1.5.2. Carbon nanotubes are capable of being chemical modified by covalent and non-covalent functionalization, which provides versatile immobilization methods for metal-chiral ligand complex.[102,103,104,105,106]

The early approach of immobilization of non-chiral ligand on CNTs is the use of metal complex coordinated on carboxylated CNTs. Banerjee et al. studied the functionalization of Vaska's complex and Wilkinson's catalyst on oxidized CNTs in 2002.[107,108] The broadened ^1H and ^{31}P NMR peak suggested coordination chemistry occurs between Rh and oxygen atom on CNT surface. The modest activity of immobilized Wilkinson catalyst was obtained in hydrogenation of cyclohexene (30% yield for 3 days). CNTs as chiral catalyst support have been rarely reported. Baleizao et al. covalently immobilized Vanadyl salen complex on single wall carbon nanotubes for the cyanosilylation of aldehydes in 2004.[109] The high conversion rate up to 95% after 4 runs was achieved, while the enantiomeric excess was dropped to 66% compared with homogenous salen (90%). But it is still higher than those supported on other inorganic supports (silica and MCM-41).

The conventional immobilization of chiral catalyst usually lowers its activity because the restricted catalyst is more difficult access to substrate. The enantioselectivity was also decreased due to losing the stereo structure. The voltage-gated ionic transportation and non-faradic impedance indicate that the conformation of charged tether is actuated under

electric field.[74,110] The tethered metal-chiral ligand complex can be functionalized on CNT membrane. The actuation of functionalized chiral complex provides mimetic homogeneous environment for organic reaction. Nonequilibrium molecular dynamic (MD) simulation (Figure 1.23) reveals that methanol primarily travels along the pore wall, which allows efficient transport of substrate to catalytic sites.[111] Fast flowing CNT membranes are considered as promising arrays of nano-reactors because the continuous reaction and separation can enhance the yield of products. Another advantage of catalytic CNT membranes is no need for separation of catalyst from products in asymmetric hydrogenation. Both voltage-gatekeeper experiment and MD simulation suggest that high efficient chiral catalysis can be achieved on CNT membranes.

1.9 Goals and summary of dissertation

Carbon nanotube (CNT) membranes provide an exciting opportunity for large-scale chemical separation, delivery and other applications. Electrochemical diazonium grafting offered versatile functionality under mild condition, which is particularly suitable for CNTs and CNT composite modification. However, it is a challenge to control the grafting density. The uncontrollable grafting polymer can block the entrance of CNT then greatly reduce the fluid, make it difficult to regulate the gatekeeper. The thick polymer dramatically reduce the current density due to insulation Pt catalyst from conductive CNT buckypaper, Therefore The efficient and controllable functionalization is critical to meet the requirement for their applications. It is important to quantify the functional density on CNTs and CNT membranes because it helps develop more controllable modification.

My research includes three main projects. The first project is to develop controllable diazonium functional chemistry and quantification of functionalization on CNTs and

CNT membranes. A near monolayer was successfully developed by electrochemical grafting of tetrafluorinated carboxylphenyl diazonium on glassy carbon, gold and CNT buckypaper. The polymer growth is limited by the inertness carbon-fluorine bond on aryl ring. Diazonium grafting efficiency on bucky paper was enhanced by 4 fold due to shortening conduction path length when grafting CNTs on more conductive glassy carbon. The functional density on glassy carbon, gold and carbon nanotube buckypaper, was successfully quantified by anion selective dye-assay. The accuracy of the dye-assay method was confirmed by X-ray photoelectron spectroscopy (XPS) of thiol-Au self-assembled monolayers (SAM) as a calibration reference. Tetrafluorinated carboxylphenyl diazonium grafting provides the most controllable functionalization chemistry allowing near monolayer levels of functionality on carbon nanotubes. This technique enables monolayer functionality at the tips of carbon nanotube membranes for biomimetic pumps and valves as well as thin conductive layers for CNT-based high area electrochemical support electrodes.

The second project is to develop single-step electrochemical functionalization of double walled carbon nanotube membranes and demonstrate ionic rectification. DWNT membranes were successfully functionalized by electrooxidation of amine in one step. Non-faradic electrical impedance spectroscopy (EIS) indicated that the gatekeeper can be actuated to mimic protein channel under bias. The functional density is quantified by dye-assay as same as that of two step functionalization. But the membrane modified by one step showed strong rectification while no apparent change of rectification was found by two step functionalization. Single-step functionalization by electrooxidation of amine

provides simple and high efficient functionalization chemistry for the application of CNT membranes.

The third project is the synthesis and immobilization of chiral ligand on carbon nanotubes for asymmetric hydrogenation. The Covalent immobilized chiral catalysts on polymers have no or very low activity. We were unable to achieve the literature precedence. The immobilized catalyst loses its activity due to the restricted conformation of catalysts after immobilization. Several Non-covalent immobilizations have been carried out, including coordination, π - π interaction and electrostatic anchoring. The immobilized chiral catalysts on CNTs showed comparable enantioselectivity and yield with homogeneous analogue, but the stability of catalyst needs to be improved.

In this dissertation, diazonium grafting density was successfully quantified on glassy carbon, gold and carbon nanotube buckypaper by dye-assay. Near monolayer control was developed by electrochemical grafting of tetrafluoro carboxylphenyl diazonium on glassy carbon and gold. The grafting efficiency on CNT buckypaper was enhanced by improvement of conductivity. Tetrafluorinated carboxylphenyl diazonium grafting provides more controllable functionalization chemistry for carbon nanotube membrane in the future. The enhanced ionic rectification indicates that electrochemical oxidation of amine provides highly efficient functionalization method for CNT membrane. Non-covalent immobilized chiral catalysts on CNTs showed promising ee and yield in first run, but the stability of catalyst needs to be improved.

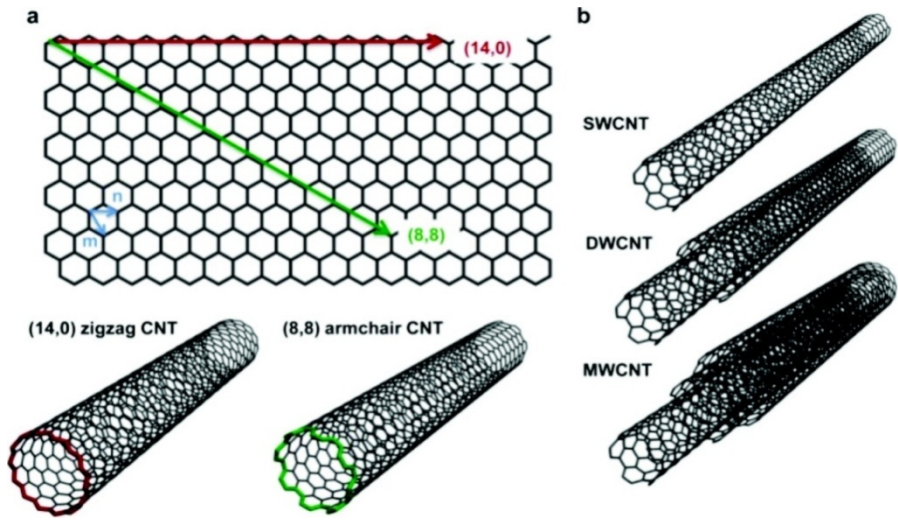


Figure 1 1 Structural varieties of carbon nanotubes (CNTs): Single (SWCNT), double (DWCNT), and multiwalled (MWCNT) CNTs. Reproduced from reference.[3]

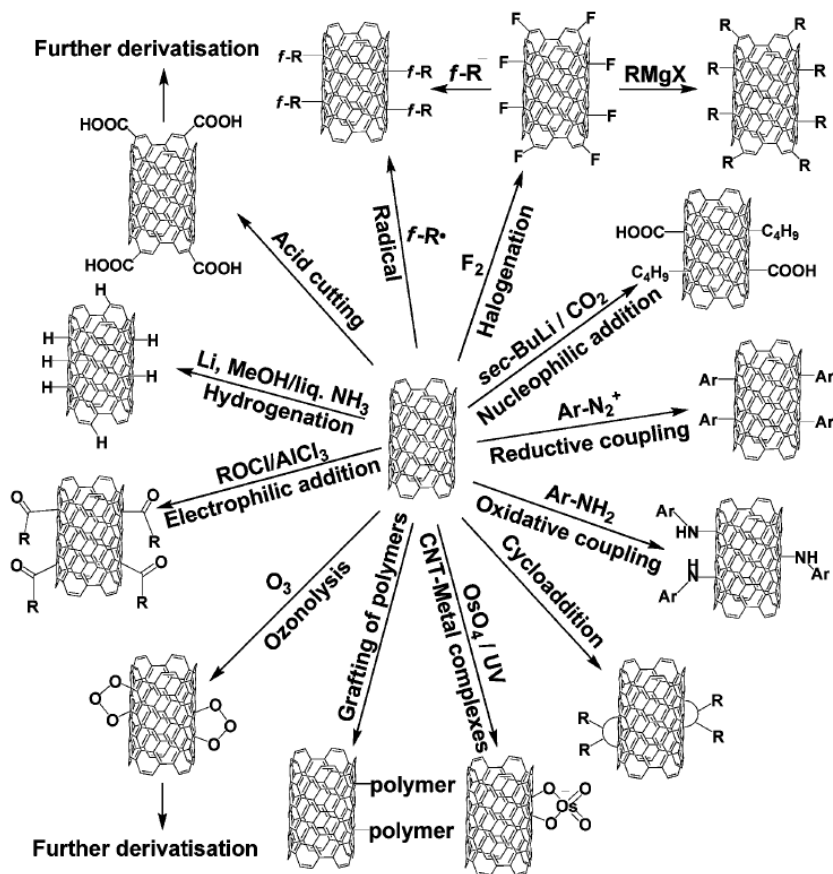


Figure 1 2 Covalent surface chemistry of CNTs. Reproduced from reference. [13]

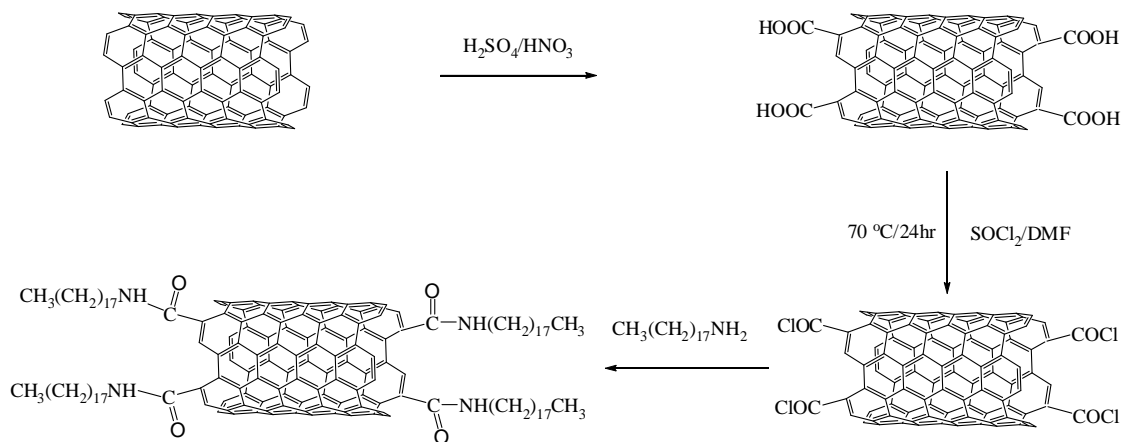


Figure 1 3 Schematic of chemical modification of CNTs by acid treatment and coupling with octadecylamine (ODA) using thionyl chloride.[15]

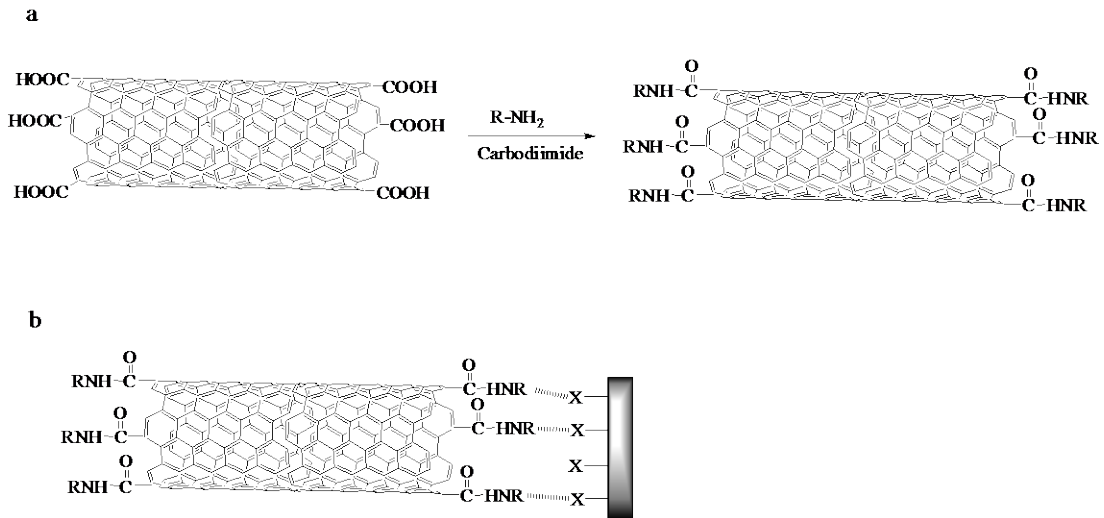


Figure 1 4 (a). Schematic of chemical modification of nanotube end with carbodiimide coupling reaction. (b). Functionalized probe to sense specific interaction with functional group (X) of a substrate. [16]

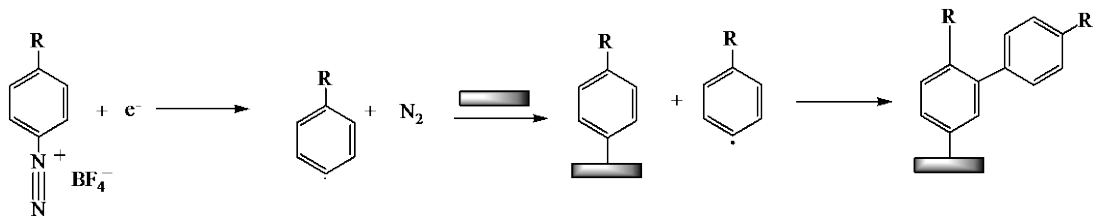


Figure 1 5 Schematic mechanism of multilayer growth in diazonium grafting.[21,26]

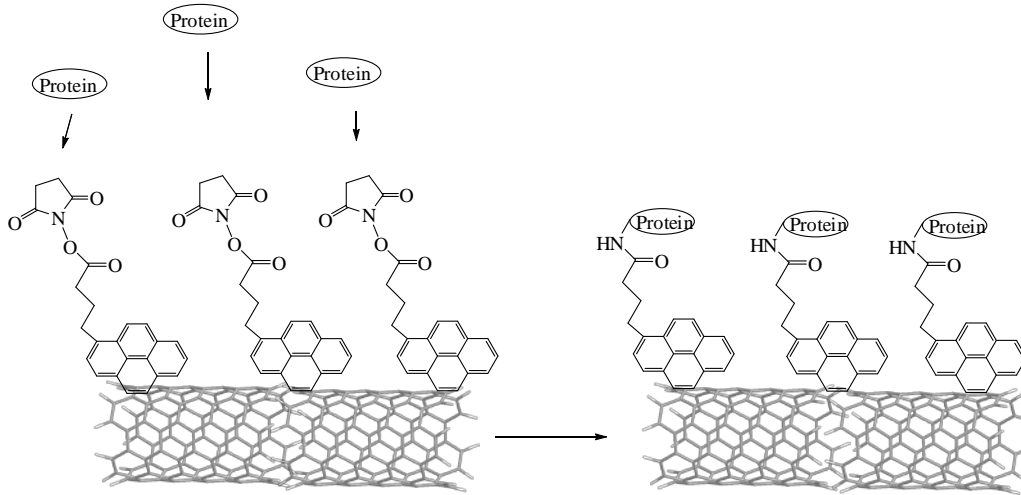


Figure 1 6 Amide coupling of protein with the irreversibly adsorbed pyrene succinimidyl ester onto sidewall of SWNT via π -stacking. Adapted from reference. [41]

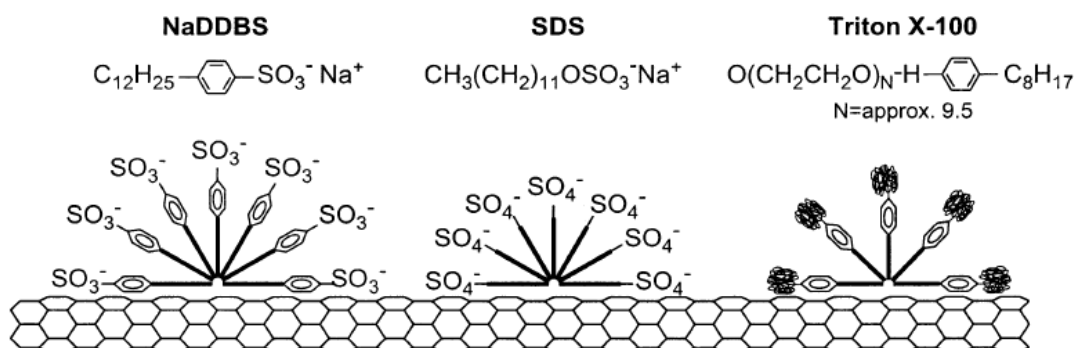


Figure 1 7 How surfactants may adsorb onto the nanotube surface. Reproduced from reference.[43]

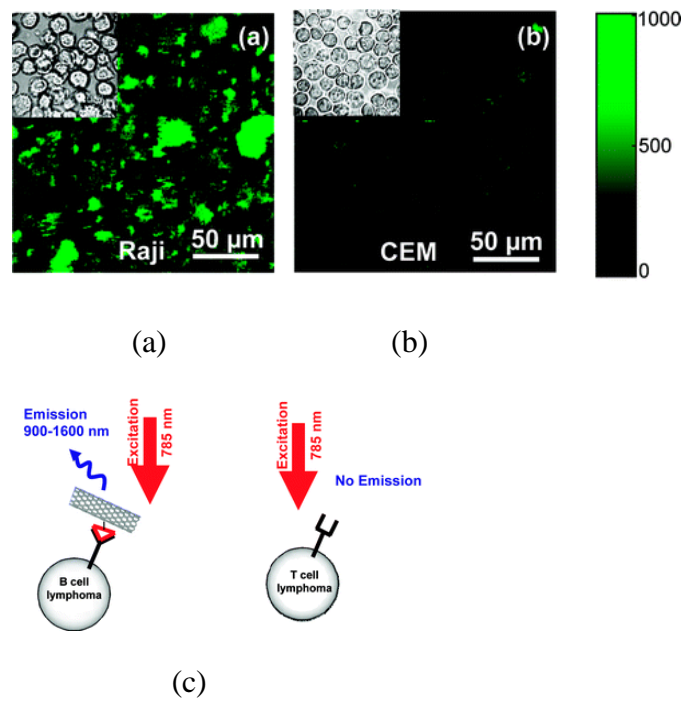


Figure 1 8 NIR fluorescence images of (a) Raji cells (B-cell lymphoma) and (b) CEM cells (T-cell lymphoma) treated with the SWNT-Rituxan conjugate. Scale bar shows intensity of total NIR emission (in the range of 900–2200 nm). Images are false-colored green. Insets show optical images of cells in the areas. (c) Schematic of NIR photoluminescence (PL) detection of SWNT-Rituxan conjugate selectively bound to CD20 cell surface receptors on B-cell lymphoma (left). The conjugate is not recognized by T-cell lymphoma (right). Reproduced from reference.[48]

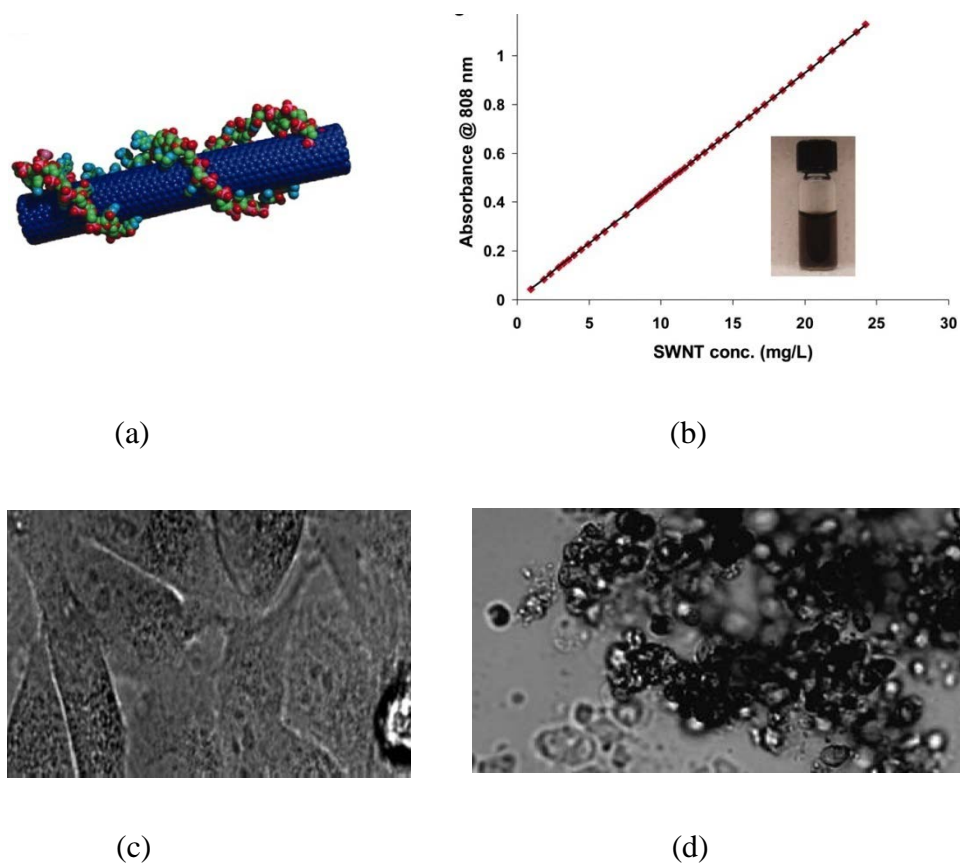


Figure 19 Carbon nanotubes as multifunctional biological transporters and near-infrared agents for selective cancer cell destruction. (a) Schematic illustration of a Cy3-DNA-functionalized SWNT. (b) Absorbance at 808 nm vs. SWNT concentration (optical path=1 cm). (Inset) A photo of a DNA-functionalized SWNT solution. (c) Image of HeLa cells without internalized SWNTs after continuous 808-nm laser radiation at 3.5 W/cm² for 5 min. No cell death was observed. (d) Image of dead and aggregated cells after internalization of DNA-SWNT and laser radiation at 1.4W/cm² for 2 min. The dead cells showed rounded and aggregated morphology as opposed to live cells in a “stretched” form in c. Reproduced from reference.[49]

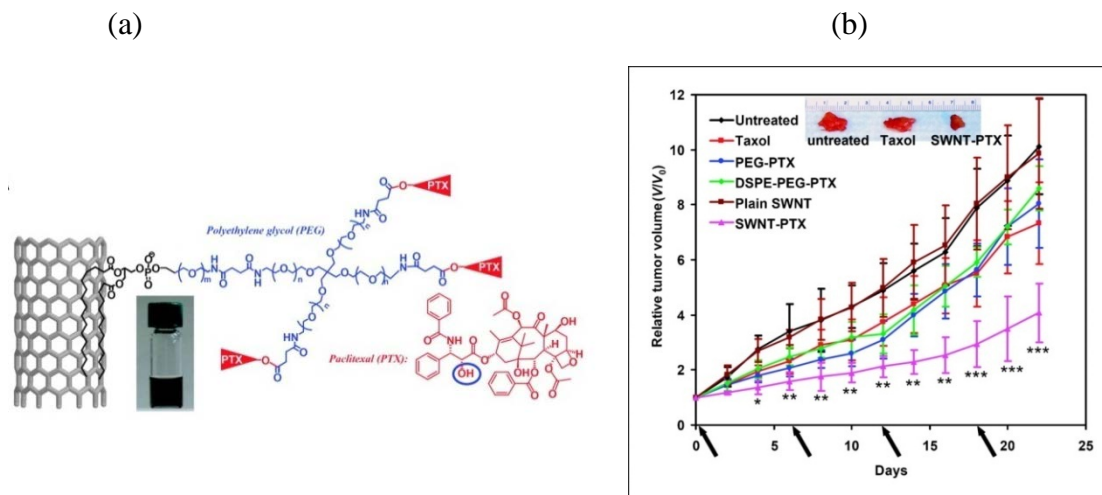


Figure 1 10 Carbon nanotube for PTX delivery. (a) schematic illustration of PTX conjugation to SWNT functionalized by phospholipids with branched PEG chains. The PTX molecules are reacted with succinic anhydride (at the circled OH site) to form cleavable ester bonds and linked to the termini of branched PEG via amide bonds. This allows for releasing of PTX from nanotubes by ester cleavage *in vivo*. The SWNT-PTX conjugate is stably suspended in normal physiologic buffer (PBS, as shown in the photo) and serum without aggregation. (b) Nanotube PTX delivery suppresses tumor growth of 4T1 breast cancer mice model. Tumor growth curves of 4T1 tumor-bearing mice that received different treatments indicated. The same PTX dose (5 mg/kg) was injected (on days 0, 6, 12, and 18, marked by *arrows*) for Taxol, PEG-PTX, DSEP-PEG-PTX, and SWNT-PTX. *, $P < 0.05$; **, $P < 0.01$; ***, $P < 0.001$, Taxol versus SWNT-PTX. Number of mice used in experiments: 8 mice per group for untreated, 5 mice per group for SWNT only, 9 mice per group for Taxol, 5 mice per group for PEG-PTX, 6 mice per

group for DSEP-PEG-PTX, and 14 mice per group for SWNT-PTX. *Inset*, a photo of representative tumors taken out of an untreated mouse (*left*), a Taxol-treated mouse (*middle*), and a SWNT-PTX-treated mouse (*right*) after sacrificing the mice at the end of the treatments. Reproduced from reference.[51]

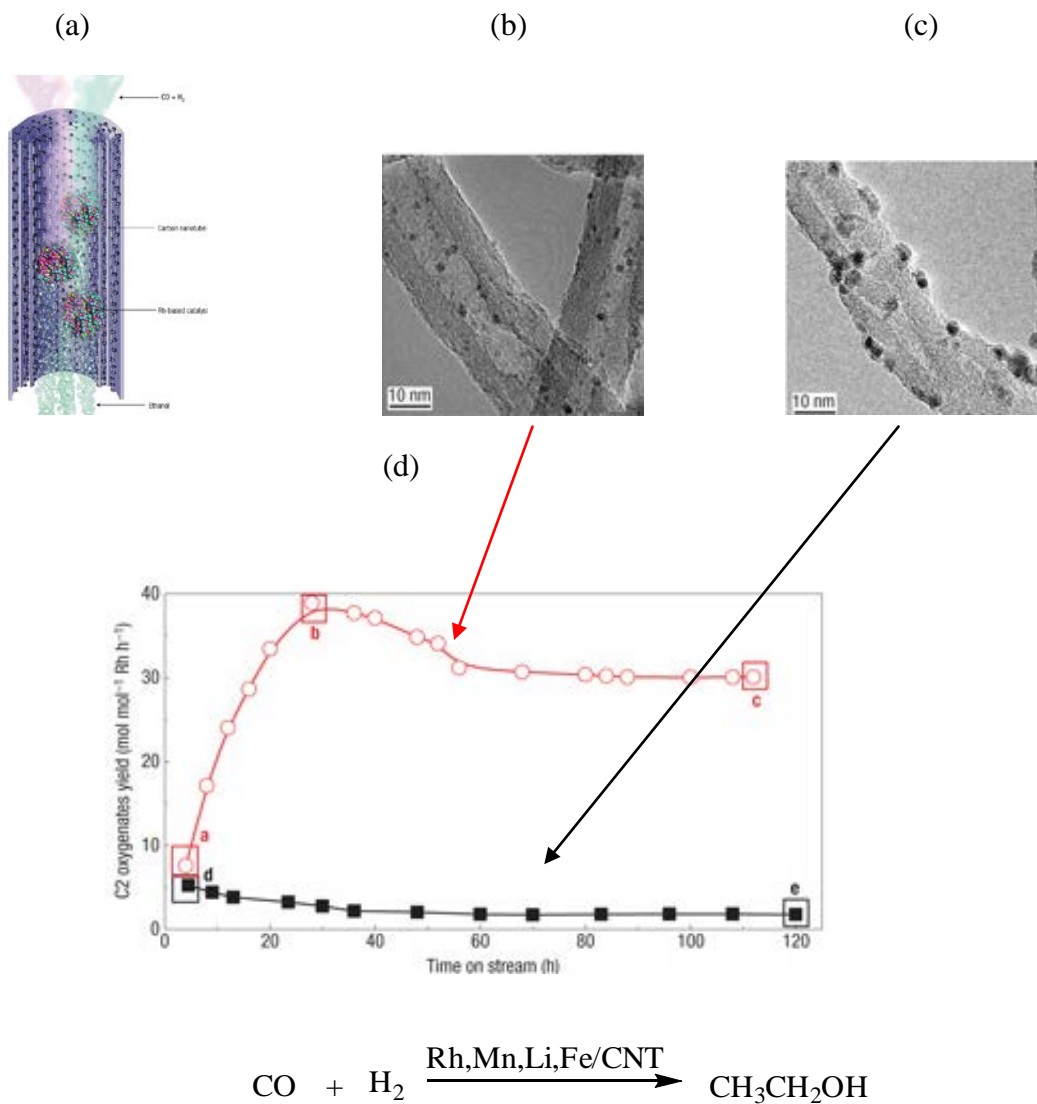


Figure 1 11 (a) Schematic diagram showing ethanol production from syngas inside Rh-loaded Carbon nanotubes. (b)TEM image of Rh, Mn-in-CNTs catalyst. (c)TEM image of Rh, Mn-out-CNT catalyst. (d) C2 oxygenate formation activities as a function of time on stream. a-c, catalyst-in-CNTs, d and e, catalyst-out-CNTs. Reproduced from reference.[57]

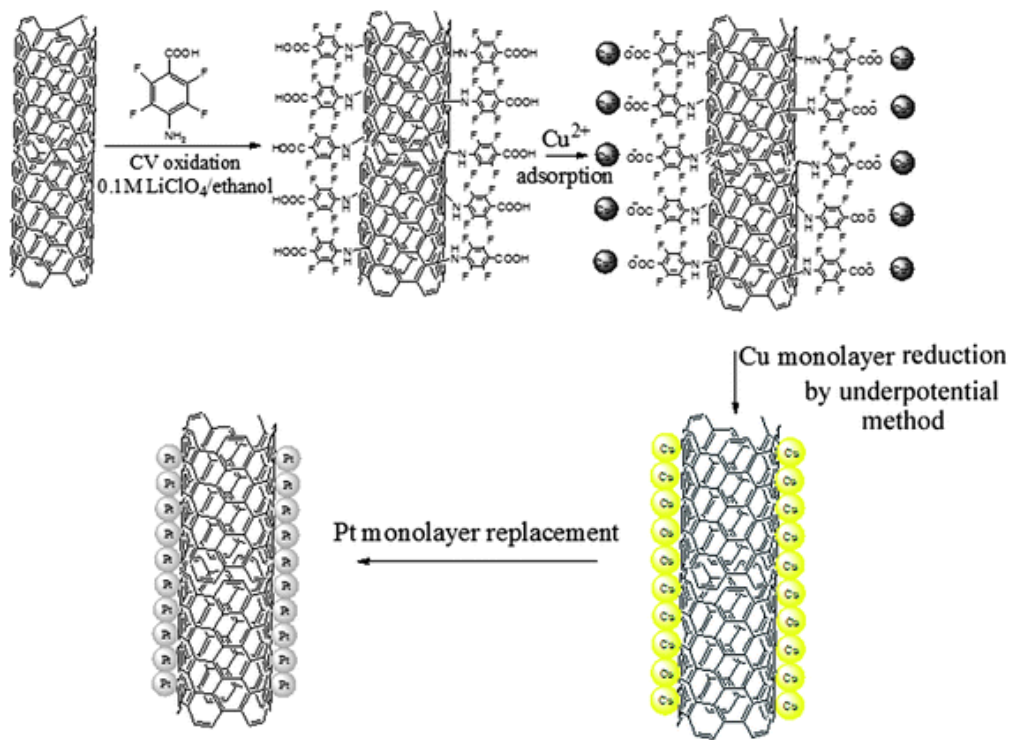


Figure 1 12 Schematic illustration of the fabrication procedure for Pt monolayer coating onto MWCNT mattes. Reproduced from reference.[59]

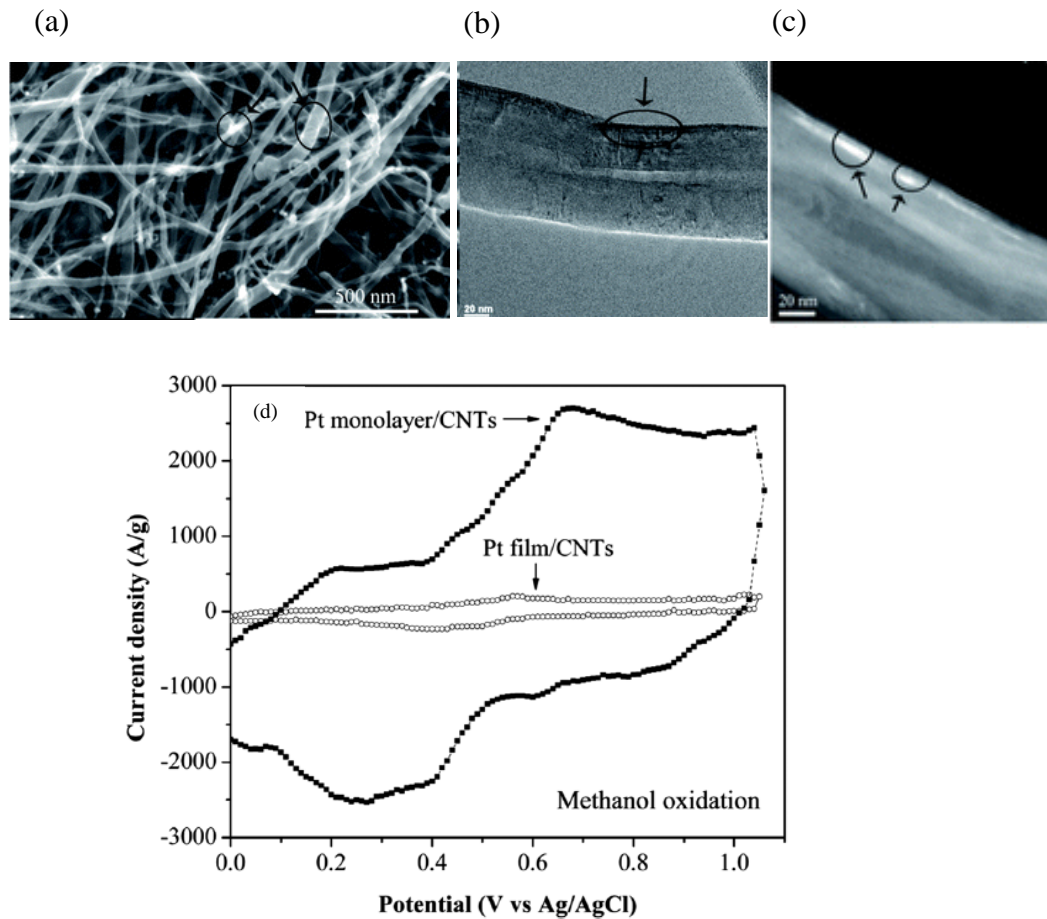


Figure 1 13 (a) SEM image, (b) TEM image in bright field and (c) STEM image in dark field of the Pt monolayer coated on MWCNTs. (d) Cyclic voltammogram of Pt monolayer and film coated on MWCNTs of buckypaper in a solution of 1 M $\text{CH}_3\text{OH}/0.5$ M H_2SO_4 and at a scan rate of 20 mV s^{-1} . Reproduced from reference.[59]

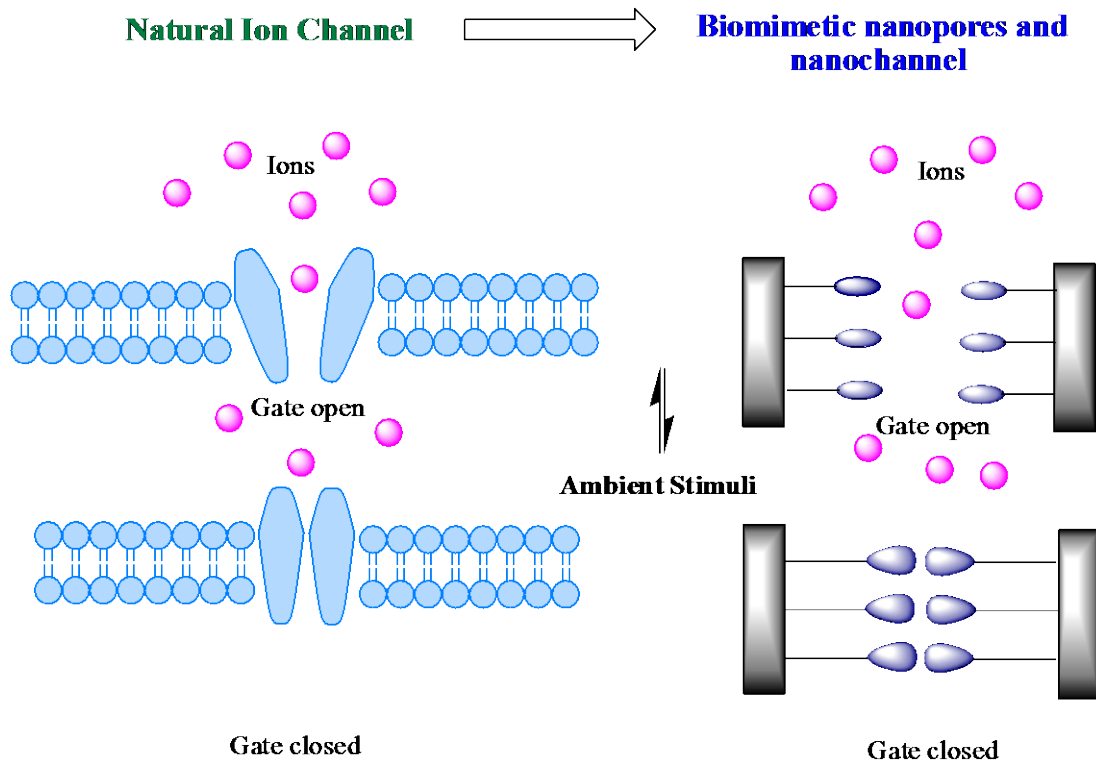


Figure 1 14 Natural ion channel inspired biomimetic nanopores and nanochannels.
Adapted from reference.[64]

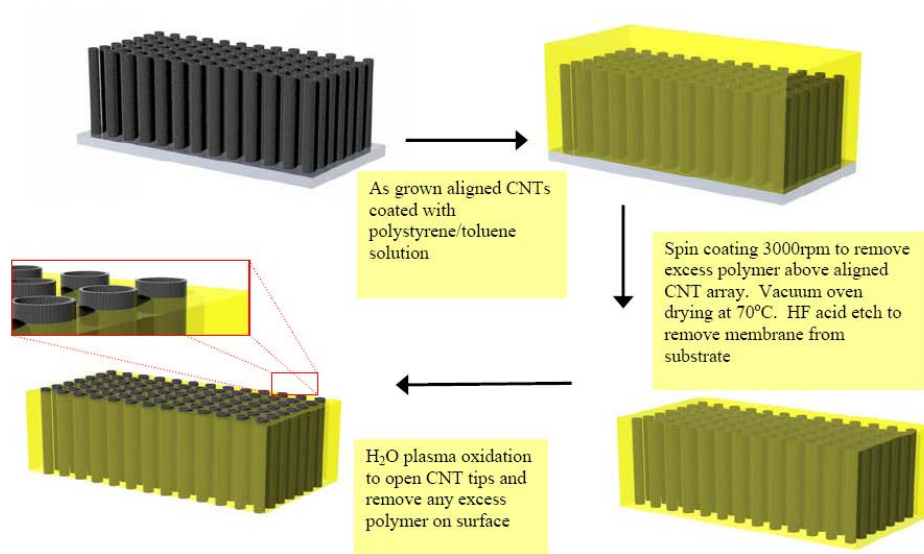


Figure 1 15 Schematic fabrication process of CNT membrane. Reproduced from reference.[68]

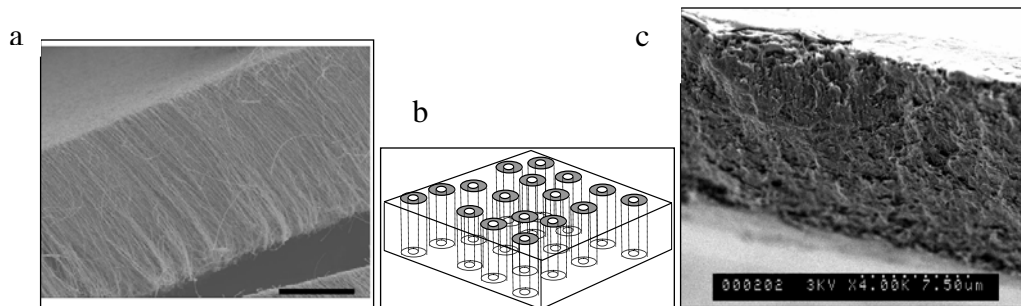


Figure 1 16 (a) An as-grown aligned multiwalled CNT array produced by Fe-catalyzed chemical vapor deposition (scale bar: 50um). (b) Idealized membrane with aligned CNT array passing across a solid polymer film. (c) Cross-sectional SEM image of CNT-polystyrene membrane. Reproduced from reference. [67]

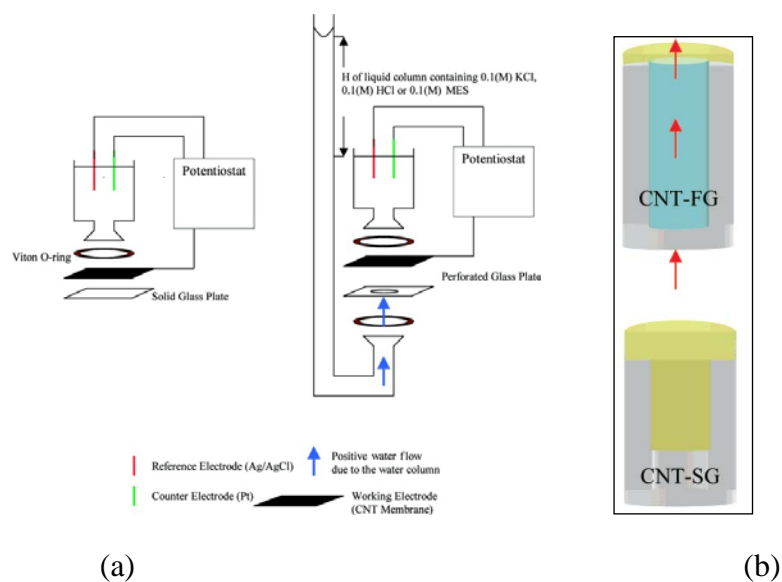


Figure 1 17 (a) Apparatus for static grafting (SG). (b) Apparatus for flow grafting (FG). H determines the height of the liquid column and hence the high flow velocity through the membrane, forcing preferential reaction at the CNT tips. Yellow section represents functionalized site. . Reproduced from reference. [112]

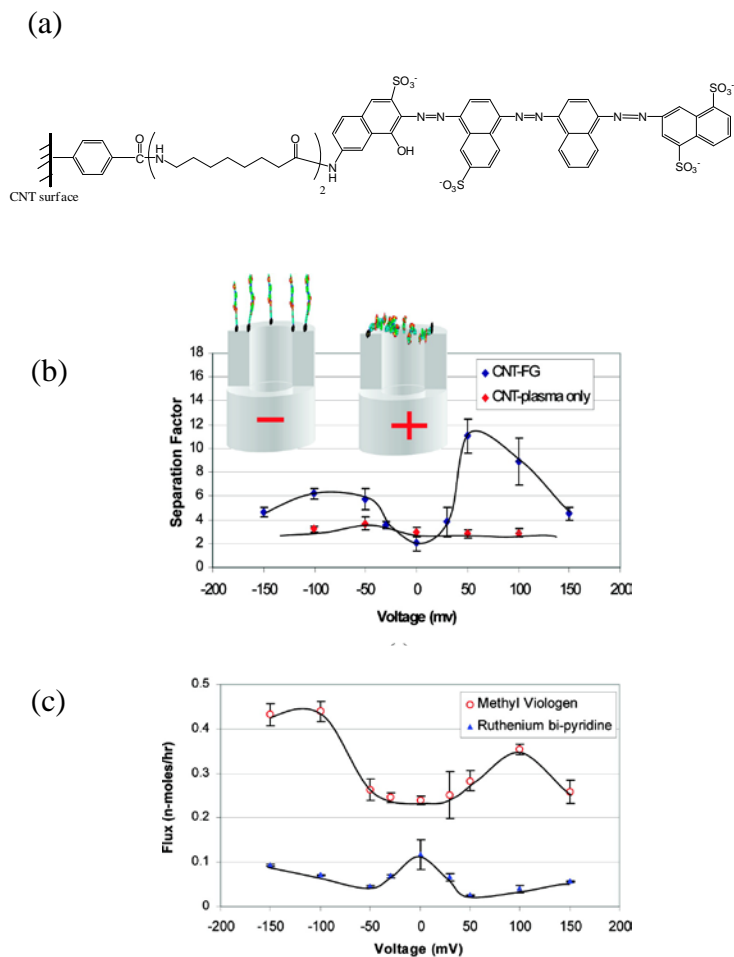


Figure 1 18 (a) Anionic dye molecule as gatekeeper on CNT membrane; (b) Change in separation co-efficient with voltage applied to the CNT- FG-spacer (polypeptide)-dye membrane. Also shown is the modest changes in observed separation factor for CNT- with low functionality (no electrochemical grafting). (c) Fluxes of the two permeates at applied voltages across CNT-FG membrane. Reproduced from reference. [112]

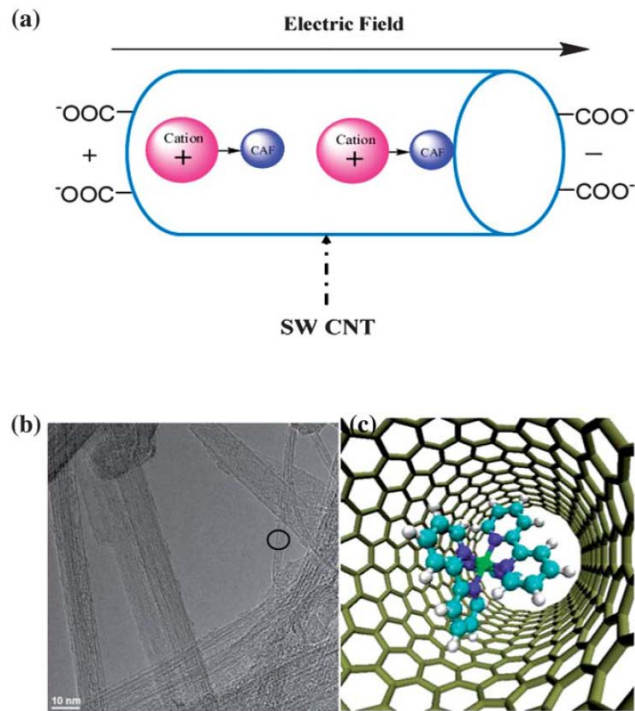


Figure 1 19 (a) Schematic of highly efficient electro-osmotic pumping of caffeine using various cations, such as $\text{Ru}(\text{bpy})_3^{2+}$ (dia. \approx 1 nm), Ca^{2+} or K^+ in SW or MWCNTs functionalized with negatively charged carboxylate groups: MWCNTs have 7 nm inner diameter; SWCNTs have inner diameters ranging from 0.8–2 nm; CAF: caffeine (\approx 0.5 nm in diameter). (b) TEM image of SWCNTs with \sim 2 nm inner diameter; (c) 3-dimensional model of $\text{Ru}(\text{bpy})_3^{2+}$ moving in a (12,12) SWCNT. Reproduced from reference.[78]

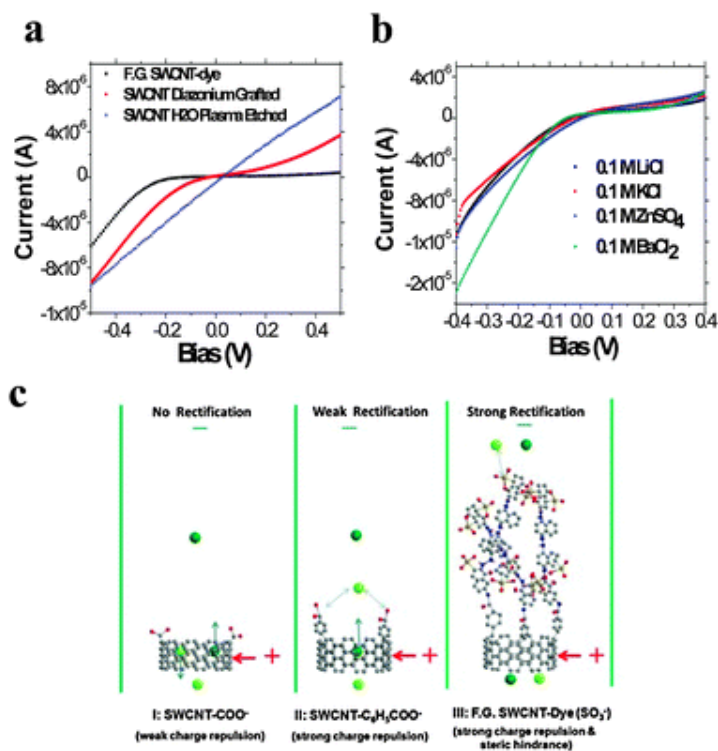


Figure 1 20 (a) Ionic rectification curves of H₂O plasma etched, diazonium grafted and dye modified SWCNT membranes when both sides of U-shape tube are filled with 0.1 M KCl, working electrode is CNT membrane, counter electrode Ag/AgCl wire. (b) Ionic rectification curve when feed side of the U-shape tube is filled with 0.1 M LiCl, KCl, ZnSO₄, or BaCl₂ and permeate side is filled with deionized (DI) water (touching Au/Pd coated SWCNT membrane). (c) Visualization of different rectification mechanisms of water plasma etched, diazonium grafted and dye modified SWCNT membranes (C, grey; N, blue; O, red; S, yellow; light green, Cl⁻; dark green, K⁺). Reproduced from reference. [110]

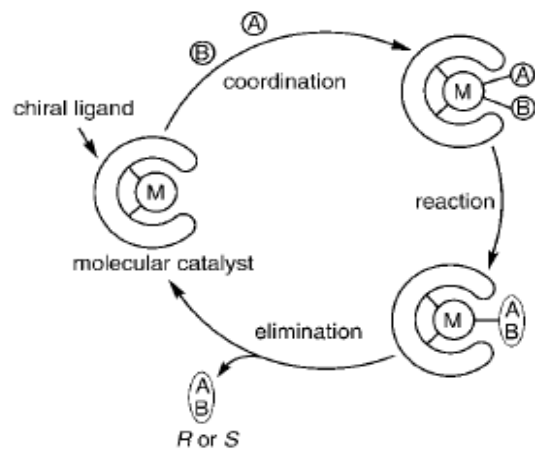


Figure 1 21 The principle of asymmetric catalysis. Reproduced from reference.[83]

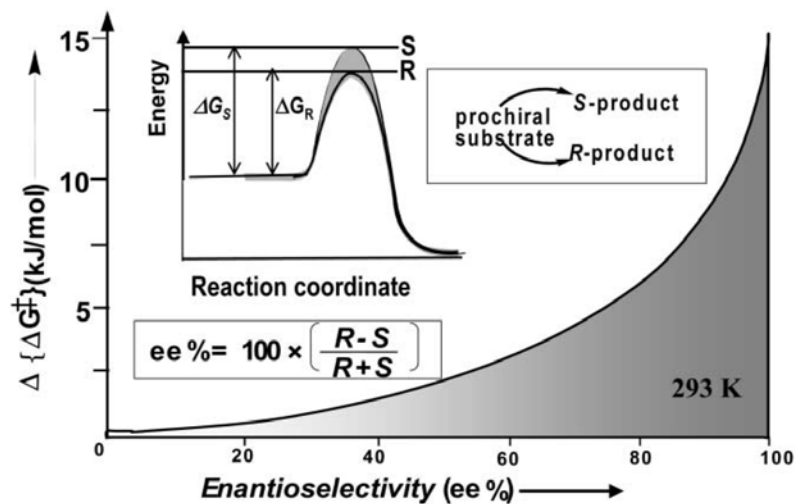


Figure 1 22 Difference in the Gibbs free energy change for the R and S transition states (at 293 K) as a function of product enantioselectivity for the reaction of a prochiral substrate for the R and S enantiomers. A subtle difference (less than 15 kJ/mol) in the energy for the R and S transition states makes a big difference in the enantioselectivity. .
 Reproduced from reference.[89]

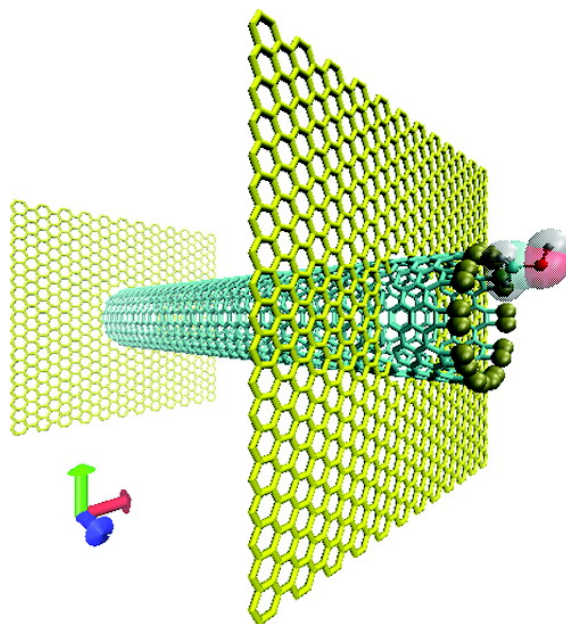


Figure 1 23 Simulation of water-methanol flux through Pt catalytic CNT membrane (Pt coated on CNT tip). . Reproduced from reference.[111]

Chapter 2 Near monolayer functionality produced by electrochemical diazonium grafting on carbon nanotubes

2.1 Introduction

Carbon nanotubes (CNTs) have unique mechanical, electronic and structure properties, however functional chemistry on CNTs is required for most applications. Generally, this functionalization is for enhanced solubility and dispersion in composites, but it also introduces functional activity for sensors and catalytic activity. Many functionalized CNT applications have been exploited, ranging from nano-composites, electronics, medicine, catalysis to membranes.[3,4,5,6,9,10,11,12] However, the conventional oxidation and addition chemistry is very aggressive, which completely cuts tubes or damages surface structure of CNTs, thereby deteriorating their unique properties. [13,45,102] Non-covalent functional chemistry on CNTs, generally using pi-pi stacking, does not significantly alter CNT properties, but the attachment is unstable and readily leaches.[41] Controlled covalent modification of CNTS without damage to CNTs is critical to advance the applications of CNTs and requires self-limiting chemistry that is strong enough to react with inert graphite.

Electrochemical grafting offers the benefits of control by current and time as well supplying up to about 1.5eV of energy for difficult reactions. The reduction of diazonium salt was first reported for the surface modification of glassy carbon in 1992.[18] It offers several advantages in surface functionalization.[17,19] First, the versatile functionality can be obtained from chemical group of the aryl ring of diazonium salts and are readily made from the activation of commercially available primary amines. Secondly, it can modify a wide variety of conductive substrates (carbon, metal, polymers, semiconductors etc). Third, the grafted molecular layer on substrate shows stronger stability due to its

covalent modification compared to thiol-Au surface modifications with weak reversible bonds.[24,25] The electrochemical grafting of diazonium on carbon nanotube was first reported by Tour's group in 2001[36] without damaging the graphitic structure of CNTs and their composites. However, the formation of multilayer polymer over the CNT was reported from electrochemical diazonium grafting.[27,29,31,34] Since electrical connectivity distances from electrode vary and there is no self-limiting mechanism, regions of CNTs will have faster deposition and polymerization. It is fundamentally important to develop controllable functional chemistry for applications of carbon nanotubes. The ideal grafting would be to have only a monolayer of coating on the CNT to maximize electron transfer from CNT to catalyst site. For instance, Pt layer can be deposited on diazonium modified CNTs for fuel cell applications, however a thick polymer would insulate the Pt layer, thereby reducing current density.[59] Carbon nanotube membranes also offer an exciting fast fluid platform which is 10,000 fold faster than pores of same diameter in conventional materials, due to atomically smooth graphite core surface.[70] Diazonium grafting was used to create sufficient density functional sites on the entrance of CNTs pores for covalently tethered dye molecules to act as a gatekeeper valve.[74] Though successful demonstrating voltage gating in larger diameter (7nm i.d.) MWCNTs, finer control of grafting thickness is critical for 1-2 nm SWCNTs where polymer growth would block pores and dramatically reduce flow rates.[113] The formation of electrochemically grafted polymers can be sterically hindered by bulky chemical groups during diazonium grafting.[114,115,116] However, this requires multiple additional steps to synthesize diazonium salt with bulky substituent and remove the protecting group after grafting, making modification more complicated. The idealized

case is to have a self-limiting monolayer of grafting at the CNT pore entrance that can act as an active biomimetic pump.[12]

In addition to preventing polymerization, it is also important to know the number of functionalized molecules at the entrances to CNTs to precisely design pump or filtering geometries. However, it has been a challenge to quantify diazonium grafting density. Highly variable results were obtained from different quantification methods.[26] Nitrophenyl diazonium grafting has been well studied and quantified using several methods, such as CV integration, XPS and Raman, however, the variable density ranged from 1.6 to 28×10^{-10} mol/cm². In addition, functional density varies among different starting diazonium salts. The diazonium grafting on gold surface has also been studied by electrochemical quartz crystal microbalance. After 20 min grafting, the different diazonium salts gave density ranging from 37 to 160×10^{-10} mole/cm².^[34] Furthermore, most reported quantification methods such as thickness measurement (AFM and ellipsometry) are only limited to flat surface and are difficult to extrapolate to CNTs.

In this paper, we report a near monolayer modification of CNTs using tetrafluorocarboxylphenyl diazonium grafting. It is hypothesized that polymerization is hindered by the inherently inert C-F bonds. The grafting density was quantified using an anion selective dye-assay. The accuracy of the dye-assay method was confirmed by X-ray photoelectron spectroscopy (XPS) of thiol-Au self-assembled monolayers (SAM) as a calibration reference.

2.2 Experimental methods

2.2.1 Reagents

Toluidine blue O(TBO), Sodium tetrafluoroborate(NaBF_4), tetrabutyl ammoniumtetrafluoroborate(NBu_4BF_4), 4-aminobenzoic acid, Pyrenebutyric acid, 12-Mercaptododecanoic acid (C-12) and 2,3,4,5,6-pentafluorothiophenol (PFBT) were purchased from Sigma (St. Louis, MO) without any purification. 4-amino-2, 3, 5, 6-tetrafluorobenzoic acid was received from Synquest (Alachua, FL). Glassy carbon (SPI-Glas™ 25 Grade) was purchase from SPI supply (West Chester, PA).

2.2.2 Synthesis of 4-carboxyphenyl diazonium tetrafluoroborate.

The synthesis was carried out from previously described method [18]. 2.74 g (0.02 mol) of 4-aminobenzoic acid was dissolved in 20 mL water at 50 °C. 0.044 mol of concentrated HCl was added dropwise to the solution, followed by cooling down the solution to -3 °C. 0.022 mol of NaNO_2 (Sigma) in 10 mL water was then slowly added to the mixture. The reaction was allowed for 1 h at -3 °C. The solution was filtered, and then 0.022 mol of NaBF_4 (Sigma) in 5 mL water was added to the filtrate at -3 °C. The light yellow precipitate was formed, which was then filtered and washed with ice water and cold ether. The product was dried in vacuum and preserved at -20°C. The yield of CP was 24%. The product was characterized by ^1H NMR (CDCl_3). There were two doublets at 8.87-8.83 and 8.46-8.42 ppm in the NMR spectra.

2.2.3 Synthesis of tetrafluorinated 4-carboxyphenyl diazonium tetrafluoroborate (TFCP).

0.6 g (2.87 mmol) of 4-amino-2, 3, 5, 6-tetrafluorobenzoic acid was dissolved in 2 mL water plus 2 mL 48% HBF_4 solution at 50 °C. The solution was cooled down to -3°C. 4.3 mmol of NaNO_2 in 8 mL water was then slowly added to the mixed solution. The reaction was sit for 1 h at -3 °C. The brown precipitate was formed, which was then filtered and

washed with ice water. The product was dried in vacuum and preserved at -20°C . The yield of tetrafluorinated carboxylphenyl diazonium salt was 17%.

2.2.4 Electrochemical reduction of diazonium salts on glassy Carbon.

Glassy carbon (SPI-GlassTM 25 Grade) was polished by 1, 0.5 and 0.02 μm Buehler alumina slurry solution, respectively. After polishing, the glassy carbon was rinsed with DI water and ultrasonicated for 5 mins in DI water. The cleaned glassy carbon was grafted by electrochemical reduction of 5 mM carboxylphenyl or TFCP diazonium in 0.1 M KCl and 0.1 M HCl aqueous solution as indicated time at potential -0.6V. The solution was deaerated by argon gas for at least 15 min. The experiment was carried out in the three-electrode cell using a potentiostat (e-Corder410) with glassy carbon as working electrode, Pt wire as counter electrode and Ag/AgCl as reference electrode. The e-Corder 410 was operated by eDAQ chart V 5.5.7 software. The grafted sample was rinsed carefully with deionized water and ethanol multiple times, and dried under nitrogen stream.

2.2.5 Electrochemical reduction of diazonium salts on Au substrate.

The Au substrate was prepared according to the literature.[24] Silica wafer was first immersed in boiling acetone bath for 5 min. Then it was rinsed by isopropanol and Milli-Q water and dried under nitrogen stream. 20 nm Cr was attached to the silica wafer as adhesion layer by thermal evaporation and then 100 nm thick gold layers were sputtered on it. The experiment was carried out in Cressington coating system 308R. The electrochemical reduction of Au substrate was similar to that of glassy carbon, except that the Au substrate was grafted with 5 mM carboxylphenyl or tetrafluorinated carboxylphenyl diazonium with 0.1M NBu_4BF_4 in anhydrous acetonitrile solution.

2.2.6 Preparation of self-assembly monolayer (SAM) on Au substrate.

In general, Au surface was pretreated by oxygen plasma (Harrick Plasma PDC-001 cleaner) at mid power for 10 min.[117] Au-S-(CH₂)₁₁-COOH: the cleaned Au layer was immersed in 1 mM 12-mercaptododecanoic acid anhydrous ethanol solution at room temperature for 20hrs under Argon protection. Au-S-C₆F₅: the cleaned Au substrate was refluxed in 1mM 2,3,4,5,6-pentafluorothiophenol anhydrous ethanol solution at 75°C for 2hrs under Argon protection. The SAM samples were rinsed carefully with deionized water and ethanol multiple times, and dried under nitrogen stream.

2.2.7 Electrochemical grafting of diazonium salts on carbon nanotube (CNT) buckypaper.

Carbon nanotube Buckypaper was prepared and grafted as shown in Figure 2.5. Basically, multiwall carbon nanotubes were grown by chemical vapor deposition method which ferrocene/xylene was used as precursors at 700 °C.[118] 10 mg multiwall CNTs was sonicated in 40 mL of ethanol at room temperature for 30 min, and then filtered by 1.0 μm Teflonunlaminated membrane (Sterlitech). The prepared CNT Buckpaper was rinsed carefully with deionized water and ethanol multiple times, dried under vacuum and then modified in 5mM diazonium salts in 0.1 M KCl and 0.1 M HCl aqueous solution at potential -0.6 Vwith indicated time.

2.2.8 Modification of CNT Buckypaper with pyrenebutyric acid.

10 mg multiwall CNTs was mixed with 1 mM pyrenebutyric acid in 30 mL dichlormethane solution. The mixture was sonicated at room temperature for 30 min and then filtered by 1.0 μm Teflon unlaminated membrane (Sterlitech). The modified CNT buckpaper was rinsed carefully with dichlormethane for multiple times and dried under vacuum.

2.2.9 Quantification of carboxyl density using Dye-Assay.

Toluidine Blue O was reported to quantify the carboxylate density on polyethylene film[119]. Glassy carbon or Au was incubated in 0.2 mM Toluidine blue O (TBO, Sigma) solution at pH=10 and room temperature for 1 hr to adsorb positively charged dye on anionic carboxylate. The glassy carbon or Au substrate was then rinsed and kept in 0.1 mM NaOH (pH=10) solution for 5 min to remove physically adsorbed TBO. The electrostatically adsorbed TBO was desorbed at pH=1 HCl solution, below the pKa of the carboxylate group. The concentration of desorbed TBO in acetic acid solution was determined by the absorbance at 632 nm using an Ocean Optics USB 4000 UV-Vis spectrometer. The calculation of carboxyl functional density was based on the assumption that positively charged TBO binds with anion carboxyl groups of CNT membrane at 1:1 ratio.

The quantification of carboxyl density on CNT buckpaper using Dye-Assay was slightly different from what for glassy carbon or Au since any dispersed CNTs are strongly absorbing in the UV-vis assay. 2 mg CNT was sonicated with 0.02 mM TBO solution at room temperature for 20 min. The solution was then centrifuged at 3500 rpm for 10 min. The precipitated CNT was resuspended in 0.1 M NaOH solution at pH=10 and then centrifuged twice. Finally, the precipitated CNT was sonicated with 14 mL of pH=1 HCl. The mixture was centrifuged and the supernatant was taken for UV-Vis measurement.

2.2.10 X-ray Photoelectron Spectroscopy (XPS).

The surface was characterized using Kratos XSAM-800 XPS spectrometer with a monochromatic Al K α X-ray source (1486.6eV). The signal was collected on 280W (20 mA \times 14 kV) at 45 $^\circ$ takeoff angle. The vacuum pressure in chamber is below 1×10^{-9} torr. Pscis software was used for data acquisition and analysis.

2.3 Results and discussions

The electrochemical reduction of diazonium salt on carbon surface is based on the mechanism of phenyl radical reaction (Figure 2.1a).[21,26,31,120] The radical produced by electrochemical reduction from diazonium can covalently attach to surface and form organic layer. However, the growth of organic layer would not stop at the initial layer since the reactive radical can continuously bind to the grafted layers. Generally, the reaction is self-limiting when a thick insulating layer is formed on the surface. However, if the film is not dense and has ionic functional groups, the electrochemical charge transfer reaction makes multilayer growth continue to over 10 nm.[34] In this report, we used an approach to limit polymerization with a relatively inert monomer with C-F bonds. Fluorinated and non-fluorinated diazonium salts, 4-carboxyl phenyl diazonium and tetrafluorinated carboxyl phenyl diazonium, were electrochemically reduced at -0.6V as a function of time. The available carboxylate sites in polymers were quantified by Dye-assay as illustrated in Figure 2.2. The positively charged dye-molecule Toluidine blue O is adsorbed on the negatively charged surface at pH=10. And those adsorbed dye molecules can be removed into 0.1 M HCl solution at pH=1. The concentration of the detached dye molecule was quantified at 632 nm by UV-Vis spectrometer. We studied the quantification of diazonium grafting on glassy carbon because it has a similar sp^2 structure to CNTs. The ideal monolayer density of carboxylphenyl (CP) was calculated as 3.8×10^{14} molecules/cm² according to the close packing model (based on molecular projection area and Van der Waals radius). Figure 2.3 shows that the carboxyl density was increased with grafting time. The carboxyl density of 4-carboxyl phenyl diazonium grafting first reached to 8.6×10^{14} molecules/cm² at 15 seconds, indicating about two organic layers may be formed. After 480 seconds, the carboxyl density of CP grafting increased up to

16×10^{14} molecules/cm², which indicates the formation of a thick film (> 4 molecular layers) with an open structure to access charged sites. These results were in good agreement with previous reports.[34] However, the grafting of tetrafluorinated carboxylphenyl showed slower deposition rates. It reached 5.6×10^{14} molecules/cm² at 15 seconds and 8.2×10^{14} molecules/cm² at 480 seconds, corresponding to 2.1 molecular layers. The reduced growth rate is likely due to the sites on aryl ring being fully occupied by four strong C-F bonds (490KJ/mole), as seen in Figure 2.1b. The use of tetrafluorinated carboxylphenyl diazonium grafting is more controllable allowing for monolayer deposition at CNT tips.

X-ray photoelectron spectroscopy was used to confirm the dye assay method. XPS has been used to quantify diazonium grafting functional density on glassy carbon[26]. However a high carbon background signal from the substrate makes the percentage of composition that includes sample and substrate carbon results inaccurate. Gold surface provides a carbon free background signal and the well-organized SAM with known density in the literature can be used as reference for quantification. 12-mercaptododecanoic acid and pentafluorobenzenethiol (PFBT) on Au was chose as reference, respectively. The density of alkanethiol SAM was calculated as 4.6×10^{14} molecules/cm², [121] while PFBT was quantified as 3.0×10^{14} molecules/cm² by scanning tunneling microscopy [122]. The diazonium grafting density is calculated by comparison to the integrated peak area of C_{1s}, at the same intensity and take-off angle conditions.

Thiolates on gold enable them to form a well-organized monolayer structure because of Van der waals force between thiolate molecules [121]. To further quantify the carboxyl density of carboxylphenyl and tetrafluorinated carboxylphenyl diazonium grafting on

gold surface, self-assembled monolayer (SAM) of thiolates was used as a reference for XPS quantification. Pentafluorobenzenethiol (PFBT) and 12-mercaptododecanoic acid (C-12) thiolate on gold were chosen as the standard references in our study. At 75 °C for 2 hours, the adsorption of (PFBT) molecules on gold leads to a long-range, well-ordered self-assembled monolayer detected by scanning tunneling microscopy (STM)[122]. Based on this work, the surface density of PFBT molecules was calculated as 3.0×10^{14} molecules/cm². The surface density of 12-mercaptododecanoic acid (C-12) thiolate on Au was calculated as 4.6×10^{14} molecules/cm² from the pattern of decane thiolate on Au. The survey scans of XPS spectra of standard C-12, PFBT SAMs, 4-carboxylphenyl and TFCP grafting samples were displayed in Figure 2.4(a-d). The C1s peak was appeared at 286ev, O1s at 532ev and F1s at 688ev. The intensity of C1s peak from the diazonium grafting samples and the standard SAMs was calculated by integration of peaks area. And the surface density of diazonium grafting on gold was quantified by comparison to the standard SAMs. The results are shown in Table 2.1. We chose C-12 and PFBT as reference to calculate the grafting density since their literature density is known. The C-12 density was calculated as 6.4×10^{14} molecules/cm² with the reference of PFBT, while the literature value is 4.6×10^{14} molecules/cm². The PFBT density was calculated as 3.8×10^{14} molecules/cm² with the reference of C-12, while the literature value is 3.0×10^{14} molecules/cm². The calculated density is close to the literature value, which supports the accuracy of quantification. By using C-12 film as reference for C1s peak area, the carboxylphenyl (CP) grafting density increases from 1.7×10^{14} to 4.7×10^{14} molecules/cm² after the grafting time was extended from 5 min to 8 min. The TFCP grafting density was 1.9×10^{14} molecules/cm² at 5 min, and increased up to 2.7×10^{14}

molecules/cm² at 8 min. After 8 min, the carboxyl density of CP is 1.7 fold to that of TFCP. The intensity of C1s peak from the diazonium grafting samples and the standard SAMs was integrated by areas of their XPS peaks. As shown in Table 2.1, using C12 thiolate as the XPS carbon reference, the surface density of TFCP grafting on gold was 1.9×10^{14} molecules/cm² at 5 min. After 8 minutes grafting, it raised up to 2.7×10^{14} molecules/cm². These values were lower than the monolayer reference SAM sample but are within 10% of PFBT (3.0×10^{14} molecules/cm²). The carboxyl density of carboxylphenyl diazonium grafting increases from 1.7×10^{14} to 4.7×10^{14} molecules/cm² after the grafting time was extended from 5 min to 8 min. The similar trend was found when PFBT was used as a reference. The results from XPS quantification were consistent with what was measured by dye-assay. Taken above data together, we demonstrated both tetrafluorinated carboxylphenyl and carboxylphenyl grafting form a near monolayer on gold surface. In both fluorinated and non-fluorinated cases, the deposition rates were lower on Au than carbon. Forming direct Au-C bonds is more difficult than C-graphite bond. The lower deposition rate of tetrafluorinated carboxylphenyl grafting indicates that the C-F bonds on aryl ring inhibit polymerization.

Carbon nanotube Bucky paper can be simply fabricated by filtration of dispersed CNT solutions. It provides mechanically flexible high surface area and corrosion free support for electrochemical electrodes, filters, scaffolds, cell culturing and composites[123]. Bucky paper can be simply functionalized using electrochemical grafting of diazonium, which produces less damage on carbon nanotube surface compared to the traditional acid oxidation methods. The modified carbon nanotube has been characterized by absorption and Raman spectra.[36] However, quantification of the functionality on carbon nanotubes

is a challenge. In this work, the dye-assay was used to quantify the carboxyl density on the carbon nanotube mat. Figure 2.5 shows the preparation steps and electrochemical modification on buckypaper where the dispersed carbon nanotubes were filtered onto PTFE membranes followed by electrochemical grafting with diazonium salt at -0.6V. Figure 2.6 shows the grafting density of carbon nanotube buckypaper on Teflon membrane using the dye-assay. The area of the CNTs was calculated by CNT weight collected times the specific surface area of 54m²/g as measured by Brunauer-Emmett-Teller (BET) test. The 4-carboxylphenyl diazonium grafting on carbon nanotube buckypaper was 0.9×10¹⁴ molecules/cm² after 10 min grafting. However, the carboxyl density of TFCEP grafting dropped to 0.3 ×10¹⁴ molecules/cm², nearly as 1/3 as that of 4-carboxylphenyl and 1/10 as the calculated monolayer density (3.8×10¹⁴ molecules/cm² as mentioned above). The significant drop in grafting efficiency was due to poor conductivity of overlapping CNTs in the lateral direction (~1cm length scale). A more conductive CNT film can be easily prepared by deposition of dispersed CNT solution on glassy carbon after ethanol evaporation[124,125,126]. By placing CNTs on a conductive substrate, the conduction path is reduced to sub-micron lengths (matte thickness instead of lateral contact under o-ring). As shown in Figure 2.7 and Table 2.2, both grafting density of carboxylphenyl and tetrafluorinated carboxyl phenyl was nearly enhanced by 4 fold and approaching monolayer efficiency.

To calibrate relative functionality, The CNT was modified with pyrenebutyric acid through π - π interaction, as seen in Figure 2.8. Pyrene molecules are the state-of-the-art surfactant for CNT dispersion due to strong π - π interaction, thus have the highest charged functional density on CNTs.[41] Theoretically, the monolayer coverage is

1.4×10^{14} molecules/cm² according to the area of each pyrene molecule, which is estimated as 72 \AA^2 by bond lengths and angles. In our experiment, the carboxyl density of pyrene acid modified carbon nanotube was quantified as 0.2×10^{14} molecules/cm² by dye-assay, which was 7 times less than that of theoretical packing. But this is sufficient for long lasting dispersion.[41] The density of the highly effective pyrene surfactant was slightly less than our TFCP grafting (0.3×10^{14} molecules/cm²) on carbon nanotubes indicating the utility of grafting method when good electrical contact is present. A significant merit of diazonium grafting is covalent bonding meaning that leaching is not an issue as it is for the pyrene system.

2.4 Conclusions

In this report, a dye-assay was successfully used to quantify the diazonium grafting density on glassy carbon, gold and carbon nanotube buckypaper and confirmed by XPS method. A near monolayer was developed by electrochemical grafting of tetrafluorinated carboxylphenyl diazonium on glassy carbon and gold. The polymer growth is limited by the inertness carbon-fluorine bond on aryl ring. CNT Buckypaper was successfully modified to near monolayer functional density by using tetrafluorinated carboxylphenyl diazonium grafting. Diazonium grafting efficiency on bucky paper was enhanced by shortening conduction path length when grafting on a conductive substrate. Tetrafluorinated carboxylphenyl diazonium grafting provides the most controllable functionalization chemistry allowing near monolayer levels of functionality on carbon nanotubes. This technique enables monolayer functionality at the tips of carbon nanotube membranes for biomimetic pumps and valves as well as thin conductive layers for CNT-based high area electrochemical support electrodes.

Table 2 1 Comparison of XPS and dye-assay quantification.

Sample	Modification	Surface density based on C peak of Au-S-(CH ₂) ₁₁ -COOH as reference (Sites/cm ²)	Surface density based on C peak of Au-S-C ₆ F ₅ as reference (Sites/cm ²)	Surface density measured by Dye-assay (Sites/cm ²)
Au-S-(CH ₂) ₁₁ -COOH	1mM thiol in ethanol for 20hrs	4.6×10 ¹⁴ *(literature value)	6.4×10 ¹⁴	N/A
Au-S-C ₆ F ₅	1mM thiol in ethanol for 2hrs at 75C	3.8×10 ¹⁴	3.0×10 ¹⁴ *(literature value)	N/A
Au-C ₆ H ₄ -COOH	5mM diazonium /0.1M NBu ₄ BF ₄ in CH ₃ CN-0.6V for 5mins	1.7±0.1 ×10 ¹⁴	1.4±0.1 ×10 ¹⁴	2.1×10 ¹⁴
Au-C ₆ H ₄ -COOH	5mM diazonium /0.1M NBu ₄ BF ₄ in CH ₃ CN-0.6V for 8 mins	4.7±0.4×10 ¹⁴	3.8±0.3 ×10 ¹⁴	3.8×10 ¹⁴
Au-C ₆ F ₄ -COOH	5mM diazonium /0.1M NBu ₄ BF ₄ in CH ₃ CN-0.6V for 5mins	1.9±0.4 ×10 ¹⁴	1.6±0.3 ×10 ¹⁴	1.9×10 ¹⁴
Au-C ₆ F ₄ -COOH	5mM diazonium /0.1M NBu ₄ BF ₄ in CH ₃ CN-0.6V for 8 mins	2.7±0.7 ×10 ¹⁴	2.2±0.6 ×10 ¹⁴	2.9×10 ¹⁴

Table 2 2 Enhanced grafting efficiency of CNT buckypaper on glassy carbon

CNT diazonium grafting	CNT on teflon membrane (Molecules/cm ²)	CNT on glassy carbon (Molecules/cm ²)
2min carboxyl phenyl grafting	0.3×10^{14}	3.4×10^{14}
10min carboxyl phenyl grafting	0.9×10^{14}	3.3×10^{14}
2min tetrafluorinated carboxyl phenyl grafting	0.3×10^{14}	1.0×10^{14}
10min tetrafluorinated carboxyl phenyl grafting	0.3×10^{14}	1.1×10^{14}

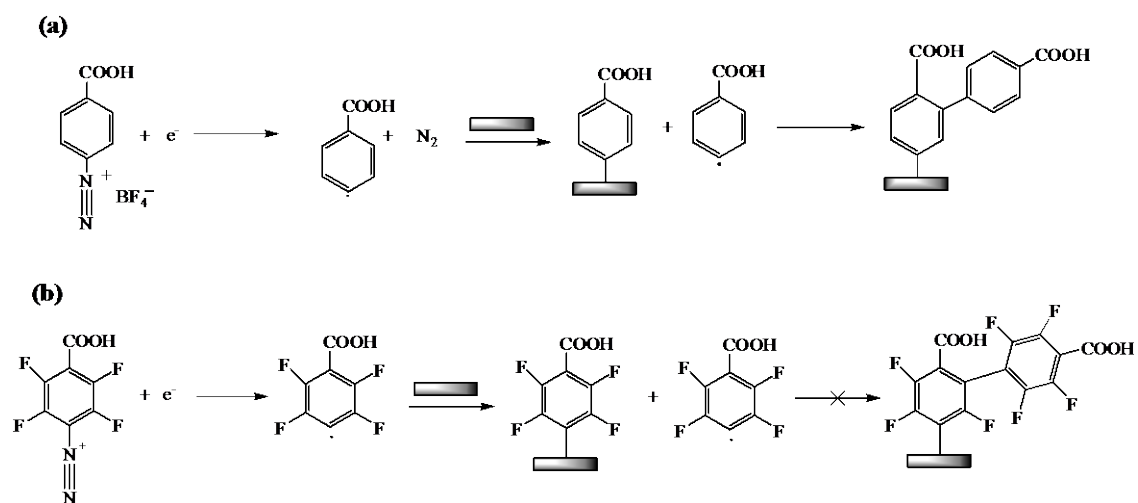


Figure 2 1 (a) The mechanism of multilayer formation by electrochemical reduction of 4-carboxylphenyl diazonium grafting. (b) Hindrance of multilayer growth by C-F bond on aryl ring.

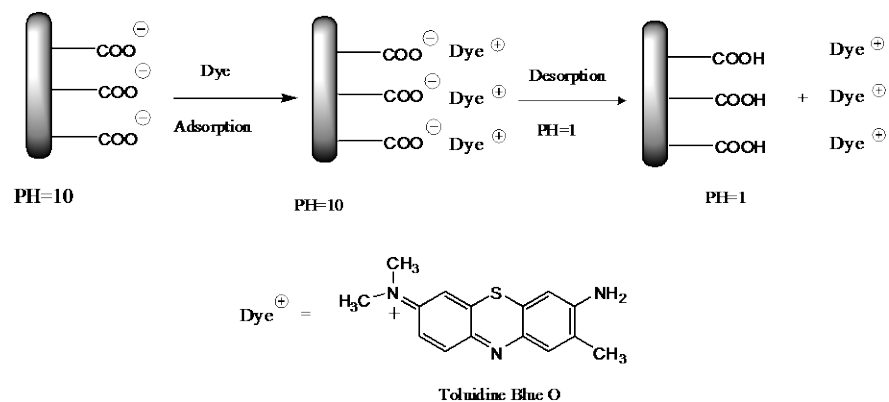


Figure 2 2 Schematic illustration of quantification of carboxylic density on surface of glassy carbon by pH dependent adsorption/desorption of charged dye molecule.

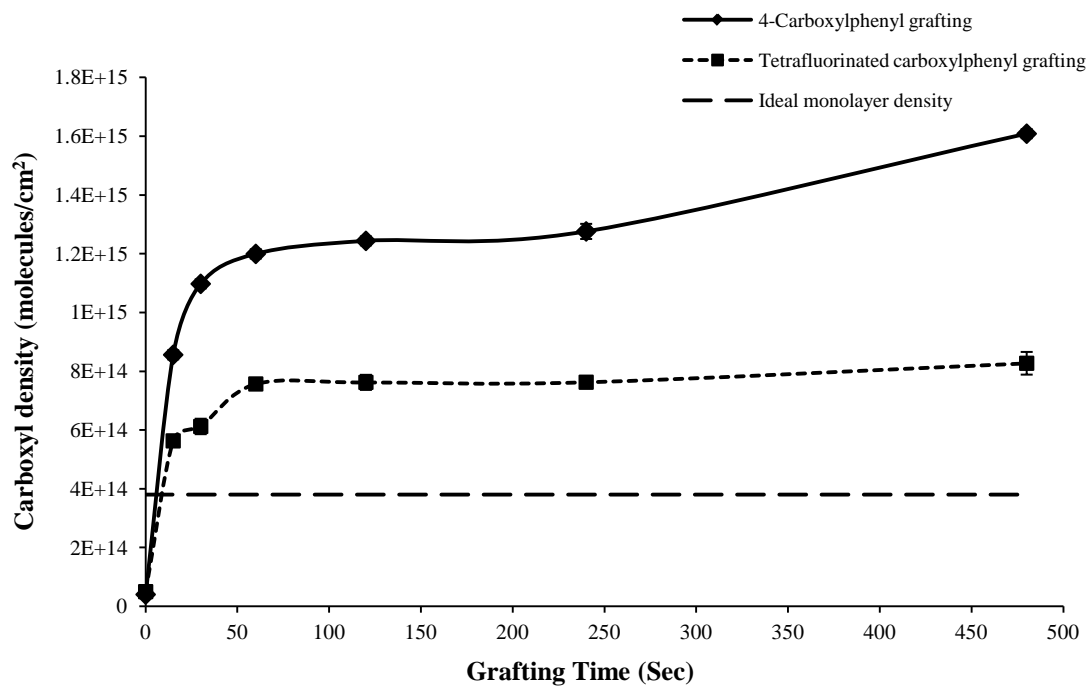


Figure 2 3 4-carboxyl phenyl diazonium and tetrafluorinated 4-carboxyl phenyl diazonium grafting density on glassy carbon as measured by TBO dye assay.

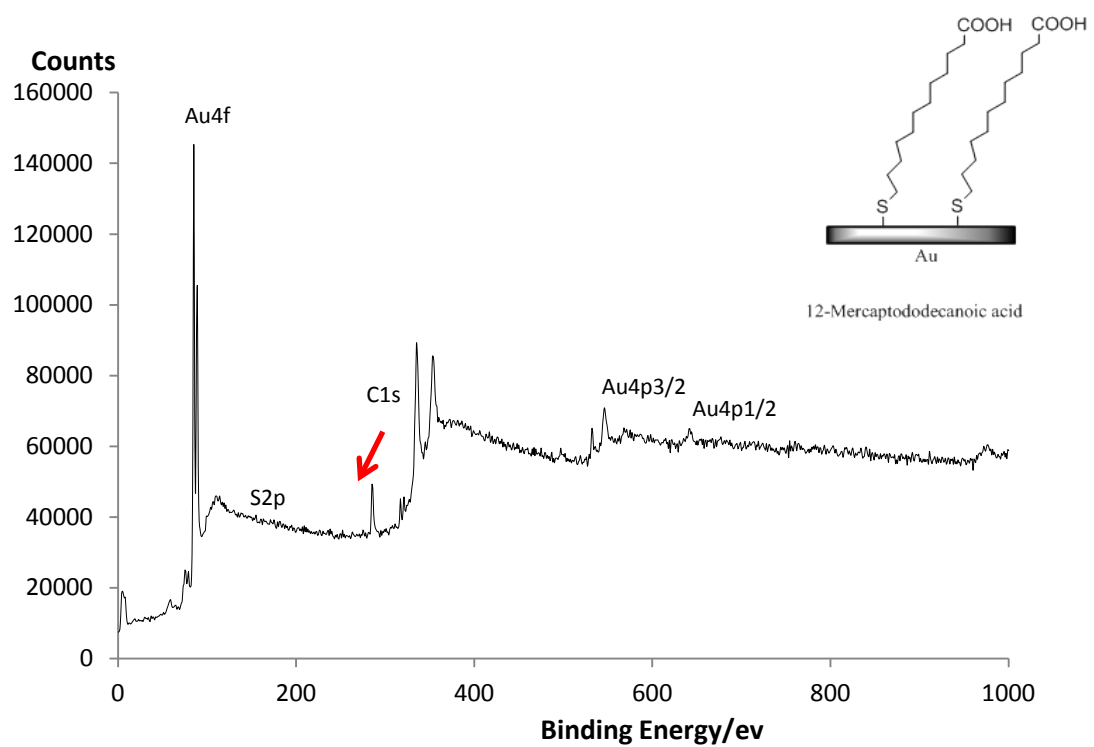


Figure 2 4 XPS spectra of Self-Assembled Monolayers (SAMs) and diazonium modified Au surface (a) XPS survey scan for 12-mercaptopropionic acid SAM on Au

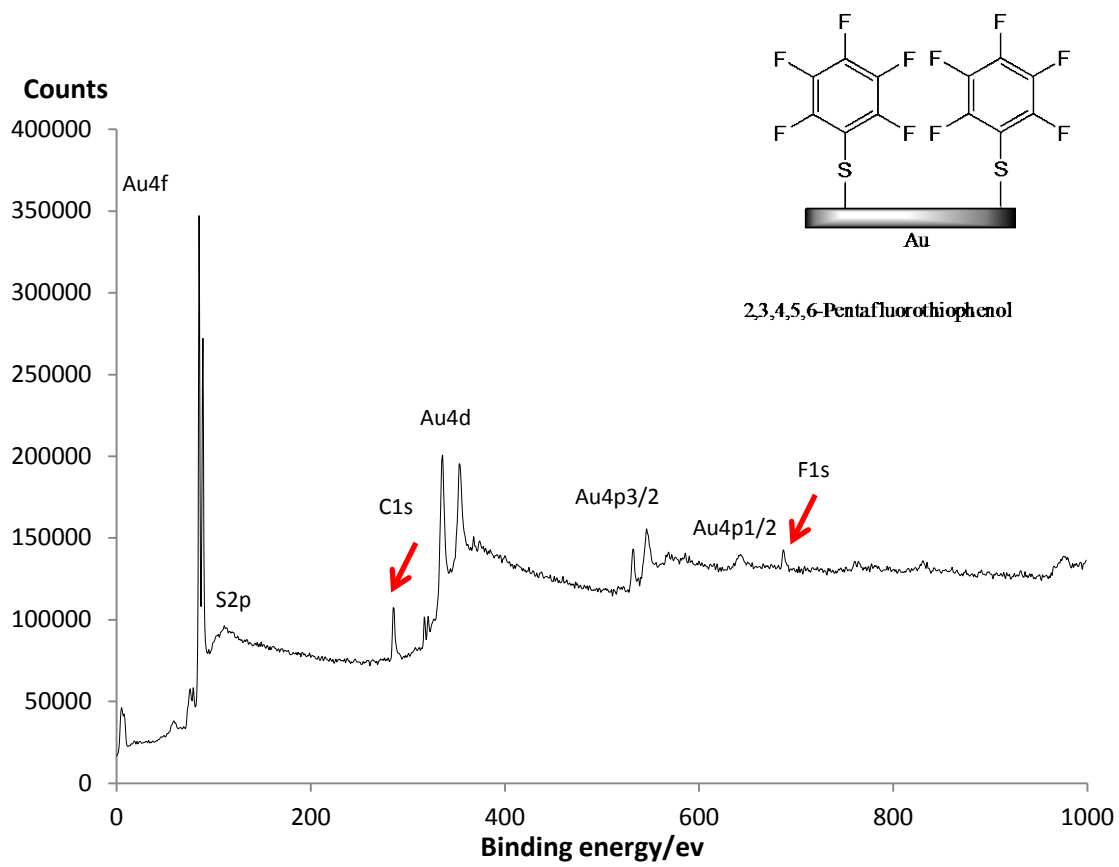


Figure 2.4 (b) XPS survey scan for 2,3,4,5,6-pentafluorothiophenol SAMs on Au

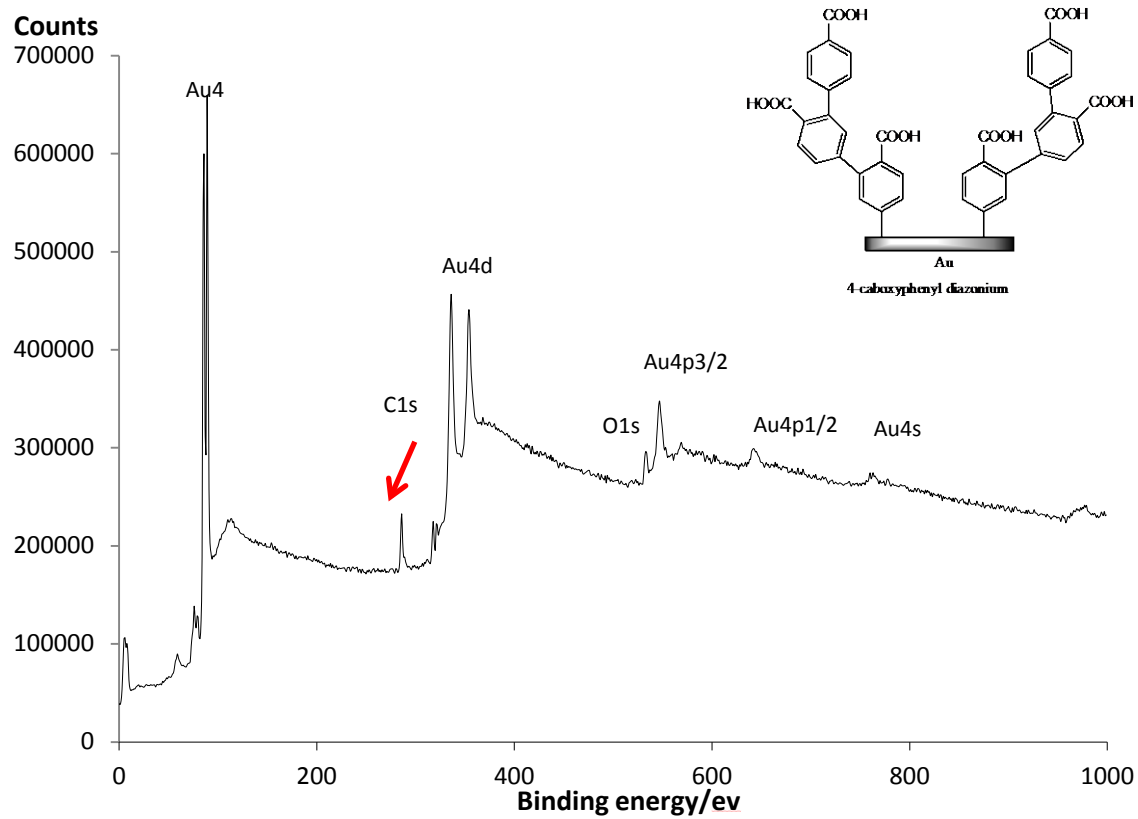


Figure 2.4 (c) XPS survey scan for 4-carboxyphenyl diazonium grafted on Au

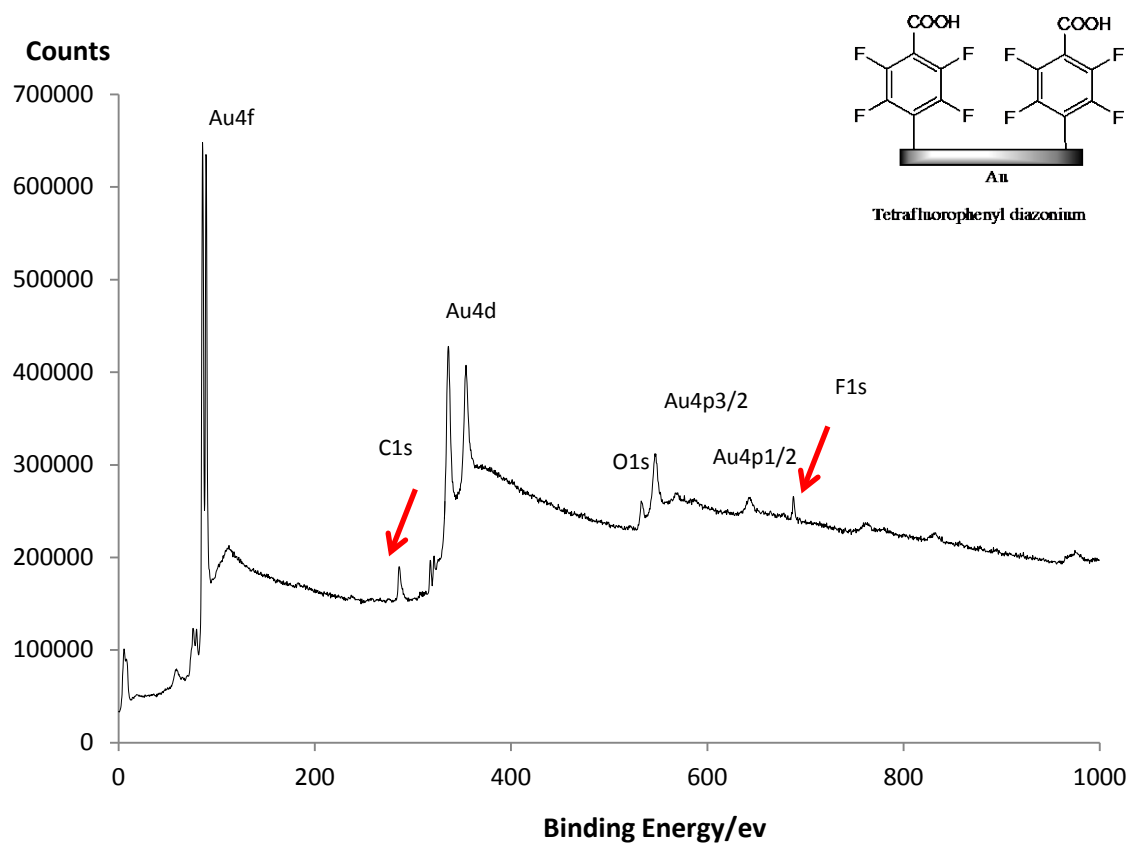


Figure 2.4 (d) XPS survey scan on tetrafluorinated 4-carboxyl phenyl on Au

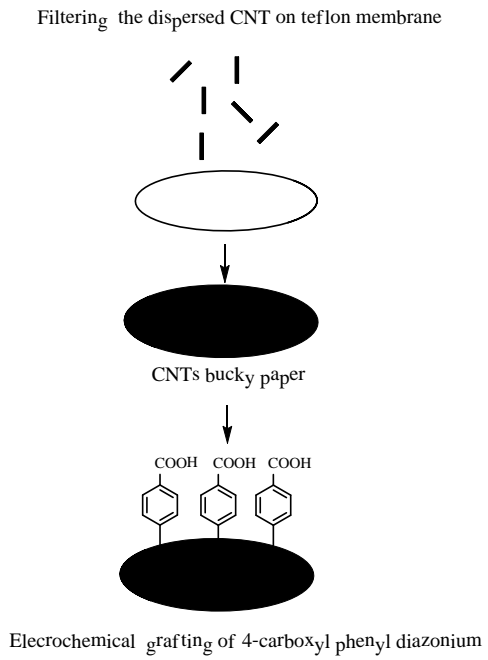


Figure 2 5 Schematic of fabrication and grafting of CNT buckypaper on Teflon membrane.

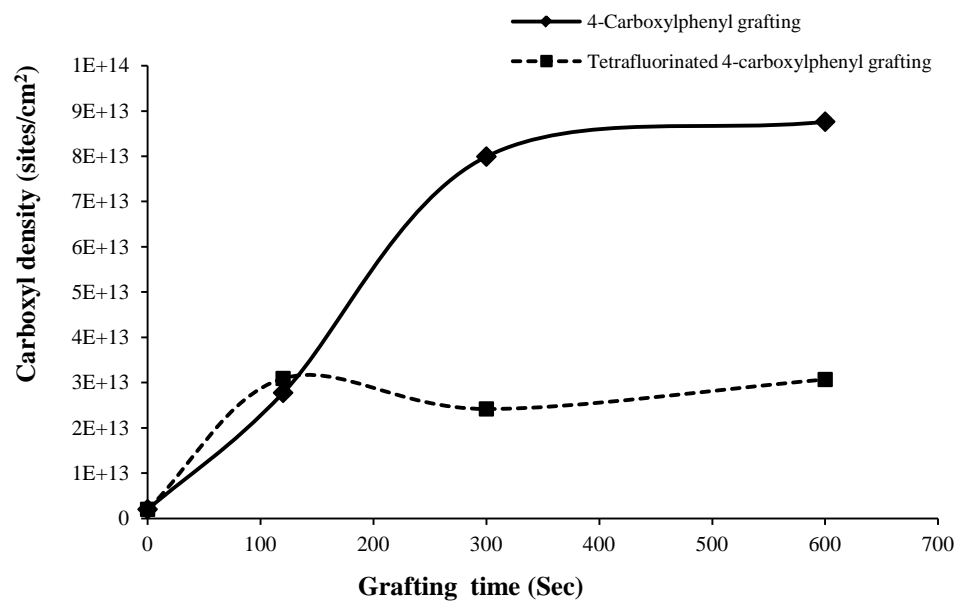


Figure 2 6 Grafting time vs carboxyl density on CNT buckypaper on Teflon membrane.
As measured by dye-assay method.

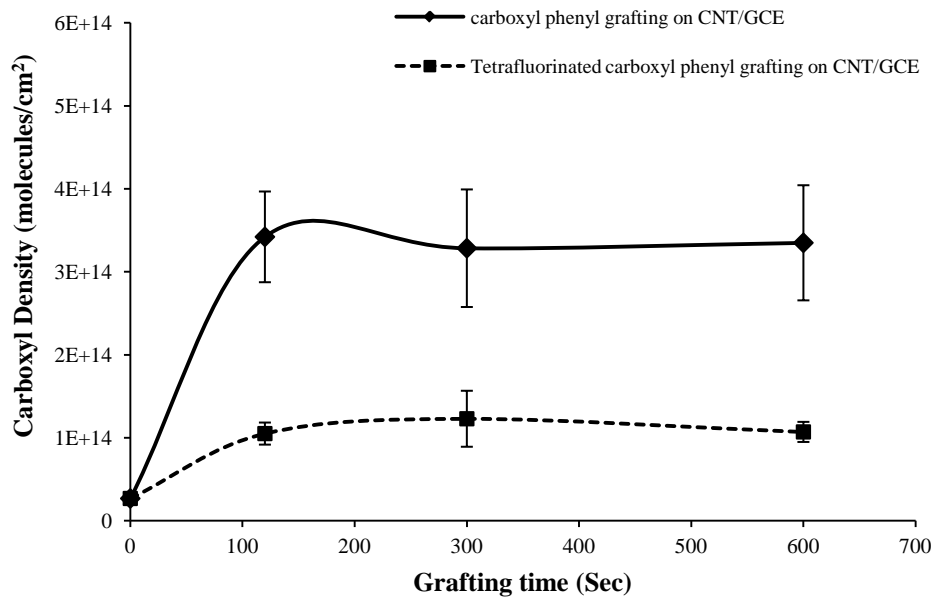


Figure 2 7 Enhanced grafting efficiency of CNT buckypaper on glassy carbon. 4-carboxyl phenyl diazonium and tetrafluorinated 4-carboxyl phenyl diazonium grafting of CNT buckypaper on glassy carbon (GCE) as substrate.

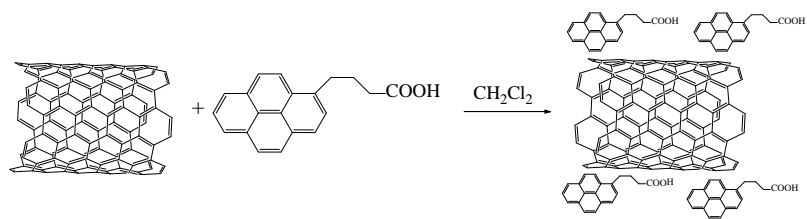


Figure 2 8 Schematic of making non-covalent functionalized CNT with pyrenebutyric acid .

Chapter 3 Single-step electrochemical functionalization of double-walled carbon nanotube (DWCNT) membranes and the demonstration of ionic rectification

3.1 Introduction

Protein channels embedded in cell membrane function as natural regulators of biological systems. Conformational change of proteins actuated by voltage can open or close the gate of channel, which regulates ions permeation with high selectivity.[61,63,127,128] This inspires researchers develop artificial nanopores and nanochannels in response to external signals (voltage, pH, temperature, light and etc) by mimicking natural ion channels.[64,129]. Transmembrane voltage is an preferred stimulus to open or close the gate of nanodevice since it is not aggressive, tunable and its input can be pulsed with digital control. [129] These devices can modulate the ionic flux and rectify the ionic transport current through the nanochannel/pore enabling applications in single molecule sensing and separation. [130,131,132,133] Carbon nanotube (CNT) membranes offer a fast fluid platform with velocity within pores is 10,000 times faster than conventional membrane of similar pore size due to atomically smooth graphite core.[70,113] Moreover, the CNT membranes have far more mechanical strength than lipid bilayer films, thus provide an exciting opportunity for chemical separation, drug delivery and other applications.[12,73] Carbon nanotube membranes can imitate ions channels with the functionalized molecules at CNT tips acting as protein-mimetic gatekeepers. Chemical functionalization of molecules (biotin[67], phosphorylation,[134] and charged dye[69]) at entrance of CNT core enables the demonstration of the modulation of ionic transportation. Further study showed that the steric hindrance of gatekeepers at pore entrance can be controlled with voltage.[74] Negative bias repels the anionic tethered molecules away from CNT entrance opening the channel while positive bias pulls the

anionic tethered molecules into the pore thus closing the channel. The voltage-gated carbon nanotube membranes have been successfully applied in drug delivery for nicotine addiction treatment.[77] Neutral molecules and solvent have also been pumped through CNT membranes via a highly efficient electroosmotic flow that is 100 fold more power efficient compared to conventional materials such as anodized Aluminum oxide (AAO) membranes.[78]

To improve gate keeper activity on CNT membranes, there needs to be a high functional density only at the pore entrances of CNTs.[113,135] This has been largely achieved with two step processes, which diazonium grafting first creates carboxyl groups at CNT tips followed by carbodiimide coupling chemistry. [69,112] Diazonium grafting generates highly reactive radicals that covalently react with the electrode or subsequent organic layer on surface under mild solvent and temperature conditions.[17,19] However, it is difficult to control the amount of carboxylate groups on CNT tip due to polymerization during diazonium grafting.[17,136] In principle, the grafting reaction is self-limiting when the formed insulating polymer layer stops the electrochemical reduction of diazonium salt. However with ionic functional groups (such as carboxylates), the reaction is not self-limiting and block carbon nanotubes. Another complication of the diazonium approach is that it generally requires a two-step functionalization since the diazonium formation reaction is not compatible with many functional groups that would be required on the gatekeeper. This adds complication and reduces overall yield. The electrochemical oxidation of amine to coat carbon fiber surface predates diazonium grafting with first report in 1990.[137] It enables immobilization of various primary amine containing molecules on different electrodes

surface.[138,139,140,141,142] The electrografted layer is characterized by AFM, XPS, ellipsometry, Time-of-Flight Secondary Ion Mass Spectrometry (ToF-SIMS) and electrochemistry methods.[143,144,145] Amine electrochemical oxidation greatly simplifies the surface modification process since it does not need complicated synthesis and surface chemistry. Even large molecules including dendrimers and metal-ligand complex can be directly functionalized on conductive surface in single step.[146,147,148,149] Electrografting of amine offers simple and efficient functional chemistry for CNT applications. Electrografting of amine provides binding sites on CNTs for coating of Pt-Ru and Ag nanoparticles that exhibit excellent electrocatalytic activity.[150,151] The more controllable electrochemical grafting of fluorinated aminobenzoic acid layer enables Pt monolayer deposition on CNT buckypaper. The highest record of mass activity has been achieved as 2711 A g^{-1} in methanol oxidation.[37]

The primary hypothesis of this paper is that the efficiency of voltage gatekeeping can be enhanced to obtain high on/off ratio using electrooxidation of amine in one step. The conformation change of tethered dye molecules under bias is proven by changes in non-faradic electrochemical impedance measurements (EIS). The EIS spectra also qualitatively show the effectiveness of this single step functionalization on double-walled carbon nanotube (DWCNT) membranes. Transmembrane ionic rectification was measured to compare the efficiency of gatekeeping. The stronger rectification indicated higher efficient gatekeeping. The gatekeeper density was quantified by dye assay on glassy carbon due to its similar structure with CNTs. Single step modification may give higher overall functional density over a more complicated two step modification.

3.2 Experimental methods

3.2.1 Fabrication of double-walled carbon nanotube membranes

Double-walled CNTs with average inner diameter of 2 nm and length of 30 μm were purchased from Sigma-Aldrich (TEM image as seen in Figure 3.1a). DWCNT membranes were fabricated using microtome-cutting method similar to the previous reports.[77,78,79] To describe it briefly, 5 wt% CNTs were mixed with Epoxy 862 epoxy resin (Miller Stephenson Chem. Co.), hardener methylhexahydrophthalic anhydride (MHHPA, Broadview Tech. Inc.) and 0.1 g surfactant Triton-X 100 (Sigma) using a Thinky™ centrifugal shear mixer. As-prepared CNTs-epoxy composite was cured at 85 °C according to the commercial epoxy procedure before being cut into CNT membranes using a microtome equipped with a glass blade. The typical thickness of as-cut CNT membrane is 5 microns (3. 1b). The membranes ($\sim 0.6 \times 0.6 \text{ cm}^2$) were glued over a 3 mm diameter hole in polycarbonate plate (1 mm thick) to act as a mechanical support. The top of the membrane was referring to the surface in the recess of the hole in the polycarbonate support while the bottom of the membrane was on the bottom plane of polycarbonate support. Pd/Au (30 nm) was sputter deposited on the bottom of membrane to give electrical contact to CNT membrane and act as effective working electrode.

3.2.2 Modification of DWCNT membranes

To avoid grafting in the inner core of CNTs, CNT membranes were placed in U-tube fittings under a 2 cm column pressure of DI water on the bottom of the membrane to have inert flow through the CNT core.[74] In two step functionalization, as-prepared double-walled carbon nanotube (DWCNT) membranes were first modified by flow electrochemical grafting (FG) with 5 mM 4-carboxy phenyl diazonium tetrafluoroborate/0.1 M KCl solution at -0.6 V for 2 minutes. In the next step, Direct Blue

71 dye (Aldrich) was coupled to the carboxyl group on the tip of CNTs with carbodiimide chemistry: 10 mg of ethyl-(N', N'-dimethylamino) propylcarbodiimide hydrochloride (EDC) and 5 mg N-hydroxysulfosuccinimide (Sulfo-NHS) were dissolved into 4 ml of 50 mM Direct Blue 71 dye in 0.1 (M) 2-(N-morpholino) ethane sulfonic acid (MES) buffer for 12 hrs at ambient temperature.

In one step functionalization, Direct Blue 71 dye, that has a primary amine, was directly grafted to CNT by electro-oxidation of amine. Before electrografting, the ethanol solution of 0.1 M LiClO₄/1 mM direct blue was purged by Argon gas for 15 min to remove adsorbed oxygen in the solution. Applying a 2 cm column pressure of DI water on the bottom of the membrane is to have inert flow through the CNT core. The electrografting was carried out under constant potential 1.0 V using potentiostat (E-corder 410) in the three electrode cell. The CNT membrane, with sputtered Pd/Au film (~30nm thick) on the membrane's back side, was used as the working electrode; Pt wire was the counter electrode and the reference electrode was Ag/AgCl. Before electrografting, the ethanol solution of 0.1 M LiClO₄/1 mM direct blue was purged by Argon gas for 15 min to remove adsorbed oxygen in the solution.

3.2.3 Rectification experimental setup

The schematic of the ionic rectification setup was shown in 3. 4b. Both U-tube sides were filled with potassium ferricyanide solution. Working electrode (W.E) was DWCNT membrane coated with 30 nm thick Pd/Au film; reference Electrode (R.E) was Ag/AgCl electrode. Voltage was controlled using an E-Corder 410 Potentiostat. Counter electrode was a sintered Ag/AgCl electrode purchased from IVM Company. The membrane area was ~0.07 cm². Linear scan was from - 0.60 V to + 0.60 V with the scan rate at 50 mV/s.

3.2.4 Dye assay quantification of carboxyl and sulfonate density on glassy carbon

Glassy carbon (SPI-Glass™ 25 Grade) was polished by 1, 0.5 and 0.02 μm Buehler alumina slurry solution, respectively. After polishing, the glassy carbon was rinsed with DI water and ultrasonicated for 5 mins in DI water. The cleaned glassy carbon was modified under same condition as modification of DWCNT membranes. The grafted sample was rinsed carefully with deionized water and ethanol multiple times, and dried under nitrogen stream.

Toluidine Blue O was reported to quantify the carboxyl group density on polymer film. Our dye-assay method was similar to the previous reports.[119,152] Glassy carbon was incubated in 0.2 mM Toluidine blue O (TBO, Sigma) solution at pH=10 and room temperature for 1 hr to adsorb positively charged dye onto the anionic carboxylate or sulfonate group. The glassy carbon was then rinsed with NaOH (pH=10) solution and further incubated in 0.1 mM NaOH (pH=10) solution for 5 min to remove physisorbed TBO dye. The adsorbed TBO on anionic glassy carbon was removed into pH=1 HCl solution. The concentration of desorbed TBO in HCl solution was determined by the absorbance at 632 nm using Ocean Optics USB 4000 UV-Vis spectrometer. The calculation of carboxyl or sulfonate density was based on the assumption that positively charged TBO binds with carboxylate or sulfonate groups at 1:1 ratio on glassy carbon.

3.3 Results and discussions

The fabrication of DWCNT membranes using microtome-cutting method was described in the experimental section. TEM image of DWCNTs and (b) SEM image of as-made DWCNT membrane in the cross-sectional view were shown in Figure 3.1a and 3.1b, respectively. Figure 3.1c shows the schematic structure of functionalized DWCNT membranes with tethered anionic dye. Carbon nanotube membranes can imitate ions

channels with the functionalized molecules acting as mimetic gatekeepers. In our previous studies, functionalization of gatekeeper includes two-step modification, [74,75] as shown in Figure 3.2. CNT membranes were first modified by 4-carboxylphenyl diazonium grafting, and then the negative charged dye molecules were linked with carboxyl sites using carbodiimide coupling chemistry. However, it is difficult to control the gatekeeper density since the oligomer is formed by diazonium grafting and the second coupling reaction may not have high yields. The functionalization chemistry at the CNT tip determines the applications for CNT membranes, with the ideal gatekeeper being a monolayer grafted at the entrance of CNT cores that can actively pump chemicals through the pores.[12] The mechanism of electrooxidation of amine includes radical generation and bonding formation on surface (Figure 3.3a). The electrooxidation of amine first generates amino radical cation. After deprotonation, the neutral aminyl radical can be covalently attached to surface but the yield is typically less than that of diazonium grafting.[153,154,155,156] By using electrooxidation of amine group of dye (as shown in Figure 3.3b), the charged dye molecules were simply covalently grafted in one-step functionalization.

Non-faradic electrochemical impedance measurements (EIS) were carried out to prove the effectiveness of the one-step electrochemical reaction on DWCNT membranes and demonstrate the conformation changes of tethered dye molecules.[79] The Nyquist plots of EIS were shown in Figure 3.5a and 3.5b, with the frequency ranging from 100 kHz to 0.2 Hz. Platinum wire, Ag/AgCl and DWCNT-dye membranes were used as counter, reference and working electrodes, respectively (Figure 3.5c). By switching bias from 0 V to + 0.6 V, charge transfer resistance was increased (R_{ct}) by 2.3 times in 20 mM KCl

(Figure 3.5a). It indicated that positive bias can draw the negative charged dye to CNT entrance, resulting in blocking the CNT tube, reducing ionic current and increasing R_{ct} . By applying negative applied bias, R_{ct} was reduced by 2 times since the dye molecules can be repelled away from the tip. Under higher concentration at 100 mM KCl, R_{ct} was increased by only 1.2 times switching bias from 0 V to + 0.6 V and a factor of 1.7 times switching bias from 0 V to -0.6 V (Figure 3.5b). The slower R_{ct} changing rate was due to ionic screening effect. The results of Non-faradic EIS indicated that the gatekeeper can be actuated to mimic protein channel under bias.

In order to compare the gatekeeping efficiency of two different functional chemistry, transmembrane ionic rectification was measured on DWCNT-dye membranes. Figure 3.4a illustrates the schematic mechanism of ionic rectification on DWCNT-dye membrane. With negative applied bias across the membrane, the dye molecules are repelled away from CNT entrance resulting in an open state and potassium ions can go through CNT channel giving easily measured current. However, at positive bias, anionic gatekeepers will be dragged into the pore entrance, thus blocking or reducing ionic current. The rectification experiment setup was diagrammed in Figure 3.4b. The DWCNT membrane coated with a layer of 30 nm thick Au/Pd film (working electrode) was placed in U-tube filled with potassium ferricyanide. Ag/AgCl electrode was used as reference/counter electrode. Constant potential was provided using a Princeton Scientific Model 263A Potentiostat. Linear scan was ranged from - 0.60 V to + 0.60 V with scan rate as 50 mV/s. The rectification factor was calculated by the ratio of ionic transport current at negative and positive 0.6 V bias.

The ionic current of potassium ferricyanide vs. trans-membrane bias for as-made and modified DWCNT membranes were shown in Figure 3.6, with a summary of rectification factors in Table 3.1. The highest experimental rectification factor of ferricyanide observed was 14.4 for the single-step grafting, which was 3.7 times as that of as-made membrane. The rectification factor dropped with the increasing ionic concentration, which was expected for the screening of charge on the gatekeepers at high ionic strength. The rectification factor dropped from 14.4 to 9.8 when the ferricyanide concentration increased from 10 mM to 50 mM. With the concentration increasing up to 100 mM, the rectification factor further dropped to 8.0. The rectification can be attributed to both charge and steric effect at low concentration while the ionic screening effects dominate under high concentration.

On another modified membrane with one-step amine grafting, we compared the rectification factor of three different ions, ferricyanide, 2, 6 naphthalene di-sulfonic acid (NDS) and sodium benzenesulfonate (SBS) to examine the role of anion size in being repelled by the modification of CNT tips. In Table 3.2, we saw that as the ion size was reduced, smaller rectification factors were seen, which was consistent with partially blocked ion channels. Due to the broad size distribution of double-walled CNT diameter, different membranes have variance in initial rectification factors and comparisons should be made within the same series. Also, due to the relatively large size of DWCNTs (~2.0 nm i.d.) compared to SWCNTs (1.4 nm), rectification of small ion pairs (i.e. KCl) was not seen as was for the SWCNT case.[110] However, larger mobile anions such as ferricyanide, NDS, and benzenesulfonate showed rectification (Table 3.2). Similar to Table 3.1, as ionic strength was increased, R_f was decreased for all of the anions. It

indicated that the rectification was partially attributed from charge effect. As a control experiment, the single-step grafted dye on DWCNT membranes used in Table 3.2 was removed by plasma oxidation. As seen in Table 3.3, the rectification factor was dropped to 2-3, close to the expected as-made membranes. The disappearance of rectification effect provided supportive evidence that functional anionic charged dye played as gatekeeper to modulate the ionic flux through DWCNT membranes.

Ferricyanide has a well-known redox potential of 0.17V (vs. Ag/AgCl), and thus an important control experiment was to make sure the observed rectification was not due to faradic current instead of trans-membrane ionic current. Cyclic voltammetry scans (-0.6 V to 0.6 V) showed no redox reaction on both as-made and one-step functionalized DWCNT membrane in 50 mM ferricyanide (Figure 3.7). We also didn't observe redox occurred on glassy carbon in 2 mM ferricyanide, as seen flat curve in Figure 3.8a. The much larger conductive area of glassy carbon electrode compared to 5% DWCNT membrane, requires the use of more dilute (2 mM) ferricyanide solution. However, with the supporting 0.5 M electrolyte KCl solution, oxidation and reduction peak were observed at 0.29 V and 0.06 V, which was similar to expected redox behaviors.[141,157] The experiment was also repeated with both oxidized and reduced species. In Figure 3.8b, no redox peak was found on glassy carbon in 50 mM ferricyanide solution and 25 mM ferricyanide/ferricyanide solution. The control experiments of cyclic voltammetry on DWCNT membrane and glassy carbon ruled out the redox reaction of ferricyanide, which supports the ionic rectification on electrochemically grafted CNT membranes.

The non-faradic EIS spectra indicated that the functionalized gatekeeper by single-step can be actuated to mimic protein channel under bias. This functional chemistry was

proved to be highly effective on enhancement of ion rectification. The disappearance of rectification also supported its effectiveness after removing the grafted gatekeeper by plasma etching. Interestingly no apparent change of rectification was seen for the two step functionalization. The likely reason is that high efficient functional density can be obtained by electrografting of amine in one step since the poor yield in the second step (carbodiimide coupling reaction) resulted in significantly lower gatekeeper density on CNT membranes. To address this question, two-step and one-step of functionalization were quantified on glassy carbon due to its well defined area and similar chemical reactivity to CNTs with dye-assay.[119] The schematic mechanism of dye-assay's absorption and desorption was shown in Figure 3.9. The sulfonate density as a function of one step amine grafting time was shown in Figure 3.10. The sulfonate density reached its saturated level as 0.9×10^{15} molecules/cm² after 2 min grafting. Since each Direct Blue 71 dye molecule contains four sulfonate groups, the dye molecule density was calculated as 2×10^{14} molecules/cm², nearly as one half of the ideal monolayer density as 3.8×10^{14} molecules/cm². The amine grafting density was less efficient than diazonium grafting, which is consistent with the prior report.[156] Comparison of total surface charge density by the two grafting methods was shown in Table 3.4. In first step of two step functionalization, the carboxyl density reached up to 1.3×10^{15} molecules/cm² after 8 mins grafting showing an efficient process. After carbodiimide coupling of dye in the second step, the charged density increased to 2.0×10^{15} molecules/cm². With each carboxyl site will be replaced by one dye molecule containing four sulfonate groups after coupling, each reacted site will have a net gain of three more charges. Going from 1.3 to 2.0×10^{15} charges/cm², with 3 charges/added dye resulted in a sulfonate density of 0.93×10^{15}

charges/cm² after the two step functionalization. The dye density was calculated as 0.23×10^{15} molecules/cm² (1/4 of sulfonate density). This resulted in a carbodiimide coupling efficiency of 18% on glassy carbon. The net sulfonate density for 1 step reaction and 2 step reaction are both comparable at 0.9×10^{15} charges/cm², where the less efficient electrochemical oxidation of amine is similar to the loss in efficiency for the carbodiimide coupling reaction. However, in the case of the DWCNT membranes, the two-step modification was not effective at showing rectification (Table 3.1). The possible reason for poor rectification is that the actual yield of the second reaction in the two-step modification on CNT membranes may be significantly below 18% yield seen on glassy carbon. The CNT surfaces can interfere in the coupling reaction, presumably through absorption of intermediates.

3.4 Conclusions

DWCNT membranes were successfully functionalized with dye for ionic rectification by electrooxidation of amine in single step demonstrating ionic channel rectification. Non-faradic EIS spectra showed changes in R_{ct} indicating that the functionalized gatekeeper was actuated to mimic protein channel under bias. This functional chemistry showed ionic current rectification up to 14.4 for $K_3Fe(CN)_6$. With decreasing ion size, we observed smaller rectification due to reduced blocking of ion channels by the grafted ligands. The rectification was decreased with the higher ionic concentration that increased ionic screening. Thus ionic current rectification is attributed to both charge and steric effects at low concentration, while steric effects are dominant at high concentration. Plasma oxidation removal of the gatekeeper from membrane removed the ionic rectification properties further supporting the role of functional gatekeeper chemistry. The saturated functionalized dye density by single step functionalization was quantified

as 2.3×10^{14} molecules/cm² on glassy carbon by dye-assay. This is similar to that of the two step functionalization, which had a low yield (~18%) for the second step of the reaction. One step functionalization by electrooxidation of amine provides simple and promising functionalization chemistry for the application of CNT membranes.

Table 3 1 Comparison of ionic current rectification factor (Rf) in K₃Fe(CN)₆ solution. Rectification factor was calculated by the ratio of ionic transport current at negative and positive 0.6 V bias. Linear scan was from - 0.60 V to + 0.60 V with the scan rate at 50 mV/s.

Concentration of K ₃ Fe (CN) ₆ (mM)	As-made Rf	Single step electrooxidation of amine Rf	Electrochemical grafting of diazonium and coupling of dye Rf	Chemical grafting of diazonium and coupling of dye Rf
10	3.9±0.8	14.4±0.6	2.9±0.2	4.0±0.4
50	4.4±0.9	9.8±0.3	2.9±0.2	3.3±0.07
100	3.4±0.1	8.0±0.4	3.2±0.3	3.6±0.2

Table 3 2 Summary of ionic rectification factor on single-step modified DWCNT-dye membrane. Rectification factor was calculated by the ratio of ionic transport current at negative and positive 0.6V bias. Linear scan was from - 0.60 V to + 0.60 V with the scan rate at 50 mV/s.

Concentration (mM)	Rf (potassium ferricyanide)	Rf (NDS)	Rf (Sodium benzenesulfonate)
10	7.2±0.3	3.1±0.3	2.4±0.2
50	6.4±1	2.0±0.1	2.0±0.1
100	5.6±1	2.3±0.1	1.7±0.1

Table 3 3 Summary of ionic rectification factor on DWCNT membrane after water plasma oxidation to remove gatekeepers.

Concentration (mM)	Rf (potassium ferricyanide)	Rf (NDS)	Rf (sodium benzenesulfonate)
10	3.2±0.3	1.7±0.2	2.4±0.2
50	2.8±0.3	1.5±0.07	2.0±0.2
100	2.4±0.2	1.4±0.02	2.0±0.2

Table 3 4 Quantification of carboxyl and sulfonate density using dye-assay.

	Modification on glassy carbon (GC)	Charge density (molecules/cm ²)	Carboxyl density (molecules/cm ²)	Sulfonate density (molecules/cm ²)
Step 1 in two step functionalization	Electrochemical grafting of 4- carboxyl phenyl diazonium for 8min	1.3×10^{15}	1.3×10^{15}	--
Step 2 in two step functionalization	Carbodiimide coupling of dye	2.0×10^{15}	1.07×10^{15}	0.93×10^{15}
One Step functionalization	Electrochemical grafting of dye by amine oxidation for 8min	0.9×10^{15}	--	0.9×10^{15}

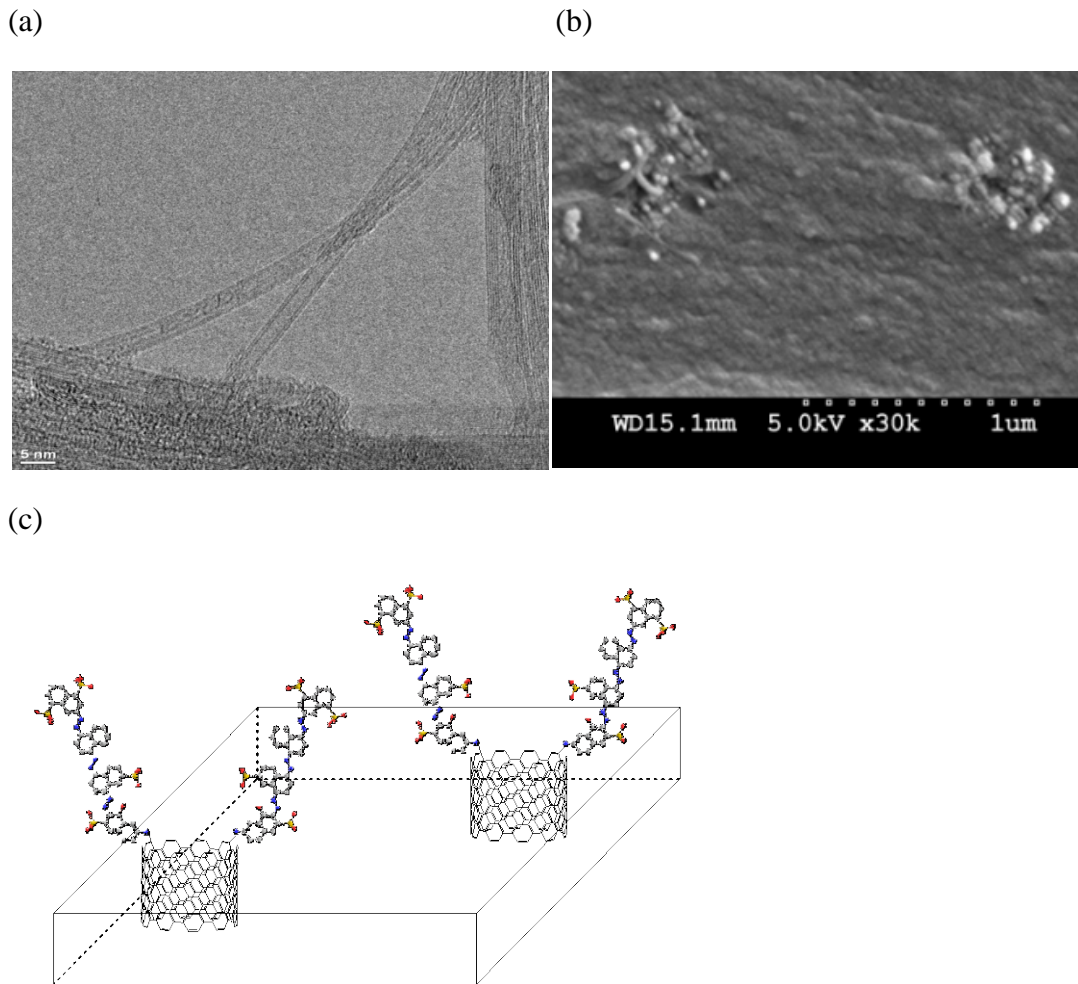


Figure 3 1 (a) TEM image of DWCNTs (purchased from Sigma-Aldrich). (b) SEM image of as-made DWCNT membrane in the cross-sectional view. (c) Schematic diagram of the functionalized anionic dye on CNT tip playing as gatekeeper (grey: C; red: O; blue: N; yellow: S).

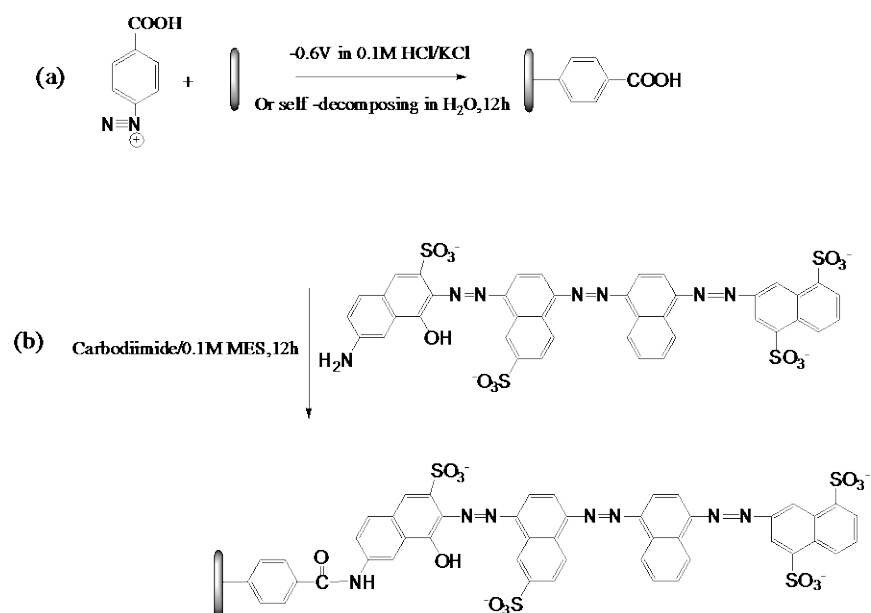
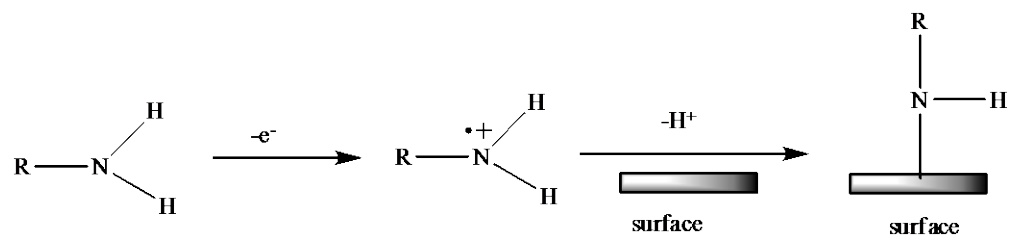


Figure 3 2 Schematic illustration of two step functionalization. (a) Electrochemical grafting or chemical grafting of 4-carboxyl phenyl diazonium. (b) Carbodiimide coupling of Direct Blue 71 dye.

(a)



(b)

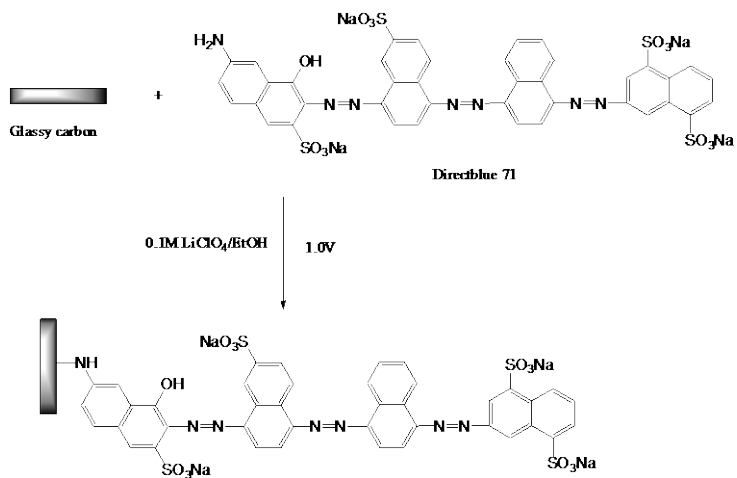
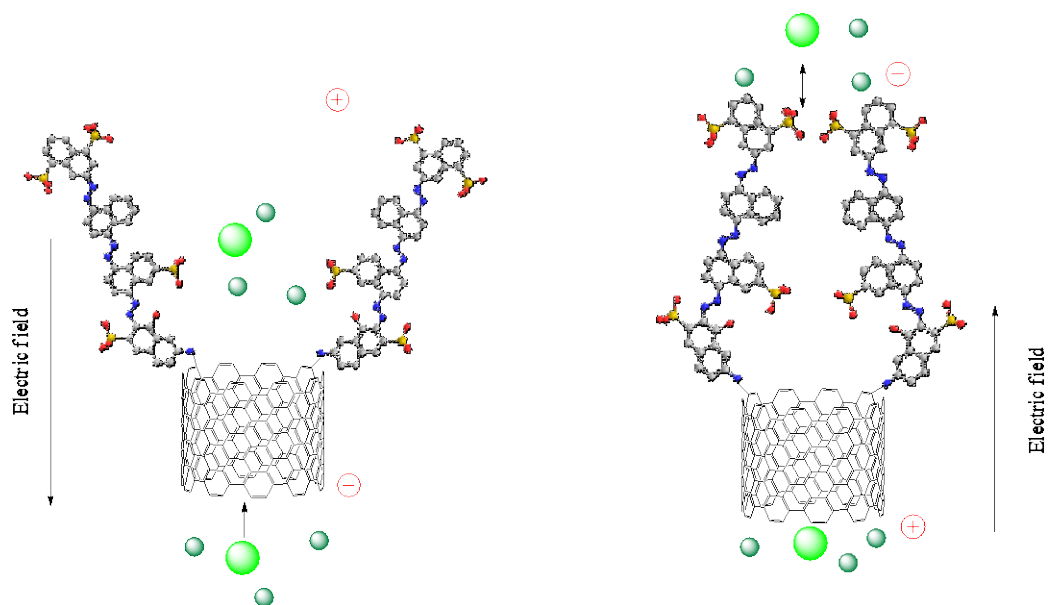


Figure 3 3 (a) Schematic mechanism of electrochemical oxidation of primary amine on conductive surface. (b) Schematic illustration of one step functionalization of Direct Blue 71 via electrooxidation of amine.

(a)



(b)

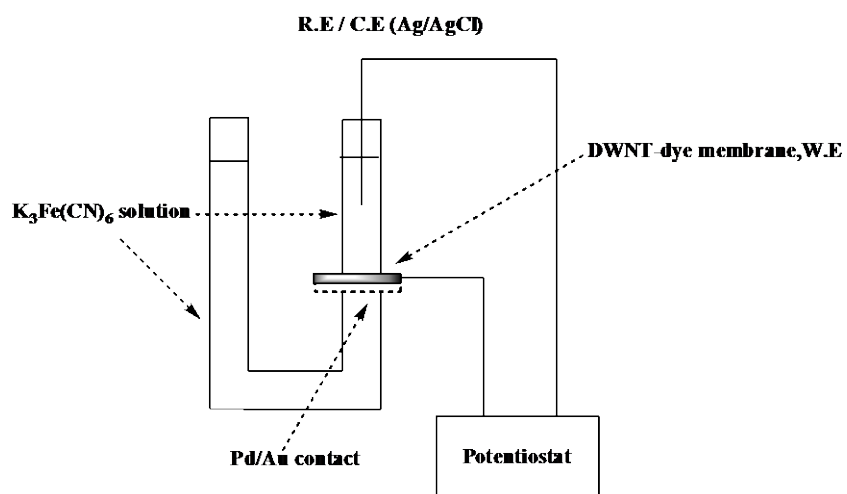
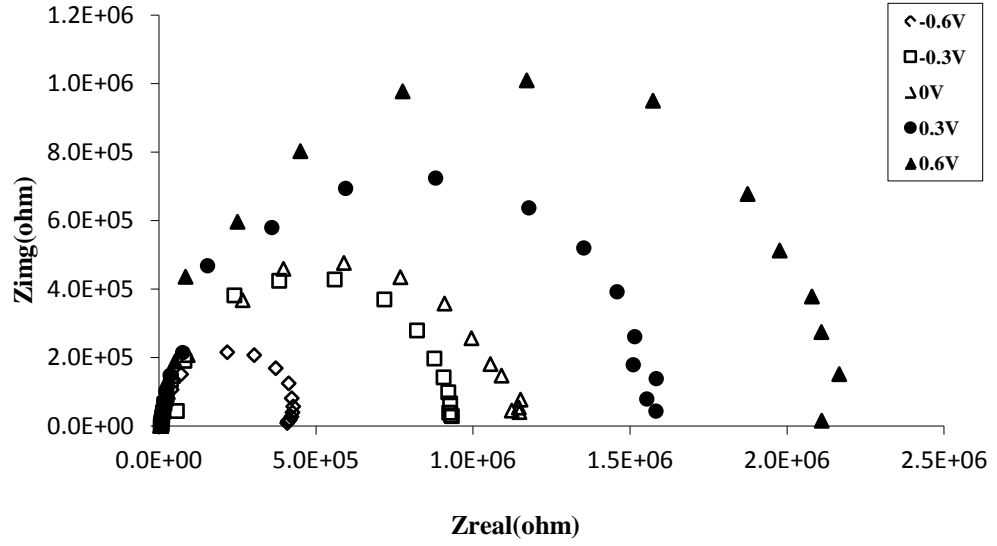
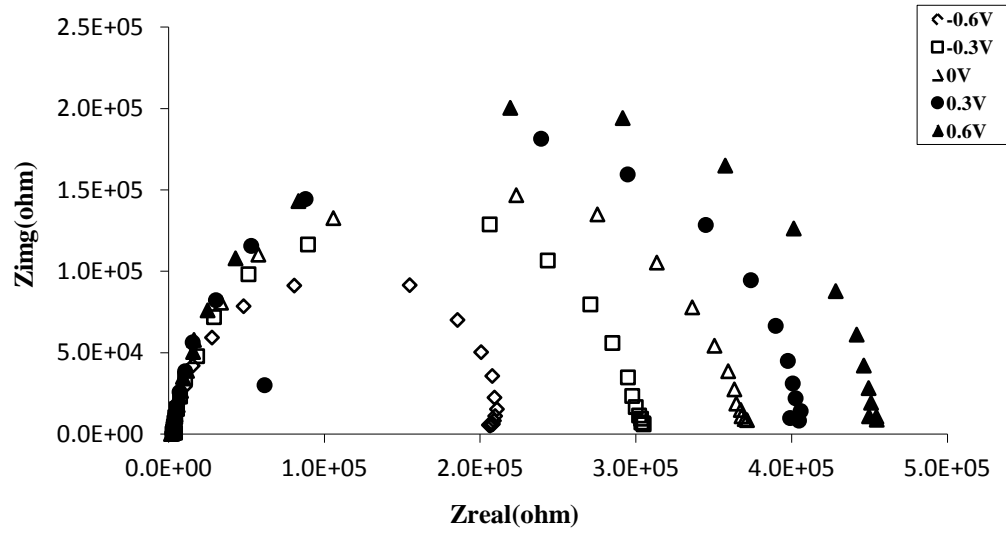


Figure 3 4 (a) Schematic mechanism of ionic rectification on DWCNT-dye membrane. (C, grey; N, blue; O, red; S, yellow; light green:Fe(CN)₆³⁻; dark green: K⁺) (b) Schematic rectification setup. Working electrode (W.E) is DWCNT membrane coated with 30 nm thick Pd/Au film; Reference/counter Electrode (R.E/C.E) is Ag/AgCl electrode. Constant potential was provided using a Princeton Scientific Model 263A Potentiostat. Both U-tube sides are filled with potassium ferricyanide (K₃Fe(CN)₆) solution. linear scan from -0.60V to +0.60V, scan rate as 50mV/s.

(a)



(b)



(c)

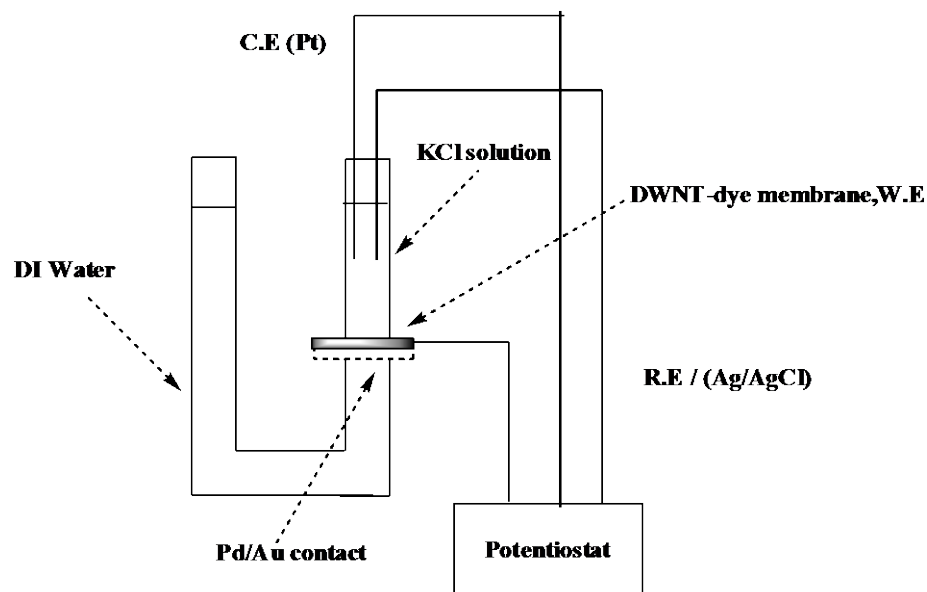
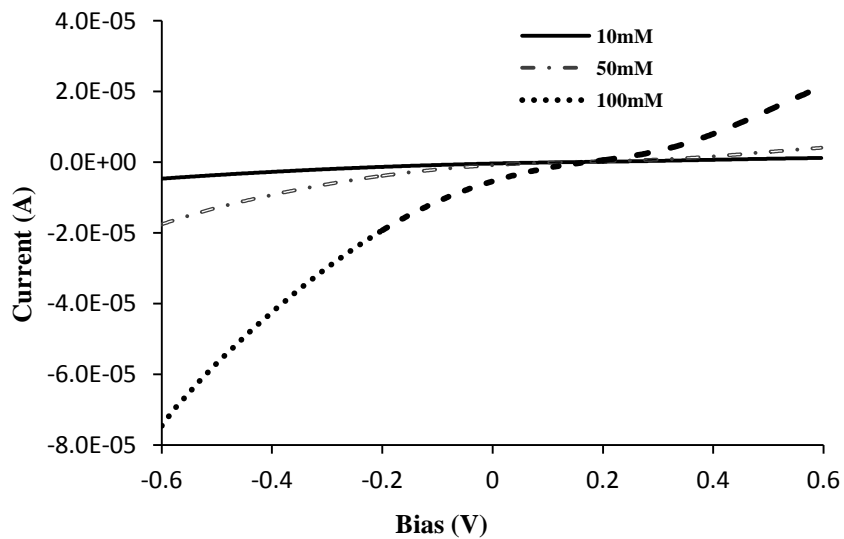
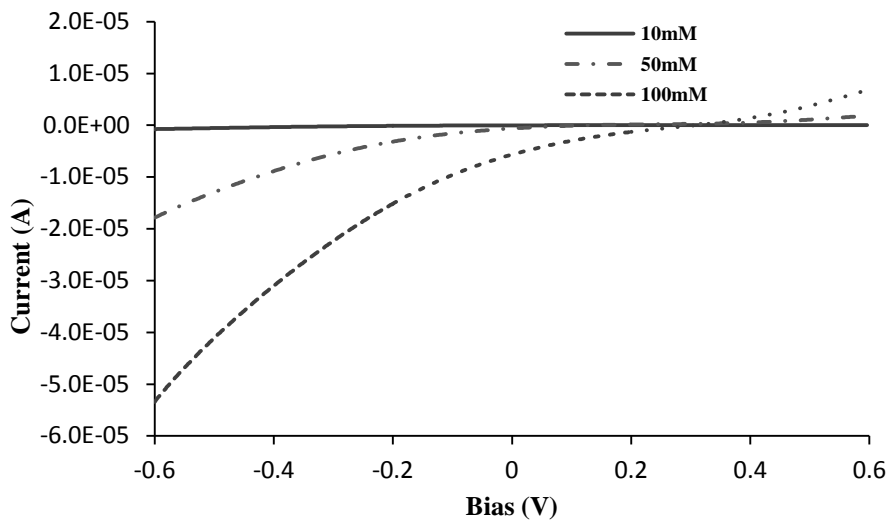


Figure 3 5 Nyquist plots of dye modified membrane in (a) 20 mM KCl (b) 100 mM KCl (c) Experimental setup for the EIS measurements. Experimental conditions: Working Electrode (W.E): DWCNTs-dye membrane; Reference Electrode (R.E): Ag/AgCl; Counter Electrode (R.E): Pt; AC magnitude:10 mV; DC magnitude: -0.6, -0.3, 0, 0.3, 0.6 V; frequency: 100 kHz to 0.2 Hz. Platinum wire, Ag/AgCl and DWCNTs-dye membrane were used as counter, reference and working electrodes, respectively.

(a) As-made DWCNT membranes



(b) DWCNT-dye membrane by single step modification



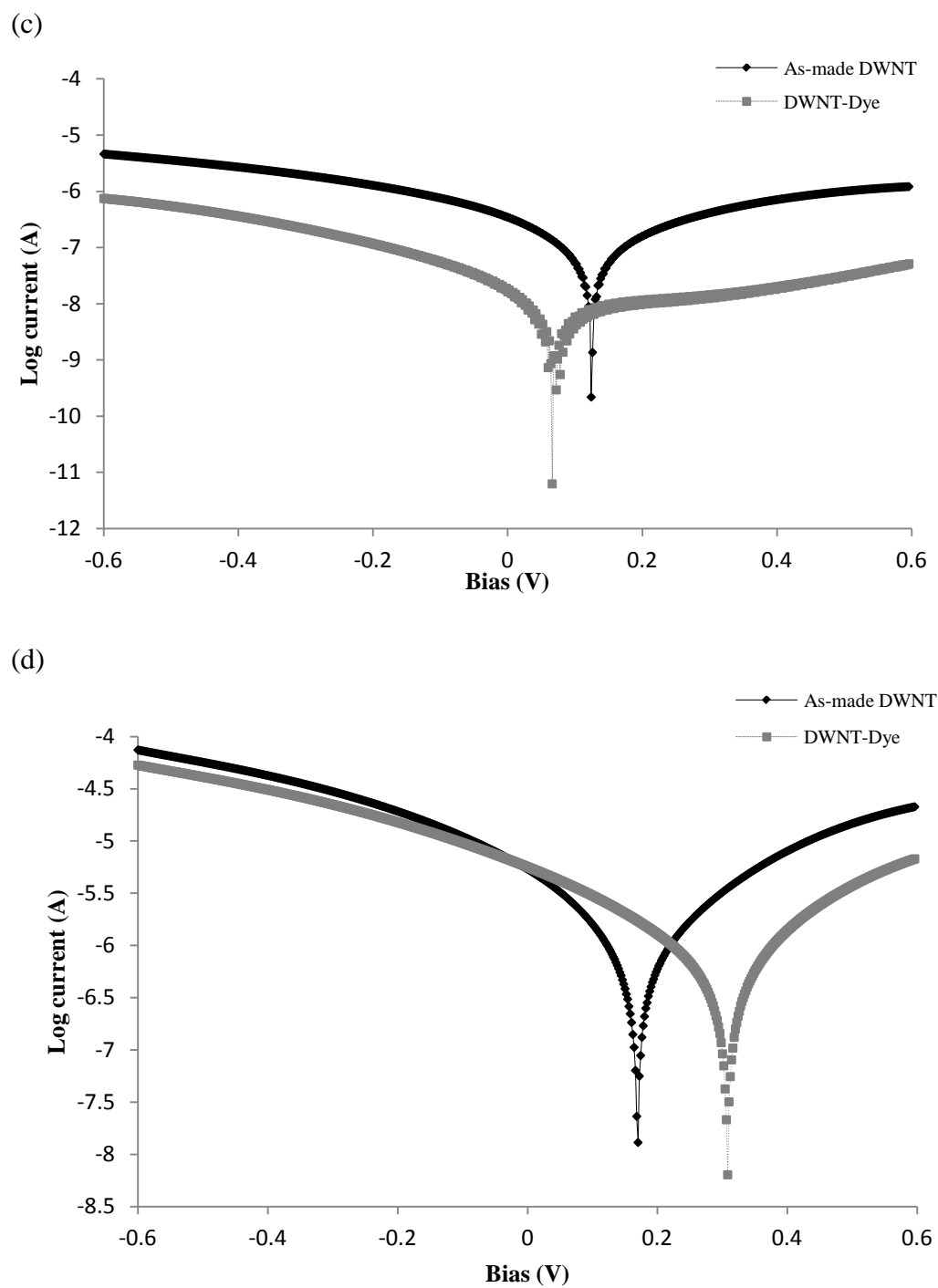


Figure 3.6 Ionic rectification curves on (a) as-made and (b) modified DWCNT membrane (electrochemical oxidation of amine) with potassium ferricyanide. (c) in 10 mM potassium ferricyanide and (d) in 100 mM potassium ferricyanide

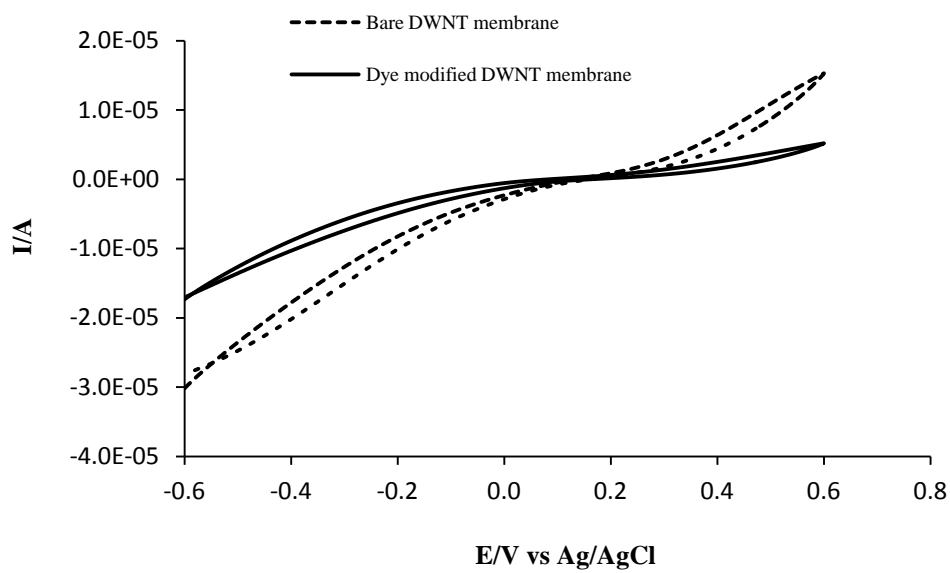
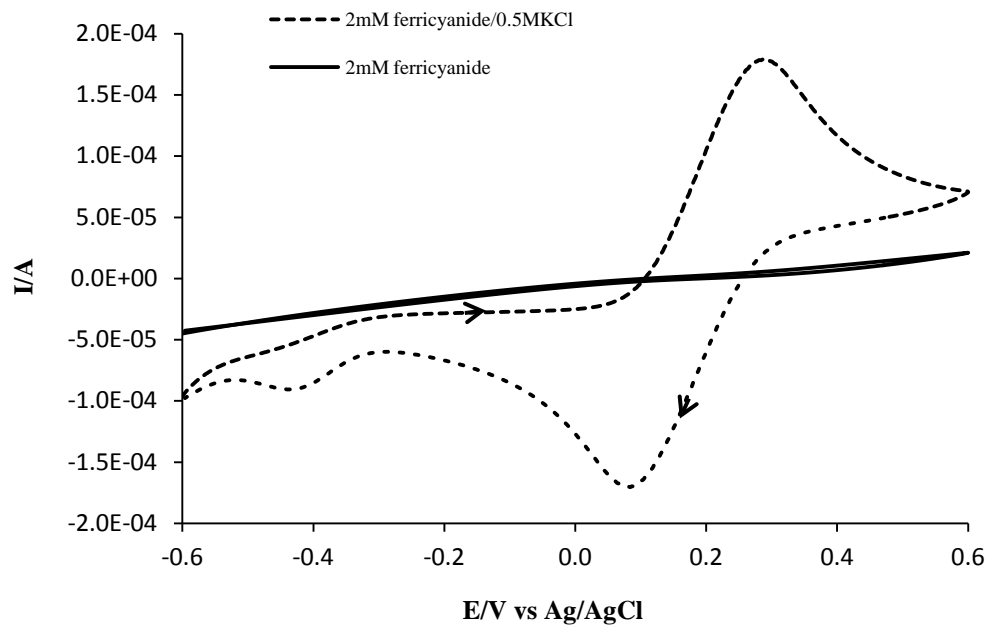


Figure 3 7 Control experiments on DWNT membrane to rule out redox current. Cyclic voltammetry scan on DWNT membrane from -0.6V to +0.6V. Reference /Counter electrode: Ag/AgCl; Working electrode: DWNT membrane. Both sides filled with 50 mM potassium ferricyanide. No Redox peak was found on bare and modified DWNT membrane, which supports the current change was from ionic rectification.

(a)



(b)

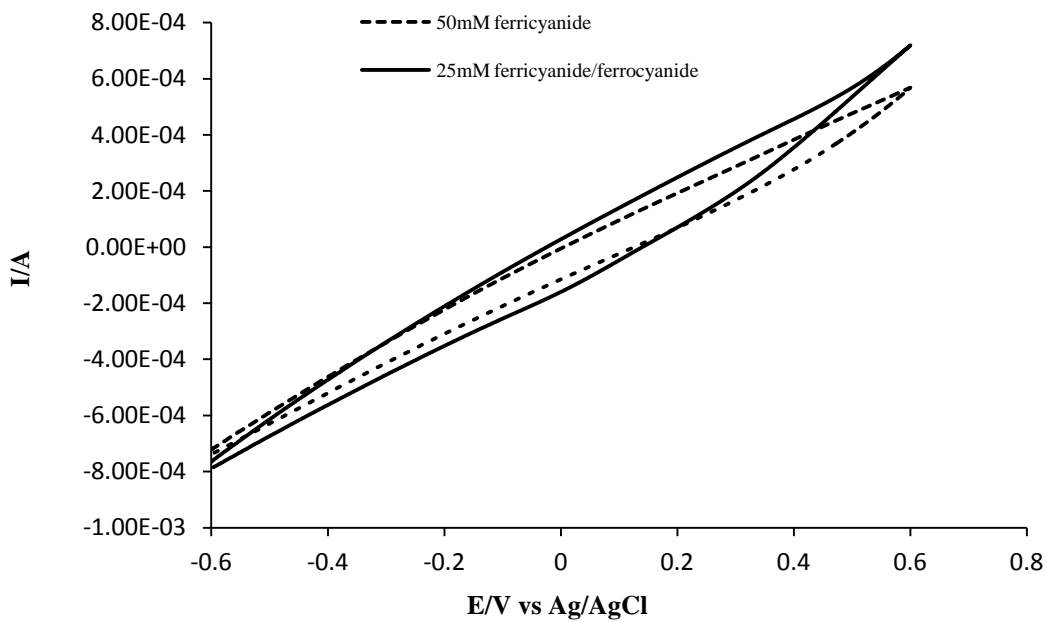


Figure 3 8 Control experiments on glassy carbon to rule out redox current. (a) Cyclic voltammetry scan on glassy carbon in 2mM ferricyanide solution and 2mM ferricyanide solution with 0.5M KCl. (b) Cyclic voltammetry scan on glassy carbon in 50 mM ferricyanide solution and 25 mM ferricyanide/ferricyanide solution (Cyclic voltammetry scan from -0.6V to +0.6V. Reference /Counter electrode: Ag/AgCl; Working electrode: glassy carbon.). With the supporting electrolyte KCl, oxidation and reduction peak were observed at 0.29V and 0.06V, respectively. However, No Redox peaks were found without KCl, which supports no redox reaction occurred in solution.

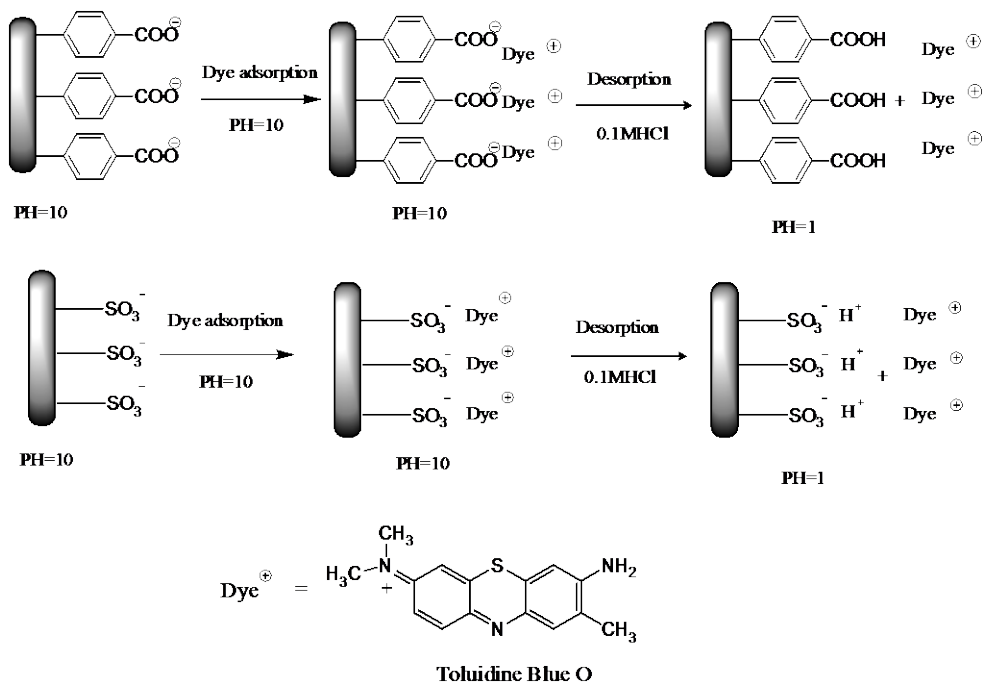


Figure 3 9 Schematic illustration of Dye-Assay quantification.(a) quantification of carboxylic density on glassy carbon by pH dependent adsorption/desorption.(b) quantification of sulfonate density by ionic screening effect. (Assuming charge: Dye =1:1).

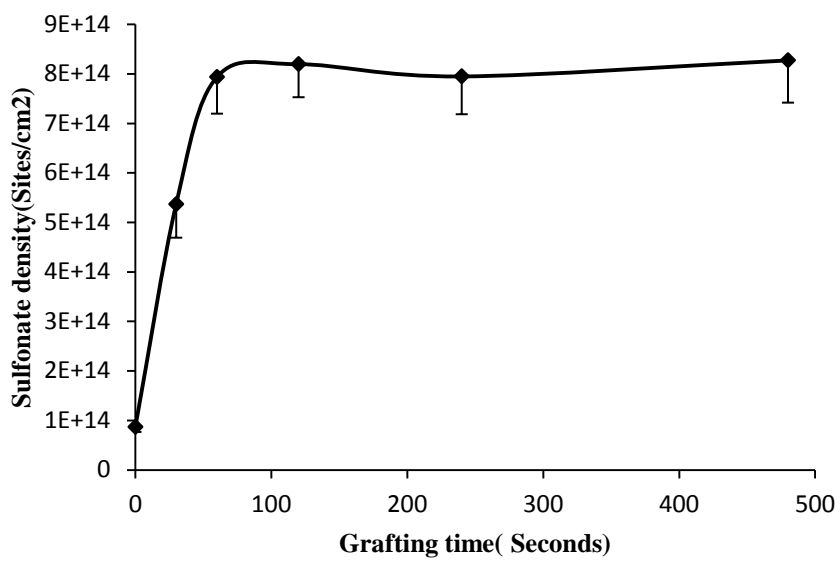


Figure 3 10 Quantification of sulfonate density as a function of grafting time using dye-assay.

Chapter 4 Covalent and noncovalent immobilization of chiral ferrocenyldiphosphine ligand on carbon nanotubes for asymmetric Rh catalyzed hydrogenation

4.1 Introduction

The ideal chiral synthesis is to use a catalyst that produces only the desired enantiomer thereby dramatically increasing yield and eliminating difficult separation steps.[85,86] The rhodium-chiral phosphine complexes were developed for high efficient asymmetric hydrogenation in 1970s, which have been successfully applied in the commercial synthesis of L-dopa (anti-Parkinson drug) and (S)-metolachlor (herbicide precursor). The increasing demand for chiral products stimulates the development of chiral ligands facilitating a wide variety of reactions.[158,159,160] Chiral ferrocenylphosphine ligands are considered as one of the most privileged ligands [161] due to their inherent stability and rigidity from the “sandwich-structured” ferrocene backbone.[162] They offer very high enantiomeric selectivity in asymmetric hydrogenation since the stereo structure combines planar and central chirality without undergoing racemization.[163] The enantiomeric excess (ee) is up to 99% in asymmetric hydrogenation and hydroboration.[164,165] The modular structure and tuned electronic features permit them in a wide range of reactions such as hydrogenation, coupling, ring opening and cycloaddition reactions.[166] Based on these superior properties, ferrocenylphosphines are well adapted in industrial use. For instance, (S)-metolachlor, a well-known herbicide precursor, has been produced on more than 10000 tons/year scale with the most successful Ir-Xyliphos since 1996.[159,166]

Homogenous catalysis has been dominant in asymmetric synthesis due to its high selectivity and activity.[91] However, these expensive chiral catalyst are single use, and an additional cost is required for separation of the products from catalysts, which limit its

application. Heterogeneous catalysis with immobilized catalysts on solids offers numerous advantages including multiple reuse and easy separation of products in solution from the solid support by simple filtration. [167,168,169] However, asymmetric heterogeneous catalysis is facing several major challenges.[89] The catalytic activity is typically decreased due to slow diffusion mass-transport and more difficult steric access to the substrate molecule. There is also a deterioration of enantioselectivity due to distortion of asymmetric stereo-configuration after immobilization. Another drawback is the catalyst can be deactivated after multiple reuses. Although a few promising immobilizations of chiral catalysts on polymers and zeolites have been achieved [90,170,171], it is a challenge to maintain their activity and selectivity after immobilization. The mechanism of the heterogeneous chiral catalysis remains unclear in many aspects. The heterogeneous system is very complicated, depending upon the asymmetric reaction, nature of ligand, support, substrate, solution and functional chemistry. The transition state and kinetics in heterogeneous chiral catalysis are greatly affected by spatial restriction, diffusion, electron transfer and adsorption of substrates and products.[89] Theoretical study shows that a small difference of enantiomeric transition state energy (less than 15kJ/mol) will dramatically change the enantioselectivity. Even weak interaction with the solid support might greatly induce a change in activity and selectivity.

Carbon nanotubes (CNTs) are considered a promising catalyst support due to high surface area ($\sim 100\text{m}^2/\text{g}$), conductivity and stability to corrosion or aggressive solvents.[3,4,6,54] Additionally, the Carbon nanotube membrane geometry with reaction flow through graphitic cores, offers a unique platform with fluid flow rates that are

10,000 fold faster than conventional materials.[12,70,113] Goldsmith et al. reported the simulation of methanol flux through a model of catalytic CNT membranes. The result showed that methanol primarily travels along the pore wall, which efficiently transport substrate to catalytic sites at the CNTs tips.[111] It suggests fast flowing CNT membranes can be converted into highly efficient arrays of nano-reactors since the continuous reaction and separation of products can significantly enhance the reaction yield. Recent progress of CNT supported nanoparticles has showed enhanced performance in heterogeneous catalysis.[52,53] For instance, Ru/CNT and Pd/CNT exhibit higher selectivity than other conventional supports in cinnamaldehyde hydrogenation though mechanism is unclear.[55,56] Due to the confinement of CNTs support, the activity of Rh inside CNTs has been enhanced 10 times than that of outside CNTs in ethanol production.[57] Banerjee et al. reported nonchiral complex are immobilized on CNTs using coordination between metal and carboxyl sites on CNTs. The immobilized Wilkinson's catalyst gives modest activity in cyclohexene hydrogenation.[107,108]

CNTs are quite innovative support for metal-chiral ligand complex. Vanadyl salen has been covalently immobilized on single-wall carbon nanotubes for the cyanosilylation of aldehydes, which is the only reported covalent immobilization of metal-chiral ligand complex.[109] The activity of heterogenized vanadyl salen was decreased to only 1/6 and enantiomer excess (ee) markedly reduced from 90% to 66%. However, this reduced activity of immobilized vanadyl salen remained for five consecutive runs. Tethered pyrene attachment ligands provides simple immobilization strategy for proteins and nanoparticles using π - π stacking interaction between aromatic pyrene ligand and graphite

surface of CNTs support.[39,40,41,42] This approach has been used to recover pyrene modified Rh-Pyrphos complex from homogenous solution onto CNTs to recycle the expensive catalyst..[172] In this cycle the pyrene modified Rh-Pyrphos complex was desorbed from CNTs and worked homogeneously in CH₂Cl₂ solution. After hydrogenation, the homogeneous chiral catalyst was captured by CNTs in ethyl acetate solution. 93% ee was obtained in the asymmetric hydrogenation of α -dehydroaminoester. The continuous running of hydrogenation deteriorated its activity that dropped to 50% at fourth run and 25% at seventh run. However in this scheme it is critical to choose proper solvent systems that can effectively precipitate catalyst onto CNTs and thus limits a more broad application. Thus only two cases of CNTs used as supports in asymmetric catalysis have been reported and showed relatively modest results compared to other support systems. Further experimental study is needed to find chemical strategies for effective chiral catalysis on CNT supports. In particular, catalyst systems that work on aromatic supports such as polystyrene beads or intermediate coatings should easily apply to CNTs.

In this paper, we synthesize tethered chiral ferrocenylphosphine ligands (commercially named as Josiphos ligand) for covalent immobilization on polymers and CNTs. The Josiphos ligand (with tether) exhibited excellent ee and activity in asymmetric homogeneous hydrogenation. But it had very low activity after immobilization onto CNTs and polystyrene beads. As an alternative strategy, three noncovalent immobilization approaches have been carried out. Coordinated Rh catalyst on CNTs support exhibited excellent activity and reuse property even after seventh run in asymmetric hydrogenation. Excellent enantiomer excess (>90%) and 100% yield were

obtained in asymmetric hydrogenation with the immobilized Rh-Josiphos complex using pyrene absorption. Moreover, the higher ee (99%) with 100% yield was achieved in same asymmetric hydrogenation using PTA as electrostatic anchoring agent.

4.2 Experimental methods

4.2.1 Chemicals

In general, air free solvents such as diethyl ether, DMF, methanol and etc. were freshly used after distillation from the appropriate drying agents under argon. Unless otherwise mentioned, all synthesis reactions were carried out under argon protection using standard Schlenk techniques. n-butyllithium(n-BuLi), N,N,N,N-tetramethylethylenediamine(TMEDA), Bis(norbornadiene)rhodium(I)tetrafluoroborate([Rh(NBD)₂]BF₄), Tris[3-heptafluoropropyl-hydroxylmethylene-(+) camphorato]europium(Eu(hfc)₃), Phosphotungstic acid hydrate H₃ [P(W₃O₁₀)₄] xH₂O(PTA) were purchased from Fluka or Sigma and used as received. Chlorosilane: 3-chloropropyl dimethylchlorosilane was obtained from Gelest. (R)-1-[(1S)-2(Diphenylphosphino)ferrocenyl]ethyl dicyclohexylphosphine:(R)-(S)-Josiphos ligand: was purchased from Sigma-Aldrich, and stored in dry box.

4.2.2 Synthesis of chiral ligand precursor:(R)-[3-(N, N-Dimethylamino) ethyl] ferrocene

4.2.2.1 Compound 4: Chiral ligand precursor, (R)-[3-(N,N-dimethylamino)ethyl] ferrocene, was synthesized in multiple steps, as seen in Scheme 4.1.[173] Acetylferrocene was synthesized via Friedel –Crafts acylation. Then the resulting ferrocenyl ketone was reduced to R-(3-hydroxyethyl) ferrocene using S-CBS catalyst. The chiral ferrocenyl alcohol was finally converted the amine (R)-[3-(N,N-dimethylamino)ethyl] ferrocene.

(R)-[3-(N, N-Dimethylamino) ethyl] ferrocene

$^1\text{H-NMR}(\text{CDCl}_3)\delta$:4.10-4.08(m,9H), 3.56(q, 1H), 2.05(s,6H), 1.42(d, 3H)

4.2.3 Synthesis of chiral tethered Josiphos ligand: (R)-1[(S)-2(Diphenylphosphino)-1'-(dimethyl-3'aminopropylsilyl)-ferrocenyl] ethyldicyclohexylphosphine

Starting from this chiral precursor, the tethered (R)-(S) Josiphos ligand was prepared following the synthetic route from Kollner et.al, as seen in Scheme 4.2 via. [94,174] the stereo group dicyclohexylphosphine and tether of chlorosilane tether was introduced into Cp ring via dilithiation. The chlorine on tether was converted to amine group via Gabriel synthesis.

4.2.3.1 Compound 5: 4.3 ml of 2.5 M n-BuLi in hexane solution was added dropwise to solution of 2g of 4 in 15ml of diethyl ether at room temperature. After stirring for 1 hour, equivalent 2.5 M n-BuLi in hexane solution was added dropwise to solution. Subsequently 1.5 ml of TMEDA was added to reaction solution which turned into reddish brown. After stirring for 5 hours, 1.5 ml of chlorodiphenyl-phosphine along with 4.6 ml of 3-chloropropyldimethylchlorosilane was added dropwise at -20°C degree. The reaction continued overnight at room temperature.

Work up: 2ml of saturated NaHCO_3 aqueous solution and 10 ml of water was added slowly to reaction solution in ice bath. The mixture was extracted by 10 ml ethyl acetate for 3 times. Then the organic phase was washed by 5 ml of distilled water for 3 times and dried by MgSO_4 . The resulting product was evaporated in rotary evaporator and dried by high vacuum. The raw product was purified by column chromatography (silica gel hexane: acetic acid=1:1 and acetone), each two times. The BPPFA can be removed by recrystallization in mixed methanol and ethanol solution (1:1). It gave yield as 40%.

$^1\text{H-NMR}(\text{CD}_2\text{Cl}_2)\delta$: 0.08(3H, Si-CH₃), 0.16(S, 3H, Si-CH₃), 0.62(m, 2H, CH₂-Si), 1.28(d, 3H, C-CH₃), 1.5-1.9(m, 2H, CH₂-CH₂-Cl), 2.0(s, 6H, N(CH₃)₂), 3.42(t, 2H, CH₂-Cl), 3.5-4.4, (m, 8H, C₅H₄FeC₅H₃CH), 7.1-7.7(m, 10H, PPh₂). $^{31}\text{P-NMR}(\text{CD}_2\text{Cl}_2)\delta$: -23.5(d, PPh₂)

4.2.3.2 Compound 6: 1.2 g of dicyclohexylphosphine was added to 3.51 g of 12 in 10 ml acetic acid solution. The reaction solution was refluxed at 96 °C for 2 hours.

Work-up: the reaction mixture was extracted by 10 ml toluene and 10 ml distilled water. The organic phase was washed by 20 ml distilled water for 3 times, and then dried by MgSO₄. It was concentrated in rotary evaporator and purified by chromatography (hexane and ethyl acetate 1:1). It gave yield as 80% (orange brown oil).

$^1\text{H-NMR}(\text{CD}_2\text{Cl}_2)\delta$: 0.10(3H, Si-CH₃), 0.17(S, 3H, Si-CH₃), 0.61(m, 2H, CH₂-Si), 0.9-2.0(m, 27H, Pcy₂, CH₂-CH₂-Cl, CH-CH₃), 3.44(t, 2H, CH₂-Cl), 3.1 4.5, (m, 8H, C₅H₄FeC₅H₃CH), 7.1-7.66(m, 20H, PPh₂). $^{31}\text{P-NMR}(\text{CD}_2\text{Cl}_2)\delta$: -23.6(d, PPh₂), 18.35(d, Pcy₂).

4.2.3.3 Compound 7 and 8: 15 was prepared by Gabriel synthesis in two-step. Chloride 13 was converted into phthalimide (compound 14). Primary amine 15 was released with hydrazine hydrate in second step. 578.6 mg of potassium phthalimide and 154.3 mg hexadecyltributylphosphonium bromide (phase transfer catalyst) were added to solution of 1.8g of 13 in 5ml DMF. The reaction solution is refluxing at 96 °C for 2 hours.

Work-up: the reaction mixture was extracted by 10 ml of mixture (water/toluene=1:1). The organic phase was washed by 10 ml distilled water for 3 times and dried by MgSO₄.

The crude product concentrated by rotary evaporator was purified by chromatography (hexane/ ethyl acetate 1:1). It gave 7 yield as 68% (orange oil product).

0.4 ml of hydrazine hydrate was added to 1.72 g of phthalimide¹⁴ in 18ml of ethanol solution. The reaction solution was refluxed for 2 hours.

Work-up: 25 ml of methylene chloride was added to the reaction mixture. The suspension was washed by methylene chloride and filtered. The product of 15 was purified by chromatography (methanol with 2% triethylamine). It gave 8 yield as 90%.

14: ¹H-NMR(CD₂Cl₂)δ:0.07(3H,Si-CH₃),0.14(S,3H,Si-CH₃),0.61(m,2H,CH₂-Si),0.9-2.0(m,27H,Pcy₂,CH₂-CH₂-Cl,CH-CH₃),3.5(t,2H,CH₂-N),3.1-4.5(m,8H,C₅H₄FeC₅H₃CH),7.6-7.7(m,10H,PPh₂). 7.7-7.9(m,4H, phthalimide).

³¹P NMR (CD₂Cl₂)δ:-26.5(d, PPh₂),15.2(d, PCy₂)

15: ¹HNMR(CD₂Cl₂)δ:0.07(3H,Si-CH₃),0.14(S,3H,Si-CH₃),0.61(m,2H,CH₂-Si),0.9-2.0(m,27H,Pcy₂,CH₂-CH₂-Cl,CH-CH₃),2.58(t,2H,CH₂-N),3.1-4.5,(m,8H,C₅H₄FeC₅H₃CH),7.6-7.7(m,10H,PPh₂).

³¹PNMR(CD₂Cl₂): δ-26.5(d, PPh₂), 15.2(d, Pcy₂)

4.2.4 General procedure of homogenous and heterogeneous hydrogenation of dimethyl itaconate

Typical homogenous hydrogenation was carried out in following steps (Scheme 4.3): 3 mmol dimethyl itaconate was dissolved in 10 ml methanol and stirred for 1hr (solvent varied in different reaction). 0.015 mmol ferrocenyldiphosphine ligand was added to equivalent [Rh (NBD)₂] BF₄ in 10 ml methanol. It allowed coordination for 0.5-1.0 hr under stirring at room temperature. Then Rh-Ligand complex catalyst was transferred to

dimethyl itaconate solution under argon protection. H₂ gas in balloon was purged for five times to remove argon in Schlenk flask. The reaction mixture was stirred for 1hr under room temperature and 1 atm H₂. In general, heterogeneous hydrogenation procedures followed the same procedures as homogenous reaction except recycling of immobilized catalysts by filtration. The hydrogenation product (dimethyl succinate) was separated from immobilized catalysts through cannula filtration. The yield of dimethyl succinate was determined by ¹H NMR.

4.2.5 Quantification of enantiomeric excess by chiral NMR

The *ee* of product was quantified by chiral NMR with Lanthanide shift reagent Eu(hfc)₃ that is capable of coordinating with Lewis bases succinate. The paramagnetic Eu³⁺ dramatically induces the chemical shift of alpha-proton, which split the NMR peak. In general, ~30mg dimethyl succinate was dissolved in 1ml CDCl₃. 27 mg Eu(hfc)₃ was subsequently added to the solution. After it was dissolved, the sample was tested by 400 M Hz Varian ¹H NMR. Optical pure R and S succinate are quantitatively mixed to prepare series standard solutions. Enantiomer excess of standard solution is obtained by calculation of the ratio of shifted peaks' area. The integrated area of S (-) peak is proportional to *ee* of standard racemic succinate solution. Standard curve of shifted NMR assay is prepared to quantify *ee* in the asymmetric hydrogenation, as shown in supplementary information Figure 4.1.

4.2.6 Fabrication and oxidation of multiwalled CNTs

Multiwall carbon nanotubes were grown by chemical vapor deposition method which ferrocene/xylene was used as precursors at 700 °C.[118] The length of CNTs varies from 30 to 100 μm, while the inner diameter is around 10 nm. CNT sample was under 70% nitric acid refluxing at 140°C for 16 hrs, then filtered and washed extensively with

distilled water until the pH is ~7. The sample was dried in vacuum by oil pump at 60 °C for 48 hrs.

4.2.7 Covalent immobilization of chiral catalyst

4.2.7.1 Immobilization with carbodiimide coupling reaction

This immobilization protocol was adapted from Slovias company patent (Scheme 4.4).[174] 2 ml of orange solution of 24 mg (0.034 mmol) tethered Josiphos ligand was dissolved in 2 ml of THF. The orange ligand solution was transferred to the mixture of solid supports with 4 ml THF and 1 ml H₂O (Amberlite IRC-50 resin, carboxylated polystyrene and carboxylated CNTs, respectively). Then 2 ml THF solution of 50 mg DCC (N,N-dicyclohexylcarbodiimide) was slowly added to the mixture of reaction. The yellow solution gradually turned colorless and polymer beads turned into orange after 2 hours. The polymer beads were filtered and washed once with THF, once with DMF, four times with THF (5 ml each time). The polymer beads were dried at 50°C under high vacuum for overnight. In coordination with Rh precursor, The Josiphos ligand loaded polymer beads was simply stirred with 0.02 mmol Rh precursor in methanol for 30mins. The yellow Rh precursor solution turned into colorless. Then the Rh-Josiphos-support was filtered and rinsed with methanol for 3 times. The loading of Rh (95%) was determined by UV-vis absorbance measurement of decant solution with calibration standard.

4.2.7.2 Immobilization with isocyanate as coupling reagents

The amine group of tethered Josiphos was conjugated with aminomethylated polystyrene with isocyanate as coupling reagents (Scheme 4.5). This detailed procedure was adapted from the report of Pugin et al.[93]

4.2.8 Non-covalent immobilization of chiral catalyst

4.2.8.1 Strategy 1. Coordination of [Rh (NBD)₂] BF₄ with carboxyl sites on CNTs

~0.1g purified CNTs were dispersed in methanol for 1hour sonication. 0.03 m mol [Rh (NBD)₂] BF₄ was dissolved in 10ml methanol. Then it was slowly transferred to solution of CNTs and stirred at 55 °C for overnight. Then the reaction mixture was filtered and washed with methanol through cannula at least three times (seen in Scheme 4.6).

4.2.8.2 Strategy 2. Pyrene modified chiral catalysts on CNT via π - π stacking interaction

The tethered Josiphos ligand was coupled with 1-pyrenebutyric acid with dicyclohexylcarbodiimide(DCC) and 4-dimethylaminopyridine(DMAP) in dichloromethane.[172]0.02mmol pyrene modified ligand was coordinated with 0.017mmol [Rh(nbd)₂]BF₄ in methanol for 30 mins at room temperature under argon protection. And the pyrene modified Rh-ligand complex was absorbed on surface of CNTs and filtered and rinsed three times with methanol (seen in Scheme 4.7).

4.2.8.3 Strategy 3. Immobilization of Rh-chiral ligand anchoring on CNT using electrostatic anchoring agent phosphotungstic acid

In general, 1g phosphotungstic acid (PTA, Aldrich) was dissolved in 20 ml H₂O (or EtOH). Subsequently, it was transferred to 0.1g acid-treated CNTs in 10 ml ethanol. The reaction mixture was sonicated for 2hrs at room temperature. Then it was stirred at 50°C overnight. The PTA modified CNT was washed by H₂O (or ethanol) for at least 3 times. For treatment with water solution, the sample was dried under vacuum for 2 days. PTA-CNT sample was stirred with pre-synthesized Rh-Ligand complex in EtOH for overnight. The (Rh-Ligand)-PTA-CNT was filtered and washed by ethanol for at least 3 times (seen in Scheme 4.8).

4.3 Results and discussions

4.3.1 Covalent immobilization of tethered Rh-josiphos ligand complex on CNT

The privileged Josiphos ligands have earned great success in both laboratory and industry settings.[161,162,163,166] It is of significant benefits to separate and recover this expensive chiral complex from products with simple filtration that can be simply achieved with CNT supports. The covalently immobilized tethered Rh-Josiphos ligand complex on dendrimers exhibits promising enantioselectivity (98%) and activity in asymmetric hydrogenation of itaconate under 1 bar. [94,95] More than 100,000 turnovers have been achieved on immobilized Ir-xyliphos in asymmetric transfer hydrogenation imine at 80 bar. The immobilized Ir-xyliphos on solid support gives the close enantioselectivity (up to 78%) in asymmetric transfer hydrogenation imine at 80 bar, But activity drops from 28571 h^{-1} to the range between 20000 to 1140 h^{-1} after immobilization on silica and polystyrene, respectively.[93] With large specific area and chemical inertness, CNTs are a compelling recovery support. We thus immobilize this catalyst onto CNTs to explore if CNTs are superior chiral catalyst support over other conventional supports. If successful, the final goal is to functionalize this catalyst at the pore exits of fast flowing CNT membrane to enhance the yield of products due to the continuous reaction and separation. We synthesized the tethered Josiphos ligand from literature route since it is not commercially available. The chiral ligand precursor, (R)-[3-(N, N-Dimethylamino) ethyl] ferrocene, was synthesized from ferrocene as backbone (Scheme 4.1).[173,175,176] The synthetic route of tethered (R)-(S) Josiphos ligand was adapted from Kollner et al. (Scheme 4.2). [94,174] The detailed synthesis of chiral precursor and tethered Josiphos ligand is described in the experimental section. The performance of catalyst was tested in homogeneous hydrogenation of dimethyl itaconate (Scheme 4.3). The activity and enantiomer excess were collected in Table 4.1. The

unbound tethered Josiphos ligand gave promising yield (100%) and ee (98%) and thus the tether on the ligand does not interfere with catalytic activity and enantioselectivity.

The tethered Josiphos ligand was covalently functionalized on Amberlite IRC-50 resin with the carbodiimide coupling reaction that was adapted from the Slovias company patent (Scheme 4.4).[174] This experiment was an attempt to confirm the literature precedence with same type of ligand, support and coupling chemistry in our laboratory. The tether structure in our experiment (Ligand-Si-(CH₃)₂-CH₂-CH₂-CH₂-NH₂) was slightly different than in patent (Ligand-CH₂-NH₂) with a longer chain that typically aids in retaining catalytic activity on solid supports. The yellow solution turned colorless and polymer beads turned into orange during amide coupling reaction, indicating that the Josiphos ligand tether was successfully immobilized onto the catalyst support. After coordination with Rh precursor, the loading of Rh (95%) was determined by UV-vis absorbance measurement with calibration standard. However, the supported catalyst did not exhibit activity in asymmetric hydrogenation at 1 atm. There was no activity found on the heterogenized tethered Josiphos ligand after immobilization on carboxylated polystyrene and carboxylated CNTs at same condition.[174] The results were summarized in Table 4.2. Besides reported carbodiimide coupling chemistry, we tried to repeat another immobilization method under nearly exact condition including same coupling reaction, support and tether. This method enabled functionalization of the tethered Ir-xylyphos ligand complex(owning very similar structure with Josiphos ligand) on aminomethylated polystyrene using isocyanate as active reagent.[93] The immobilized catalyst also gave no activity in hydrogenation of itaconate at room temperature and atmosphere pressure. Even though the temperature and pressure was elevated at 50°C and

34 atm, it only gave poor yield as 11% (Table 4.3). The chiral complex lost its activity because linkage between ligand and support may still restrict the conformational flexibility making it difficult for the substrate to access to catalyst site. It seems that it is very sensitive to any subtle change such as tether, nature of ligand, functional chemistry and etc. In fact the tethered Josiphos ligand is no longer commercial available presumably due to these heterogenous catalysts being far more complicated and expensive in industrial use than their homogeneous analogue.[169] Another promising approach for this catalyst system is using noncovalent immobilization on a suitable support.[177]

4.3.2 Three non-covalent immobilizations of Rh-Josiphos on carbon nanotubes

Non-covalent immobilization of chiral catalyst has recently received considerable attention.[91,100,178] The weak interaction between catalyst and support provides more homogeneous environment to obtain high activity and enantioselectivity. The chiral catalysts are simply functionalized on solid supports using versatile noncovalent strategies such as adsorption, encapsulation and electrostatic interaction. The primary advantage is no need of tedious and expensive synthesis of tethered chiral ligand. It simulates homogeneous environment to obtain high activity and enantioselectivity due to weak interaction between chiral catalyst and support. However, the common problem are stability issues associated with leaching into solution. Three non-covalent immobilization approaches were carried out onto CNTs via coordination, pyrene attachment and phosphotungstic anchoring, respectively.

4.3.2.1 Immobilization of Rh-Josiphos ligand on CNT using coordination chemistry

The immobilized Rh precursor $[\text{Rh}(\text{nbd})_2]\text{BF}_4$ was coordinated to carboxyl groups on acid treated CNT for 16 hrs in methanol at 50°C and then it was filtered and rinsed by

methanol. The hydrogenation results were collected in Table 4.4. The immobilized Rh catalyst gave promising activity that was only slightly lower than that of homogeneous analogue. The activity remained even after seventh runs (100%, 2hr). The chiral modification of immobilized Rh on CNTs by (R)-(S)-Josiphos ligand was tried (entry 5 to 7 in Table 4.4). However, it seemed that chiral ligand was not able to coordinate with the immobilized Rh on CNT since the hydrogenation product is racemate. In addition, we attempted to directly coordinate Rh-Josiphos ligand complex with carboxyl sites on CNT, but zero yield in hydrogenation indicated that it was unable to attach to CNTs. There are two possible reasons for the failure of coordination between immobilized Rh and chiral ligand. First, the bulky ligand is difficult to access to Rh due to steric hindrance of the support. The second reason is that the coordination sites of immobilized Rhodium might be fully occupied by the carboxyl group.

4.3.2.2 Immobilization of Rh-Josiphos ligand on CNT using Pyrene attachment

CNTs were used as scavenger to recycle the pyrene modified Rh-Pyrphos complex since the flat polyaromatic ring can be absorbed onto CNT graphite surface via π - π stacking interaction.[172] In our experiment, the tethered catalyst containing a primary amine on Josiphos ligand was conjugated with 1-pyrenebutyric acid using same carbodiimide coupling chemistry. The pyrene modified Josiphos ligand was coordinated with $[\text{Rh}(\text{nbd})_2]\text{BF}_4$ in methanol solution and mixed with CNTs under argon protection. The orange yellow complex solution gradually turned into colorless after its absorption onto CNT surface. The CNTs loaded with catalyst were filtered and rinsed by methanol three times (seen in scheme 4.7). The immobilized chiral catalyst gave 72% yield and 90% ee in first run. However, it dramatically dropped to 10% in next run (Table 4.5). This indicated that there was serious leaching problem. It seemed that the pyrene modified Rh-

ligand complex is susceptible to be removed from CNTs in hydrogenation and effectively is a homogeneous catalysis reaction away from CNT support..

4.3.2.3 Immobilization of Rh-Josiphos ligand on CNT using phosphotungstic acid as electrostatic anchoring agent

Augustine et al. studied the immobilization of Rh-chiral ligand complex for asymmetric hydrogenation using phosphotungstic acid (PTA, $H_3PW_{12}O_{40}$) as anchoring agent.[179,180,181] Phosphotungstic acid (PTA, $H_3PW_{12}O_{40}$) is one of heteropolyacids (HPAs) with Keggin structure that a central phosphate group is surrounded by twelve octahedral tungsten oxyanion. Its anion (polyoxometalate) is considered as superacid that can have strong electrostatic attraction with positive charged Rh-ligand complex. The Rh(Dipamp)-PTA-Montmorillonite catalyst maintained activity and enantioselectivity after fifteen times reuse in hydrogenation of methyl 2-acetamidoacrylate.[179] In hydrogenation of dimethyl itaconate, more than 10000 TON and 92% ee still remained using the Rh(BoPhoz)-PTA-carbon at 75psig after fourth run. [181] PTA offered a simple noncovalent immobilization method with electrostatic interaction. The immobilized catalysts are capable of being reused a few times without deactivation. By using different HPAs as anchoring agents, it was found the nature of HPAs can have a significant effect on both the activity and selectivity of anchored catalyst. It suggested that there is a direct interaction between HPA and Rh-ligand complex.[180]

The anionic PTA molecules can be physically absorbed on CNT due to electrostatic attraction between PTA and graphite surface of CNTs. PTA-CNTs solution can be stable for weeks due to the charge repulsion.[182,183] The procedure of anchoring Rh-Josiphos ligand complex on CNT using phosphotungstic acid was described in experimental. The result of hydrogenation of dimethyl itaconate by Rh(Josiphos)-PTA-CNTs was listed in

Table 4.6. It gave very promising result in first run (100% yield and 99% ee). The activity remained 71% in the second run. However the yield went down to 20% in third run and had similarly modest yields in subsequent runs. The ideal anchoring requires appropriate interaction between Rh-chiral ligand complex and support. Strong interaction could restrict the motion of catalyst and distort its stereostructure, which may deteriorate its activity and selectivity. However, weak interaction is unable to prevent catalyst leaching from support.

4.4 Conclusions

Covalent and noncovalent immobilization of Rh-chiral ligand complex on CNTs were systematically studied for asymmetric hydrogenation. The unbound tethered Rh-Josiphos complex exhibits excellent ee and activity in hydrogenation of dimethyl itaconate. But it was deactivated after covalent immobilization on conventional resin and polystyrene supports as well as CNTs. Three noncovalent functionalization approaches have been carried out to immobilize Rh-Josiphos complex on CNTs for asymmetric hydrogenation of dimethyl itaconate. Coordinated Rh catalyst on CNTs exhibited excellent activity and reuse ability even after seventh run in hydrogenation but no enantiomeric excess as expected for lacking a chiral directing ligand. The catalyst using pyrene absorption gave 100% yield and excellent enantiomer excess (>90%) but suffered from leaching into solution. The phosphotungstic acid (PTA) anchored catalyst gave 100% yield and higher ee (99%) and better reusability over pyrene absorbed catalyst but had significant leaching after the second run. At this point it remains a significant challenge to utilize CNTs as a chiral catalyst support.

Table 4 1 Asymmetric homogeneous hydrogenation of dimethyl itaconate with Rh-Josiphos ligand (S/C=100, 1 atm and room temperature)

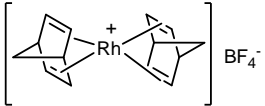
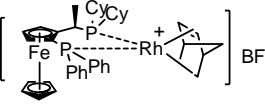
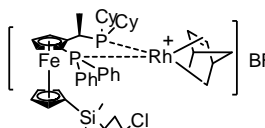
Catalysts (S/C=100)	Time	Yield	ee
 <p>a: [Rh(nbd)₂]BF₄</p>	1hr	100%	0%
 <p>b: Rh-(R)-(S)-PPh₂-PCy₂</p>	1hr	92%	99%
 <p>c: Rh-tethered-(R)-(S)-PPh₂-PCy₂</p>	2hrs	100%	98%

Table 4 2 Heterogeneous hydrogenation with the covalent immobilized Josiphos ligand-Rh complex on polystyrene. (S/C=100 in methanol solution).

Support	Pressure(atm)	Time(hours)	Solvent	Temperature(°C)	Yield
IRC-50 resin	1	24	Methanol	25	0%
carboxylated polystyrene	1	24	Methanol	25	0%
carboxylated CNT	1	24	Methanol	25	0%

Table 4 3 Heterogeneous hydrogenation with the covalent immobilized Josihpis ligand-Rh complex on polystyrene. (S/C=100 in methanol solution).

Number of runs	Pressure(atm)	Time(hours)	Solvent	Temperature(°C)	Yield
1	1	2	MeOH	25	0%
2	1	20	DCM/MeOH	25	9%
3	34	24	DCM/MeOH	25	3%
4	34	20	Toluene/MeOH	50	11%

Table 4 4 Heterogeneous hydrogenation with coordinated [Rh(nbd)2]⁺ BF₄⁻ on CNTs
(S/C=100)

Number of runs	Yield	Time(hours)
1	100%	6
2	100%	6
3	100%	6
4	100%	3
5 a*	100%	2
6 b*	100%	2
7 c*	100%	2
8	77%	1

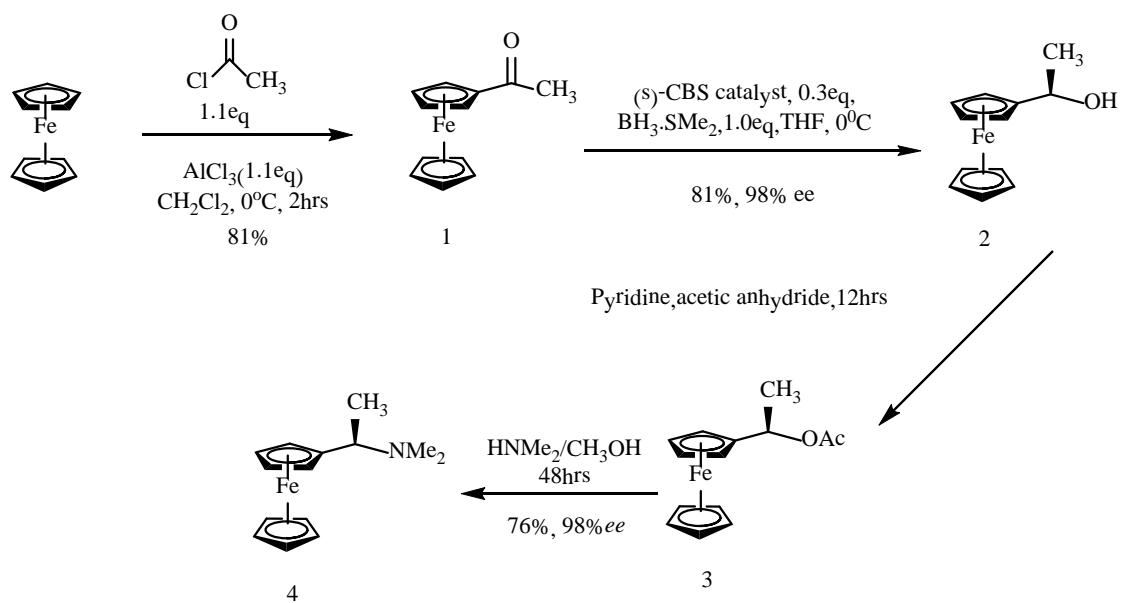
a*.Coordination with R,S-Josiphos ligand 2hours (no enantioselectivity); b*. Coordination with R,S-Josiphos ligand 5hours (no enantioselectivity); c*. Coordination with R,S-Josiphos ligand 16 hours (no enantioselectivity)

Table 4 5 Heterogeneous hydrogenation with immobilized pyrene modified chiral catalysts on CNTs(S/C=100)

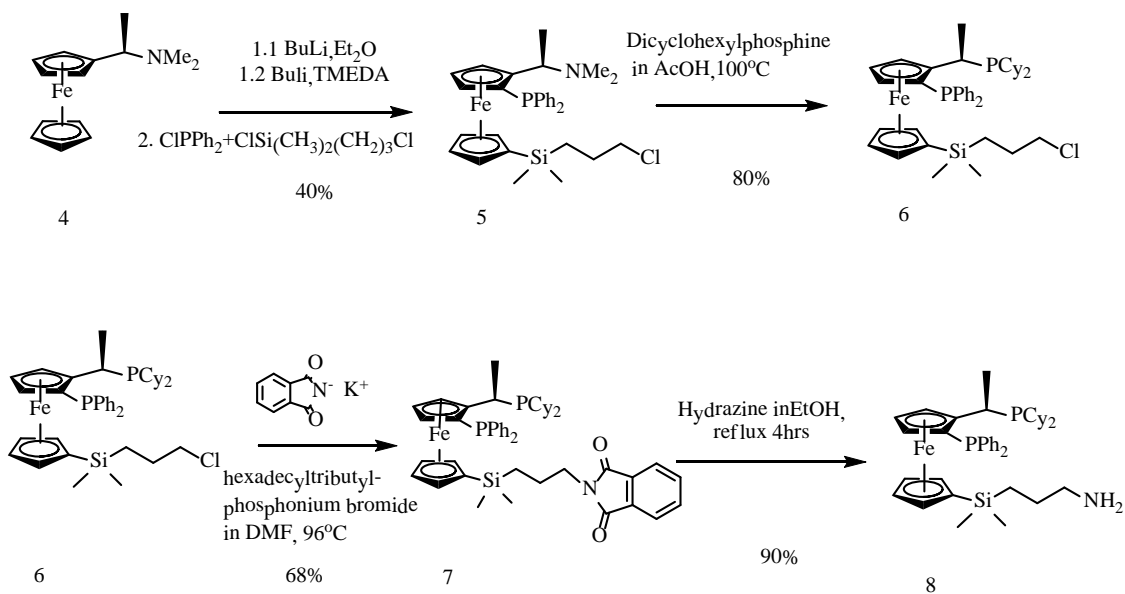
Number of Runs	Time	Yield %	% ee
1	2hrs	72	90
2	3hrs	10	N/A

Table 4 6 Heterogeneous hydrogenation with immobilized Rh-Josiphos ligand complex using phosphotungstic acid(S/C=100)

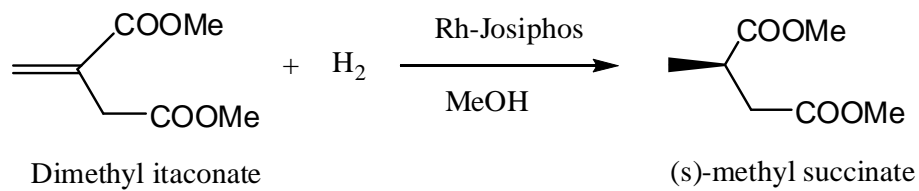
Number of runs	Yield	ee	Time(hrs)
1	100%	99%	2
2	71%	99%	2
3	20%	N/A	3.5



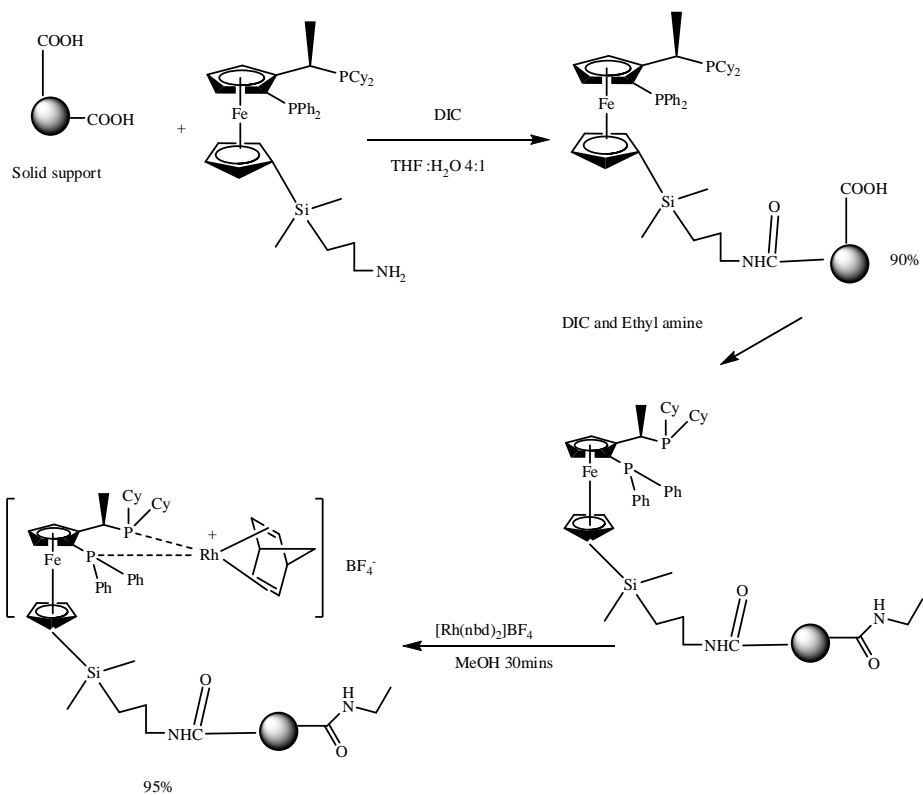
Scheme 4 1 Synthesis of chiral ligand precursor: (R)-[3-(N, N-Dimethylamino) ethyl] ferrocene.



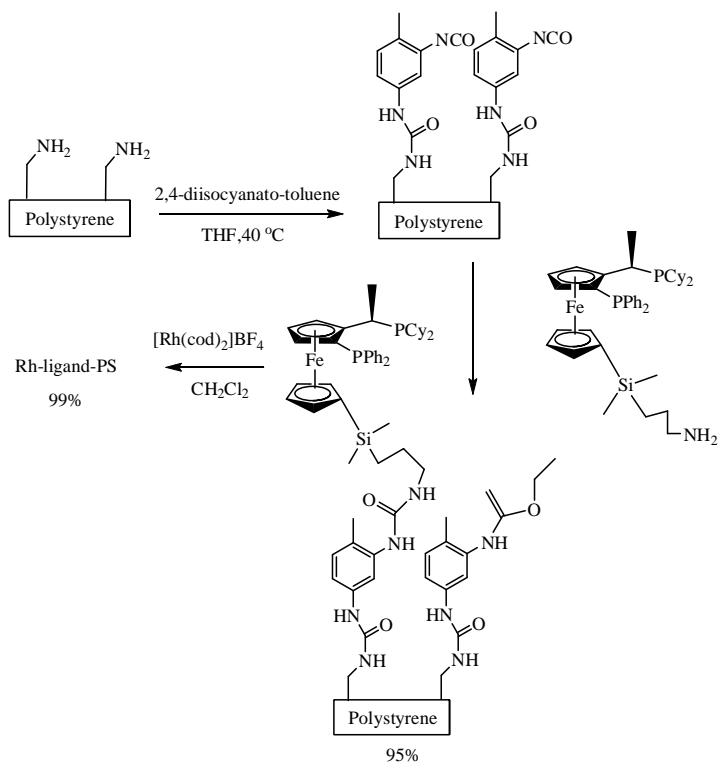
Scheme 4.2 Synthesis of tethered Josiphos ligand: (R)-1[(S)-2(Diphenylphosphino)-1'-(dimethyl-3'aminopropylsilyl)-ferrocenyl] ethyldicyclohexylphosphine.



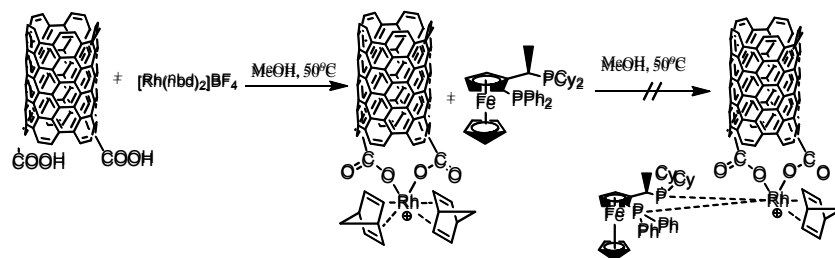
Scheme 4 3 Asymmetric hydrogenation of dimethyl itaconate.



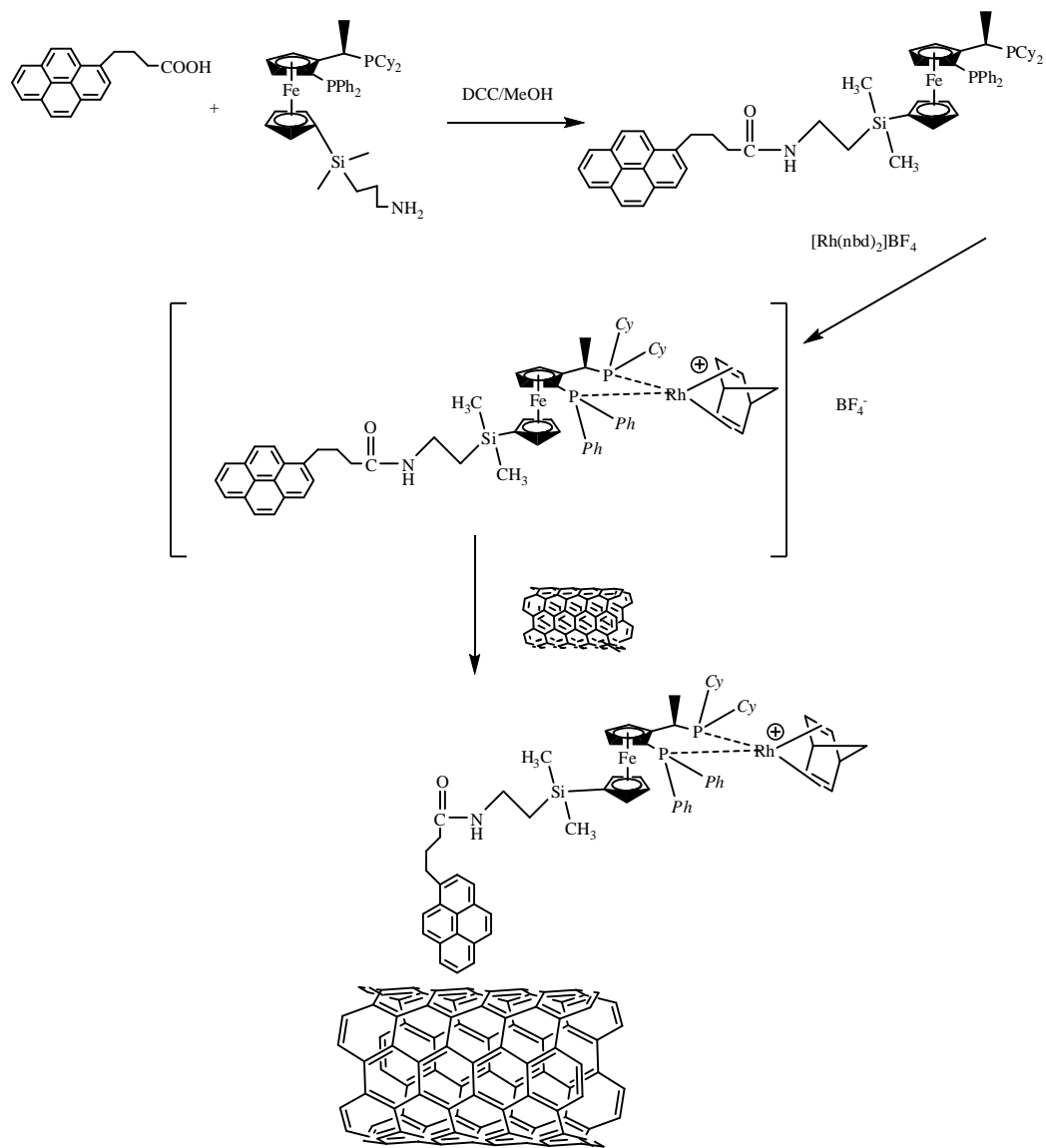
Scheme 4 4 Covalent immobilization of chiral tethered ligand on three different solid supports: Amberlite IRC-50 resin, carboxylated polystyrene and carboxylated CNT, respectively.



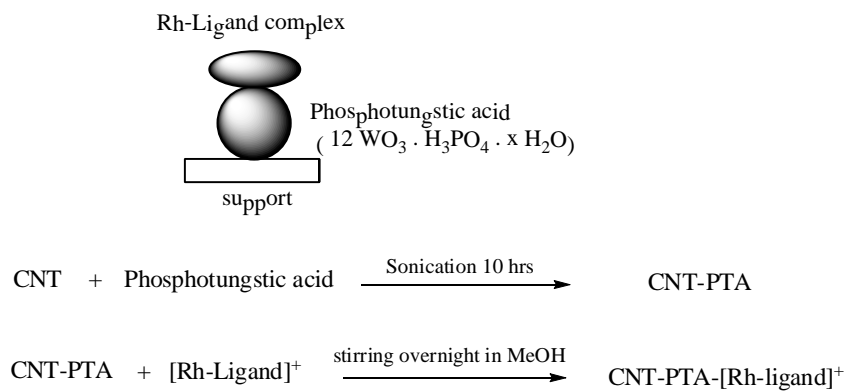
Scheme 4 5 Covalent immobilization of chiral tethered ligand on Polystyrene-NH₂.



Scheme 4.6 Coordination of Rh–ligand complex with carboxylate on CNT.



Scheme 4 7 Pyrene modified chiral catalysts on CNTs via π - π stacking interaction.



Scheme 4 8 Rh-chiral ligand anchoring on CNT using phosphotungstic acid.

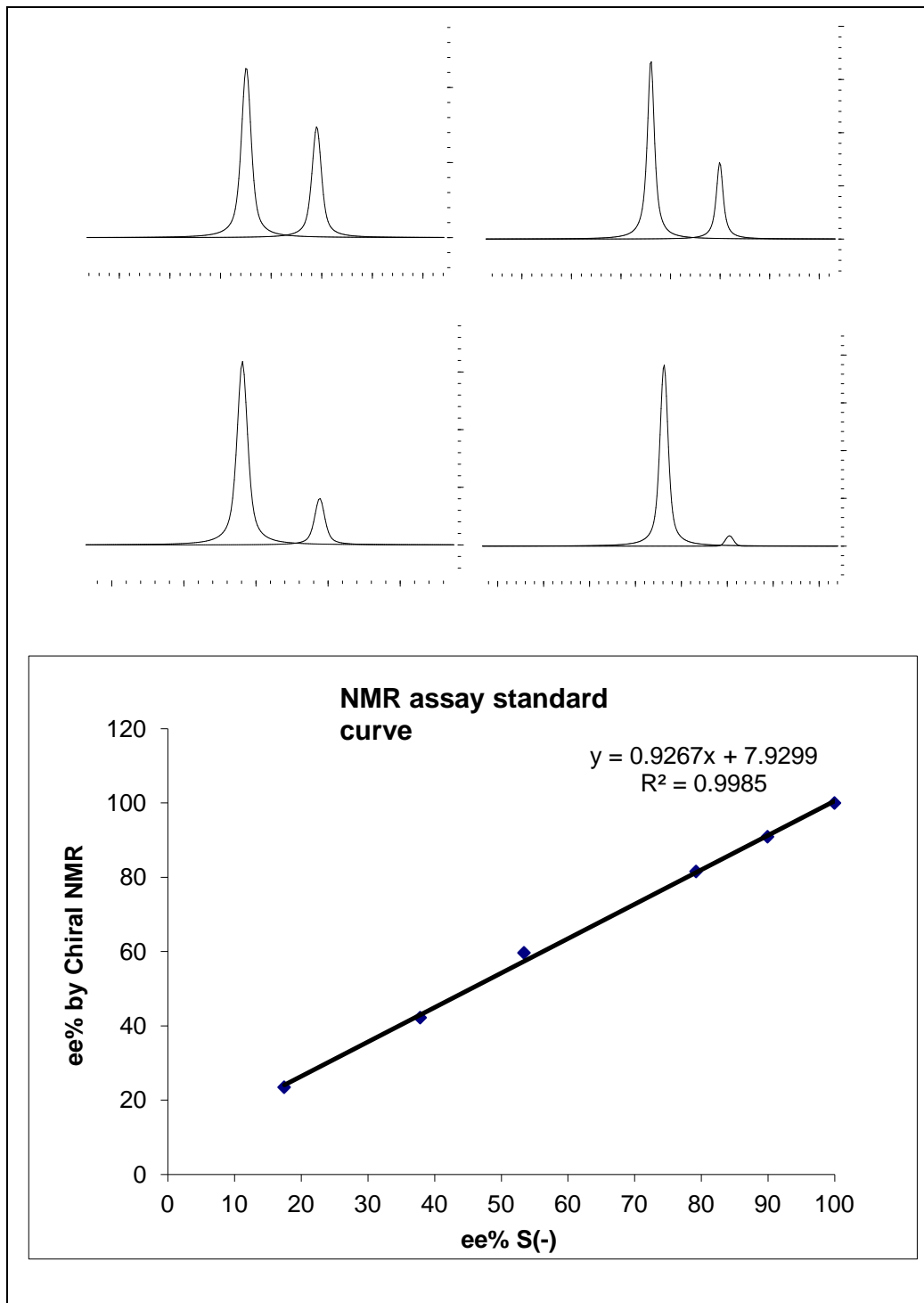


Figure 4 1 Quantification of enantiomer excess (*ee* %) by ¹H NMR with lanthanide shift reagent. (A) to (D) Shifted ¹H NMR Peak by Eu³⁺ reagent: larger integrated area of S(-) peak with increasing of S(-) *ee*%. (A) 17.5%; (B) 38.0%; (C) 53.4%; (D) 90%; Left peak: S(-), right peak: R(+); (E) Shifted NMR assay standard curve

Chapter 5 Conclusions and future research direction

Carbon nanotubes have been intensively studied due to their unique physical and chemical properties. However, the pristine CNTs are insoluble and chemically inert. All of the CNT applications are based on the CNT functional chemistry.[184] Electrochemical diazonium grafting offers versatile functionality under mild condition, which is particularly suitable for CNTs and CNT membranes modification.[74,135] However, it is a challenge to control the grafting density and quantify the number of functional molecules. Carbon nanotube membranes allow mimicking natural ion channels for exciting applications in drug delivery and chemical separation.[12] This was achieved by placing gatekeeper at pores of CNTs in two-step functionalization. However, the uncontrollable grafting polymer can block the entrance of CNT then greatly reduce the fluid, make it difficult to regulate the gatekeeper. The diazonium modified CNT buckypaper was used as catalytic platform for fuel cell.[37] However, the thick polymer dramatically reduces the current density due to insulation Pt catalyst from conductive CNT buckypaper. This dissertation has mainly focused on developing efficient electrochemical functionalization of CNTs and CNTs membrane for energy, drug delivery and catalysis. These efforts were summarized in three directions, and the future research were discussed.

- 1.) Development of controllable electrochemical diazonium grafting and quantification for CNTs and CNTs membranes application.
- 2.) Development of single-step electrochemical oxidation of amine on double-walled carbon nanotube (DWCNT) membranes and the demonstration of ionic rectification.

3.) Synthesis and immobilization of chiral ferrocenyldiphosphine ligand on carbon nanotubes for asymmetric hydrogenation.

5.1. Electrochemical diazonium grafting and quantification of its surface functional density.

A near monolayer was successfully developed by electrochemical grafting of tetrafluorinated carboxylphenyl diazonium on glassy carbon, gold and CNT buckypaper. The polymer growth is limited by the inertness carbon-fluorine bond on aryl ring. Diazonium grafting efficiency on CNT buckypaper was enhanced by 4 fold due to shortening conduction path length when grafting CNTs on more conductive glassy carbon.

Tetrafluorinated carboxylphenyl diazonium grafting provides the most controllable functionalization chemistry allowing near monolayer levels of functionality on carbon nanotubes and carbon nanotube membranes. The future work is to use this technique enables monolayer functionality at the tips of carbon nanotube membranes for biomimetic pumps and valves as well as thin conductive layers for CNT-based high area electrochemical support electrodes.

The functional density on glassy carbon, gold and carbon nanotube buckypaper, was successfully quantified by anion selective dye-assay. The accuracy of the dye-assay method was confirmed by X-ray photoelectron spectroscopy (XPS) of thiol-Au self-assembled monolayers (SAM) as a calibration reference. However, it is a challenge to directly quantify functional density on CNT membrane due to small number of CNTs and complicated 3D structure. In current stage, we have to use the functional density on glassy carbon and CNTs buckypaper to estimate the number of functionalized molecules

on CNT membranes. There needs to develop dye-assay quantification on CNT membranes.

5.2 Single-step electrochemical oxidation of amine on double-walled carbon nanotube (DWCNT) membranes and the demonstration of ionic rectification

DWNT membranes were simply functionalized with dye in single step instead of previous two-step functionalization. Non-faradic EIS spectra indicated that the functionalized gatekeeper by single-step modification can be actuated to mimic protein channel under bias. This functional chemistry was proved by highly efficient ion rectification, which the highest experimental rectification factor of ferricyanide was up to 14.4. It was found that the rectification is attributed to both charge and steric effect at low concentration while the steric effect is dominant at high concentration. Single step electrooxidation of amine provides simple and promising functionalization chemistry that demonstrates highly efficient ionic rectification.

However, there are few questions to be addressed. Two-step functionalization enables gatekeepers partially blocking large cation on MWNT membranes and effectively blocking small cation on SWCNT membranes. However, no apparent change of rectification was observed on DWCNT membranes after two step functionalization though functional density by single step functionalization was quantified as same as that of two step functionalization on glassy carbon by dye-assay. It is possible that the single step modified dye molecules on membrane are more responsive to applied bias because it is directly bonded to conductive CNT surface, instead of organic layer by diazonium grafting. It required the experiment to prove it. Another possible reason is that the actual yield of the second step of the two-step modification on CNT membranes may be much less than the calculated 18% yield on glassy carbon. It requires the quantification of

functional density on CNT membranes. It is important to systematical study on tube size, functional chemistry and conductivity for CNT membranes.

5.3 Synthesis and immobilization of chiral ferrocenyldiphosphine ligand on carbon nanotubes for asymmetric hydrogenation.

The primary advantages of immobilization of chiral catalyst are multiple reuse and easy separation in asymmetric synthesis. However, the catalytic activity and enantioselectivity are typically decreased after immobilization. Carbon nanotubes (CNTs) are considered a promising catalyst support due to high surface area, conductivity and stability. CNTs are quite innovative support for metal-chiral ligand complex. Thus only two cases of CNTs used as supports in asymmetric catalysis have been reported and showed relatively modest results compared to other support systems. We systematically studied Covalent and noncovalent immobilizations of Rh-chiral ligand complex on CNTs for asymmetric hydrogenation. We synthesized the tethered Josiphos ligand from literature route since it is not commercially available. The unbound tethered Rh-Josiphos complex exhibits excellent ee and activity in hydrogenation of dimethyl itaconate. However, it was deactivated after covalent immobilization on conventional resin and polystyrene supports as well as CNTs even though we tried to repeat the immobilization and asymmetric hydrogenation in literature at nearly same condition. It seems that it is very sensitive to any subtle change such as tether, nature of ligand, functional chemistry and etc. In fact the tethered Josiphos ligand is no longer commercial available presumably due to these heterogenous catalysts being far more complicated and expensive in industrial use than their homogeneous analogue. The future direction is to develop

Three noncovalent functionalization approaches have been carried out to immobilize Rh-Josiphos complex on CNTs for asymmetric hydrogenation of dimethyl itaconate. Coordinated Rh catalyst on CNTs exhibited excellent activity and reuse ability even after seventh run in hydrogenation but no enantiomeric excess as expected for lacking a chiral directing ligand. The catalyst using pyrene absorption gave 100% yield and excellent enantiomer excess (>90%) but suffered from leaching into solution. The phosphotungstic acid (PTA) anchored catalyst gave 100% yield and higher ee (99%) and better reusability over pyrene absorbed catalyst but had significant leaching after the second run. Noncovalent immobilization of chiral catalyst provides promising activity and enantioselectivity, but suffered significant leaching problem in continuous use. It is urgent to enhance its stability. Although asymmetric heterogeneous catalysis is very complicated, remained many unknown questions. It is important to study asymmetric reaction, nature of ligand, support, substrate, solvent and functional chemistry.

Besides developing promising immobilization methods, we need to be out of box to emerge areas with electrocatalysis and catalytic CNT membrane. The catalytic efficiency can be enhanced with traditional overpotential and molecular catalysis. Molecular dynamic (MD) simulation reveals that methanol can primarily travel along the pore wall, which allows efficient transport of substrate to catalytic sites.[111] Fast flowing CNT membranes are considered as promising arrays of nano-reactors because the continuous reaction and separation can enhance the yield of products. We have proved that gatekeeper on CNT membrane can be actuated by changing the conformation under applied bias. It suggests the actuation of immobilized ligand conformation may overcome

the slow diffusion and enhance its turnover frequency. CNT membranes can be converted to highly efficient catalytic platform.

LIST OF ABBREVIATIONS

AAO	Aluminum oxide
AFM	Atomic force microscopy
BET	Brunauer-Emmett-Teller
CNT	Carbon nanotube
CP	Carboxylphenyl
CVD	Chemical vapor deposition
DCC	N,N-dicyclohexylcarbodiimide
DWCNT	Double-walled carbon nanotube
EDC	Ethyl-(N', N'-dimethylamino) propylcarbodiimide hydrochloride
ee	Enantiomer excess
EIS	Electrical impedance spectroscopy
EQCM	Electrochemical quartz crystal microbalance
FG	Flowing grafting
HiPco	High pressure carbon monoxide
ICP-AES	Inductively coupled plasma atomic emission spectroscopy
IRRAS	Infrared-Reflection-Absorption Spectroscopy
MD	Molecular dynamic
MHHPA	Methylhexahydrophthalic anhydride
MV ²⁺	Methyl viologen
MWCNT	Multi-walled carbon nanotube
NIR	Near-infrared
PEG	Polyethylene glycol
PFBT	Pentafluorobenzenethiol
PTA	Phosphotungstic acid
SAM	Self-assembled monolayers
SEM	Scanning electron microscope
STM	Scanning tunneling microscopy
Sulfo-NHS	N-hydroxysulfosuccinimide
SWCNT	Single-Walled carbon nanotube
TBO	Toluidine blue O
TEM	Transmission electron microscopy
TFCP	Tetrafluorinated 4-carboxylphenyl
TGI	Tumor growth inhibition
TOF	Turnover frequency
ToF-SIMS	Time-of-Flight Secondary Ion Mass Spectrometry
TON	Turnover number
Rf	Rectification factor
XPS	X-ray Photoelectron Spectroscopy

REFERENCES

- [1] C.A.M. Mihail C. Roco, Mark C. Hersam, *Nanotechnology Research Directions for Societal Needs in 2020: Retrospective and outlook*, Springer, 2011.
- [2] S. Iijima, Helical microtubules of graphitic carbon, *Nature* 354 (1991) 56-58.
- [3] J.M. Schnorr, T.M. Swager, Emerging Applications of Carbon Nanotubes†, *Chemistry of Materials* 23 (2010) 646-657.
- [4] H. Chu, L. Wei, R. Cui, J. Wang, Y. Li, Carbon nanotubes combined with inorganic nanomaterials: Preparations and applications, *Coordination Chemistry Reviews* 254 (2010) 1117-1134.
- [5] M. Valcárcel, S. Cárdenas, B.M. Simonet, Role of Carbon Nanotubes in Analytical Science, *Analytical Chemistry* 79 (2007) 4788-4797.
- [6] D. Eder, Carbon Nanotube–Inorganic Hybrids, *Chemical Reviews* 110 (2010) 1348-1385.
- [7] A. Peigney, C. Laurent, E. Flahaut, R.R. Bacsa, A. Rousset, Specific surface area of carbon nanotubes and bundles of carbon nanotubes, *Carbon* 39 (2001) 507-514.
- [8] X. Wang, Q. Li, J. Xie, Z. Jin, J. Wang, Y. Li, K. Jiang, S. Fan, Fabrication of Ultralong and Electrically Uniform Single-Walled Carbon Nanotubes on Clean Substrates, *Nano Letters* 9 (2009) 3137-3141.
- [9] Y. Zhang, Y. Bai, B. Yan, Functionalized carbon nanotubes for potential medicinal applications, *Drug Discovery Today* 15 (2010) 428-435.
- [10] L. Hu, D.S. Hecht, G. Grüner, Carbon Nanotube Thin Films: Fabrication, Properties, and Applications, *Chemical Reviews* 110 (2010) 5790-5844.
- [11] G. Lota, K. Fic, E. Frackowiak, Carbon nanotubes and their composites in electrochemical applications, *Energy & Environmental Science* 4 (2011) 1592-1605.
- [12] H. Bruce, Dramatic transport properties of carbon nanotube membranes for a robust protein channel mimetic platform, *Current Opinion in Solid State and Materials Science* 16 (2012) 1-9.
- [13] H.-C. Wu, X. Chang, L. Liu, F. Zhao, Y. Zhao, Chemistry of carbon nanotubes in biomedical applications, *Journal of Materials Chemistry* 20 (2010) 1036-1052.
- [14] J. Liu, A.G. Rinzler, H. Dai, J.H. Hafner, R.K. Bradley, P.J. Boul, A. Lu, T. Iverson, K. Shelimov, C.B. Huffman, F. Rodriguez-Macias, Y.-S. Shon, T.R. Lee, D.T. Colbert, R.E. Smalley, Fullerene Pipes, *Science* 280 (1998) 1253-1256.
- [15] J. Chen, M.A. Hamon, H. Hu, Y. Chen, A.M. Rao, P.C. Eklund, R.C. Haddon, Solution Properties of Single-Walled Carbon Nanotubes, *Science* 282 (1998) 95-98.
- [16] S.S. Wong, E. Joselevich, A.T. Woolley, C.L. Cheung, C.M. Lieber, Covalently functionalized nanotubes as nanometre- sized probes in chemistry and biology, *Nature* 394 (1998) 52-55.
- [17] D. Belanger, J. Pinson, Electrografting: a powerful method for surface modification, *Chemical Society Reviews* 40 (2011) 3995-4048.
- [18] M. Delamar, R. Hitmi, J. Pinson, J.M. Saveant, Covalent modification of carbon surfaces by grafting of functionalized aryl radicals produced from electrochemical reduction of diazonium salts, *Journal of the American Chemical Society* 114 (1992) 5883-5884.

- [19] J. Pinson, F. Podvorica, Attachment of organic layers to conductive or semiconductive surfaces by reduction of diazonium salts, *Chemical Society Reviews* 34 (2005) 429-439.
- [20] S. Baranton, D. Bélanger, Electrochemical Derivatization of Carbon Surface by Reduction of in Situ Generated Diazonium Cations, *The Journal of Physical Chemistry B* 109 (2005) 24401-24410.
- [21] P. Allongue, M. Delamar, B. Desbat, O. Fagebaume, R. Hitmi, J. Pinson, J.-M. Savéant, Covalent Modification of Carbon Surfaces by Aryl Radicals Generated from the Electrochemical Reduction of Diazonium Salts, *Journal of the American Chemical Society* 119 (1997) 201-207.
- [22] B.P. Corgier, C.A. Marquette, L.J. Blum, Diazonium-protein adducts for graphite electrode microarrays modification: Direct and addressed electrochemical immobilization, *Journal of the American Chemical Society* 127 (2005) 18328-18332.
- [23] R. Polsky, J.C. Harper, S.M. Dirk, D.C. Arango, D.R. Wheeler, S.M. Brozik, Diazonium-Functionalized Horseradish Peroxidase Immobilized via Addressable Electrodeposition: Direct Electron Transfer and Electrochemical Detection, *Langmuir* 23 (2006) 364-366.
- [24] D.M. Shewchuk, M.T. McDermott, Comparison of Diazonium Salt Derived and Thiol Derived Nitrobenzene Layers on Gold, *Langmuir* 25 (2009) 4556-4563.
- [25] L. Civit, A. Fragoso, C.K. O'Sullivan, Thermal stability of diazonium derived and thiol-derived layers on gold for application in genosensors, *Electrochemistry Communications* 12 (2010) 1045-1048.
- [26] Y.-C. Liu, R.L. McCreery, Reactions of Organic Monolayers on Carbon Surfaces Observed with Unenhanced Raman Spectroscopy, *Journal of the American Chemical Society* 117 (1995) 11254-11259.
- [27] C. Saby, B. Ortiz, G.Y. Champagne, D. Bélanger, Electrochemical Modification of Glassy Carbon Electrode Using Aromatic Diazonium Salts. 1. Blocking Effect of 4-Nitrophenyl and 4-Carboxyphenyl Groups, *Langmuir* 13 (1997) 6805-6813.
- [28] P.R. Marcoux, P. Hapiot, P. Batail, J. Pinson, Electrochemical functionalization of nanotube films: growth of aryl chains on single-walled carbon nanotubes, *New Journal of Chemistry* 28 (2004) 302-307.
- [29] P.A. Brooksby, A.J. Downard, Multilayer Nitroazobenzene Films Covalently Attached to Carbon. An AFM and Electrochemical Study, *The Journal of Physical Chemistry B* 109 (2005) 8791-8798.
- [30] F. Anariba, S.H. DuVall, R.L. McCreery, Mono- and Multilayer Formation by Diazonium Reduction on Carbon Surfaces Monitored with Atomic Force Microscopy "Scratching", *Analytical Chemistry* 75 (2003) 3837-3844.
- [31] J.K. Kariuki, M.T. McDermott, Formation of Multilayers on Glassy Carbon Electrodes via the Reduction of Diazonium Salts, *Langmuir* 17 (2001) 5947-5951.
- [32] J.K. Kariuki, M.T. McDermott, Nucleation and Growth of Functionalized Aryl Films on Graphite Electrodes, *Langmuir* 15 (1999) 6534-6540.
- [33] M. Ceccato, L.T. Nielsen, J. Iruthayaraj, M. Hinge, S.U. Pedersen, K. Daasbjerg, Nitrophenyl Groups in Diazonium-Generated Multilayered Films: Which are Electrochemically Responsive?, *Langmuir* 26 (2010) 10812-10821.

- [34] A. Laforgue, T. Addou, D. Bélanger, Characterization of the Deposition of Organic Molecules at the Surface of Gold by the Electrochemical Reduction of Aryldiazonium Cations, *Langmuir* 21 (2005) 6855-6865.
- [35] M. Ceccato, A. Bousquet, M. Hinge, S.U. Pedersen, K. Daasbjerg, Using a Mediating Effect in the Electroreduction of Aryldiazonium Salts To Prepare Conducting Organic Films of High Thickness, *Chemistry of Materials* 23 (2011) 1551-1557.
- [36] J.L. Bahr, J.P. Yang, D.V. Kosynkin, M.J. Bronikowski, R.E. Smalley, J.M. Tour, Functionalization of carbon nanotubes by electrochemical reduction of aryl diazonium salts: A bucky paper electrode, *Journal of the American Chemical Society* 123 (2001) 6536-6542.
- [37] X. Su, X. Zhan, B.J. Hinds, Pt monolayer deposition onto carbon nanotube mattes with high electrochemical activity, *Journal of Materials Chemistry* 22 (2012) 7979-7984.
- [38] T. Lin, V. Bajpai, T. Ji, L.M. Dai, Chemistry of carbon nanotubes, *Australian Journal of Chemistry* 56 (2003) 635-651.
- [39] B. Pan, B. Xing, Adsorption Mechanisms of Organic Chemicals on Carbon Nanotubes, *Environmental Science & Technology* 42 (2008) 9005-9013.
- [40] Y.-L. Zhao, J.F. Stoddart, Noncovalent Functionalization of Single-Walled Carbon Nanotubes, *Accounts of Chemical Research* 42 (2009) 1161-1171.
- [41] R.J. Chen, Y.G. Zhang, D.W. Wang, H.J. Dai, Noncovalent sidewall functionalization of single-walled carbon nanotubes for protein immobilization, *Journal of the American Chemical Society* 123 (2001) 3838-3839.
- [42] X. Li, Y. Qin, S.T. Picraux, Z.-X. Guo, Noncovalent assembly of carbon nanotube-inorganic hybrids, *Journal of Materials Chemistry* 21 (2011) 7527-7547.
- [43] M.F. Islam, E. Rojas, D.M. Bergey, A.T. Johnson, A.G. Yodh, High Weight Fraction Surfactant Solubilization of Single-Wall Carbon Nanotubes in Water, *Nano Letters* 3 (2003) 269-273.
- [44] L. Vaisman, H.D. Wagner, G. Marom, The role of surfactants in dispersion of carbon nanotubes, *Advances in Colloid and Interface Science* 128-130 (2006) 37-46.
- [45] N. Karousis, N. Tagmatarchis, D. Tasis, Current Progress on the Chemical Modification of Carbon Nanotubes, *Chemical Reviews* 110 (2010) 5366-5397.
- [46] X. Tu, S. Manohar, A. Jagota, M. Zheng, DNA sequence motifs for structure-specific recognition and separation of carbon nanotubes, *Nature* 460 (2009) 250-253.
- [47] A. Bianco, K. Kostarelos, C.D. Partidos, M. Prato, Biomedical applications of functionalised carbon nanotubes, *Chemical Communications* (2005) 571-577.
- [48] K. Welsher, Z. Liu, D. Daranciang, H. Dai, Selective Probing and Imaging of Cells with Single Walled Carbon Nanotubes as Near-Infrared Fluorescent Molecules, *Nano Letters* 8 (2008) 586-590.
- [49] N.W.S. Kam, M. O'Connell, J.A. Wisdom, H. Dai, Carbon nanotubes as multifunctional biological transporters and near-infrared agents for selective cancer cell destruction, *Proceedings of the National Academy of Sciences of the United States of America* 102 (2005) 11600-11605.

- [50] Z. Liu, S. Tabakman, K. Welsher, H. Dai, Carbon nanotubes in biology and medicine: In vitro and in vivo detection, imaging and drug delivery, *Nano Research* 2 (2009) 85-120.
- [51] Z. Liu, K. Chen, C. Davis, S. Sherlock, Q. Cao, X. Chen, H. Dai, Drug Delivery with Carbon Nanotubes for In vivo Cancer Treatment, *Cancer Research* 68 (2008) 6652-6660.
- [52] G.G. Wildgoose, C.E. Banks, R.G. Compton, Metal Nanoparticles and Related Materials Supported on Carbon Nanotubes: Methods and Applications, *Small* 2 (2006) 182-193.
- [53] X. Peng, J. Chen, J.A. Misewich, S.S. Wong, Carbon nanotube-nanocrystal heterostructures, *Chemical Society Reviews* 38 (2009) 1076-1098.
- [54] A. Schaez, M. Zeltner, W.J. Stark, Carbon Modifications and Surfaces for Catalytic Organic Transformations, *ACS Catalysis* 2 (2012) 1267-1284.
- [55] J.M. Planeix, N. Coustel, B. Coq, V. Brotons, P.S. Kumbhar, R. Dutartre, P. Geneste, P. Bernier, P.M. Ajayan, Application of Carbon Nanotubes as Supports in Heterogeneous Catalysis, *Journal of the American Chemical Society* 116 (1994) 7935-7936.
- [56] J.-P. Tessonnier, L. Pesant, G. Ehret, M.J. Ledoux, C. Pham-Huu, Pd nanoparticles introduced inside multi-walled carbon nanotubes for selective hydrogenation of cinnamaldehyde into hydrocinnamaldehyde, *Applied Catalysis A: General* 288 (2005) 203-210.
- [57] X. Pan, Z. Fan, W. Chen, Y. Ding, H. Luo, X. Bao, Enhanced ethanol production inside carbon-nanotube reactors containing catalytic particles, *Nat Mater* 6 (2007) 507-511.
- [58] X. Su, J. Wu, B.J. Hinds, Catalytic activity of ultrathin Pt films on aligned carbon nanotube arrays, *Carbon* 49 (2011) 1145-1150.
- [59] X. Su, X. Zhan, B.J. Hinds, Pt monolayer deposition onto carbon nanotube mattes with high electrochemical activity, *Journal of Materials Chemistry* (2012).
- [60] J.L.T. Jeremy M. Berg, Lubert stryer, *Biochemistry* 5th ed., W. H. Freeman and Company, New York, 2002.
- [61] D.A. Doyle, J.M. Cabral, R.A. Pfuetzner, A. Kuo, J.M. Gulbis, S.L. Cohen, B.T. Chait, R. MacKinnon, The Structure of the Potassium Channel: Molecular Basis of K⁺ Conduction and Selectivity, *Science* 280 (1998) 69-77.
- [62] Y.X. Jiang, A. Lee, J.Y. Chen, V. Ruta, M. Cadene, B.T. Chait, R. MacKinnon, X-ray structure of a voltage-dependent K⁺ channel, *Nature* 423 (2003) 33-41.
- [63] W.W.L. Cheng, J.G. McCoy, A.N. Thompson, C.G. Nichols, C.M. Nimigean, Mechanism for selectivity-inactivation coupling in KcsA potassium channels, *Proceedings of the National Academy of Sciences* 108 (2011) 5272-5277.
- [64] X. Hou, W. Guo, L. Jiang, Biomimetic smart nanopores and nanochannels, *Chemical Society Reviews* 40 (2011) 2385-2401.
- [65] G. Hummer, J.C. Rasaiah, J.P. Noworyta, Water conduction through the hydrophobic channel of a carbon nanotube, *Nature* 414 (2001) 188-190.
- [66] L. Sun, R.M. Crooks, Single Carbon Nanotube Membranes: A Well-Defined Model for Studying Mass Transport through Nanoporous Materials, *Journal of the American Chemical Society* 122 (2000) 12340-12345.

- [67] B.J. Hinds, N. Chopra, T. Rantell, R. Andrews, V. Gavalas, L.G. Bachas, Aligned multiwalled carbon nanotube membranes, *Science* 303 (2004) 62-65.
- [68] N. Chopra, SELECTIVE GROWTH OF CARBON NANOTUBES AND OXIDE NANOWIRES: APPLICATIONS IN SHADOW LITHOGRAPHY AND FABRICATION OF ALIGNED CARBON NANOTUBE MEMBRANES, PhD dissertation (2006).
- [69] M. Majumder, N. Chopra, B.J. Hinds, Effect of Tip Functionalization on Transport through Vertically Oriented Carbon Nanotube Membranes, *Journal of the American Chemical Society* 127 (2005) 9062-9070.
- [70] M. Majumder, N. Chopra, R. Andrews, B.J. Hinds, Nanoscale hydrodynamics: Enhanced flow in carbon nanotubes (vol 438, pg 44, 2005), *Nature* 438 (2005) 930-930.
- [71] J.K. Holt, H.G. Park, Y. Wang, M. Stadermann, A.B. Artyukhin, C.P. Grigoropoulos, A. Noy, O. Bakajin, Fast Mass Transport Through Sub-2-Nanometer Carbon Nanotubes, *Science* 312 (2006) 1034-1037.
- [72] D.S. Sholl, J.K. Johnson, Making High-Flux Membranes with Carbon Nanotubes, *Science* 312 (2006) 1003-1004.
- [73] A.I. López-Lorente, B.M. Simonet, M. Valcárcel, The Potential of Carbon Nanotube Membranes for Analytical Separations, *Analytical Chemistry* 82 (2010) 5399-5407.
- [74] M. Majumder, X. Zhan, R. Andrews, B.J. Hinds, Voltage Gated Carbon Nanotube Membranes, *Langmuir* 23 (2007) 8624-8631.
- [75] M. Majumder, K. Keis, X. Zhan, C. Meadows, J. Cole, B.J. Hinds, Enhanced electrostatic modulation of ionic diffusion through carbon nanotube membranes by diazonium grafting chemistry, *Journal of Membrane Science* 316 (2008) 89-96.
- [76] M. Majumder, B. Corry, Anomalous decline of water transport in covalently modified carbon nanotube membranes, *Chemical Communications* 47 (2011) 7683-7685.
- [77] J. Wu, K.S. Paudel, C. Strasinger, D. Hammell, A.L. Stinchcomb, B.J. Hinds, Programmable transdermal drug delivery of nicotine using carbon nanotube membranes, *Proceedings of the National Academy of Sciences* (2010).
- [78] J. Wu, K. Gerstandt, M. Majumder, X. Zhan, B.J. Hinds, Highly efficient electroosmotic flow through functionalized carbon nanotube membranes, *Nanoscale* 3 (2011) 3321-3328.
- [79] J. Wu, X. Zhan, B.J. Hinds, Ionic rectification by electrostatically actuated tethers on single walled carbon nanotube membranes, *Chemical Communications* 48 (2012) 7979-7981.
- [80] B. Corry, Designing Carbon Nanotube Membranes for Efficient Water Desalination, *The Journal of Physical Chemistry B* 112 (2007) 1427-1434.
- [81] F. Fornasiero, H.G. Park, K.H. Jason, M. Stadermann, C.P. Grigoropoulos, A. Noy, O. Bakajin, Ion Exclusion by sub-2-nm Carbon Nanotube Pores, *Proceedings of the National Academy of Sciences of the United States of America* 105 (2008) 17250-17255.
- [82] G.Q. Lin, Yue-Ming Li, Albert S. C. Chan, Principles and Applications of Asymmetric Synthesis, (2002).

- [83] R. Noyori, *Asymmetric Catalysis: Science and Opportunities* (Nobel Lecture), *Angewandte Chemie International Edition* 41 (2002) 2008-2022.
- [84] A.M. Thayer, Centering on chirality, *Chemical & Engineering News* 85 (2006) 11-19.
- [85] J. Halpern, B.M. Trost, *Asymmetric Catalysis*, *Proceedings of the National Academy of Sciences of the United States of America* 101 (2004) 5347.
- [86] J.M. Hawkins, T.J.N. Watson, *Asymmetric Catalysis in the Pharmaceutical Industry*, *Angewandte Chemie International Edition* 43 (2004) 3224-3228.
- [87] J. Halpern, B.M. Trost, *Asymmetric Catalysis*, *Proc Natl Acad Sci U S A* 101 (2004) 5347.
- [88] R. Noyori, *Asymmetric catalysis: Science and opportunities* (Nobel lecture), *Angewandte Chemie-International Edition* 41 (2002) 2008-2022.
- [89] C. Li, Chiral synthesis on catalysts immobilized in microporous and mesoporous materials, *Catalysis Reviews-Science and Engineering* 46 (2004) 419-492.
- [90] C. Li, H.D. Zhang, D.M. Jiang, Q.H. Yang, Chiral catalysis in nanopores of mesoporous materials, *Chemical Communications* (2007) 547-558.
- [91] M. Heitbaum, F. Glorius, I. Escher, *Asymmetric heterogeneous catalysis*, *Angewandte Chemie-International Edition* 45 (2006) 4732-4762.
- [92] K. Aoki, T. Shimada, T. Hayashi, Immobilization of chiral phosphine ligands on silica gel by means of the allylsilane method and their use for catalytic asymmetric reactions, *Tetrahedron-Asymmetry* 15 (2004) 1771-1777.
- [93] B. Pugin, H. Landert, F. Spindler, H.U. Blaser, More than 100,000 turnovers with immobilized Ir-diphosphine catalysts in an enantioselective imine hydrogenation, *Advanced Synthesis & Catalysis* 344 (2002) 974-979.
- [94] C. Kollner, B. Pugin, A. Togni, Dendrimers containing chiral ferrocenyl diphosphine ligands for asymmetric catalysis, *Journal of the American Chemical Society* 120 (1998) 10274-10275.
- [95] C. Kollner, A. Togni, Synthesis, characterization, and application in asymmetric catalysis of dendrimers containing chiral ferrocenyl diphosphines, *Canadian Journal of Chemistry-Revue Canadienne De Chimie* 79 (2001) 1762-1774.
- [96] H.D. Zhang, S. Xiang, C. Li, Enantioselective epoxidation of unfunctionalised olefins catalyzed by Mn(salen) complexes immobilized in porous materials via phenyl sulfonic group, *Chemical Communications* (2005) 1209-1211.
- [97] H.D. Zhang, Y.M. Zhang, C. Li, Enantioselective epoxidation of unfunctionalized olefins catalyzed by the Mn(salen) catalysts immobilized in the nanopores of mesoporous materials, *Journal of Catalysis* 238 (2006) 369-381.
- [98] H. Zhang, C. Li, Asymmetric epoxidation of 6-cyano-2,2-dimethylchromene on Mn(salen) catalyst immobilized in mesoporous materials, *Tetrahedron* 62 (2006) 6640-6649.
- [99] C.E. Song, 5 Immobilisation of chiral catalysts: easy recycling of catalyst and improvement of catalytic efficiencies, *Annual Reports on the Progress of Chemistry Section C* 101 (2005) 143-173.
- [100] J.M. Fraile, J.I. García, J.A. Mayoral, Noncovalent Immobilization of Enantioselective Catalysts, *Chemical Reviews* 109 (2008) 360-417.

- [101] W.P. Hems, P. McMorn, S. Riddell, S. Watson, F.E. Hancock, G.J. Hutchings, Asymmetric hydrogenation using chiral Rh complexes immobilised with a new ion-exchange strategy, *Organic & Biomolecular Chemistry* 3 (2005) 1547-1550.
- [102] D. Tasis, N. Tagmatarchis, A. Bianco, M. Prato, Chemistry of carbon nanotubes, *Chemical Reviews* 106 (2006) 1105-1136.
- [103] S. Banerjee, T. Hemraj-Benny, S.S. Wong, Covalent surface chemistry of single-walled carbon nanotubes, *Advanced Materials* 17 (2005) 17-29.
- [104] K. Balasubramanian, M. Burghard, Chemically functionalized carbon nanotubes, *Small* 1 (2005) 180-192.
- [105] Y.P. Sun, K.F. Fu, Y. Lin, W.J. Huang, Functionalized carbon nanotubes: Properties and applications, *Accounts of Chemical Research* 35 (2002) 1096-1104.
- [106] D. Tasis, N. Tagmatarchis, V. Georgakilas, M. Prato, Soluble carbon nanotubes, *Chemistry-a European Journal* 9 (2003) 4001-4008.
- [107] S. Banerjee, S.S. Wong, Structural characterization, optical properties, and improved solubility of carbon nanotubes functionalized with Wilkinson's catalyst, *J Am Chem Soc* 124 (2002) 8940-8948.
- [108] S. Banerjee, S.S. Wong, Functionalization of carbon nanotubes with a metal-containing molecular complex, *Nano Letters* 2 (2002) 49-53.
- [109] C. Baleizao, B. Gigante, H. Garcia, A. Corma, Vanadyl salen complexes covalently anchored to single-wall carbon nanotubes as heterogeneous catalysts for the cyanosilylation of aldehydes, *Journal of Catalysis* 221 (2004) 77-84.
- [110] J. Wu, X. Zhan, B.J. Hinds, Ionic rectification by electrostatically actuated tethers on single walled carbon nanotube membranes, *Chemical Communications* (2012).
- [111] J. Goldsmith, B.J. Hinds, Simulation of Steady-State Methanol Flux through a Model Carbon Nanotube Catalyst Support, *The Journal of Physical Chemistry C* 115 (2011) 19158-19164.
- [112] M. Majumder, X. Zhan, R. Andrews, B.J. Hinds, Voltage gated carbon nanotube membranes, *Langmuir* 23 (2007) 8624-8631.
- [113] M. Majumder, N. Chopra, B.J. Hinds, Mass Transport through Carbon Nanotube Membranes in Three Different Regimes: Ionic Diffusion and Gas and Liquid Flow, *ACS Nano* 5 (2011) 3867-3877.
- [114] C. Combellas, F. Kanoufi, J. Pinson, F.I. Podvorica, Sterically Hindered Diazonium Salts for the Grafting of a Monolayer on Metals, *Journal of the American Chemical Society* 130 (2008) 8576-8577.
- [115] C. Combellas, D.E. Jiang, F. Kanoufi, J. Pinson, F.I. Podvorica, Steric Effects in the Reaction of Aryl Radicals on Surfaces, *Langmuir* 25 (2009) 286-293.
- [116] Y.R. Leroux, H. Fei, J.-M. Noël, C.m. Roux, P. Hapiot, Efficient Covalent Modification of a Carbon Surface: Use of a Silyl Protecting Group To Form an Active Monolayer, *Journal of the American Chemical Society* 132 (2010) 14039-14041.
- [117] T. Smith, The hydrophilic nature of a clean gold surface, *Journal of Colloid and Interface Science* 75 (1980) 51-55.
- [118] R. Andrews, D. Jacques, A.M. Rao, F. Derbyshire, D. Qian, X. Fan, E.C. Dickey, J. Chen, Continuous production of aligned carbon nanotubes: a step closer to commercial realization, *Chemical Physics Letters* 303 (1999) 467-474.

- [119] S. Sano, K. Kato, Y. Ikada, Introduction of functional groups onto the surface of polyethylene for protein immobilization, *Biomaterials* 14 (1993) 817-822.
- [120] A. Wetzel, V. Ehrhardt, M.R. Heinrich, Synthesis of Amino- and Hydroxybiphenyls by Radical Chain Reaction of Arenediazonium Salts, *Angewandte Chemie International Edition* 47 (2008) 9130-9133.
- [121] J.C. Love, L.A. Estroff, J.K. Kriebel, R.G. Nuzzo, G.M. Whitesides, Self-Assembled Monolayers of Thiolates on Metals as a Form of Nanotechnology, *Chemical Reviews* 105 (2005) 1103-1170.
- [122] H. Kang, N.-S. Lee, E. Ito, M. Hara, J. Noh, Formation and Superlattice of Long-Range-Ordered Self-Assembled Monolayers of Pentafluorobenzenethiols on Au(111), *Langmuir* 26 (2010) 2983-2985.
- [123] M. Endo, H. Muramatsu, T. Hayashi, Y.A. Kim, M. Terrones, M.S. Dresselhaus, Nanotechnology: 'Buckypaper' from coaxial nanotubes, *Nature* 433 (2005) 476-476.
- [124] W. Kangbing, J. Xiaobo, F. Junjie, H. Shengshui, The fabrication of a carbon nanotube film on a glassy carbon electrode and its application to determining thyroxine, *Nanotechnology* 15 (2004) 287.
- [125] J.B. Raoof, R. Ojani, M. Baghayeri, M. Amiri-Aref, Application of a glassy carbon electrode modified with functionalized multi-walled carbon nanotubes as a sensor device for simultaneous determination of acetaminophen and tyramine, *Analytical Methods* 4 (2012) 1579-1587.
- [126] M. Raicopol, L. Necula, M. Ionita, L. Pilan, Electrochemical reduction of aryl diazonium salts: a versatile way for carbon nanotubes functionalisation, *Surface and Interface Analysis* (2012) n/a-n/a.
- [127] Y. Jiang, A. Lee, J. Chen, V. Ruta, M. Cadene, B.T. Chait, R. MacKinnon, X-ray structure of a voltage-dependent K⁺ channel, *Nature* 423 (2003) 33-41.
- [128] M.Ø. Jensen, D.W. Borhani, K. Lindorff-Larsen, P. Maragakis, V. Jogini, M.P. Eastwood, R.O. Dror, D.E. Shaw, Principles of conduction and hydrophobic gating in K⁺ channels, *Proceedings of the National Academy of Sciences* 107 (2010) 5833-5838.
- [129] Z.S. Siwy, S. Howorka, Engineered voltage-responsive nanopores, *Chemical Society Reviews* 39 (2010) 1115-1132.
- [130] Z. Siwy, E. Heins, C.C. Harrell, P. Kohli, C.R. Martin, Conical-Nanotube Ion-Current Rectifiers: The Role of Surface Charge, *Journal of the American Chemical Society* 126 (2004) 10850-10851.
- [131] I. Vlassiuk, Z.S. Siwy, Nanofluidic Diode, *Nano Letters* 7 (2007) 552-556.
- [132] N.R. Scruggs, J.W.F. Robertson, J.J. Kasianowicz, K.B. Migler, Rectification of the Ionic Current through Carbon Nanotubes by Electrostatic Assembly of Polyelectrolytes, *Nano Letters* 9 (2009) 3853-3859.
- [133] R. Yan, W. Liang, R. Fan, P. Yang, Nanofluidic Diodes Based on Nanotube Heterojunctions, *Nano Letters* 9 (2009) 3820-3825.
- [134] P. Nednoor, V.G. Gavalas, N. Chopra, B.J. Hinds, L.G. Bachas, Carbon nanotube based biomimetic membranes: Mimicking protein channels regulated by phosphorylation, *Journal of Materials Chemistry* 17 (2007) 1755-1757.
- [135] J.L. Bahr, J.M. Tour, Covalent chemistry of single-wall carbon nanotubes, *Journal of Materials Chemistry* 12 (2002) 1952-1958.

- [136] R.L. McCreery, *Advanced Carbon Electrode Materials for Molecular Electrochemistry*, *Chemical Reviews* 108 (2008) 2646-2687.
- [137] B. Barbier, J. Pinson, G. Desarmot, M. Sanchez, *Electrochemical Bonding of Amines to Carbon Fiber Surfaces Toward Improved Carbon-Epoxy Composites*, *Journal of the Electrochemical Society* 137 (1990) 1757-1764.
- [138] R.S. Deinhammer, M. Ho, J.W. Anderegg, M.D. Porter, *Electrochemical oxidation of amine-containing compounds: a route to the surface modification of glassy carbon electrodes*, *Langmuir* 10 (1994) 1306-1313.
- [139] G. Herlem, C. Goux, B. Fahys, F. Dominati, A.M. Gonçalves, C. Mathieu, E. Sutter, A. Trokourey, J.F. Penneau, *Surface modification of platinum and gold electrodes by anodic oxidation of pure ethylenediamine*, *Journal of Electroanalytical Chemistry* 435 (1997) 259-265.
- [140] G. Herlem, K. Reybier, A. Trokourey, B. Fahys, *Electrochemical Oxidation of Ethylenediamine: New Way to Make Polyethyleneimine-Like Coatings on Metallic or Semiconducting Materials*, *Journal of The Electrochemical Society* 147 (2000) 597-601.
- [141] J. Liu, L. Cheng, B. Liu, S. Dong, *Covalent Modification of a Glassy Carbon Surface by 4-Aminobenzoic Acid and Its Application in Fabrication of a Polyoxometalates-Consisting Monolayer and Multilayer Films*, *Langmuir* 16 (2000) 7471-7476.
- [142] M. Herlem, B. Fahys, G. Herlem, B. Lakard, K. Reybier, A. Trokourey, T. Diaco, S. Zairi, N. Jaffrezic-Renault, *Surface modification of p-Si by a polyethylenimine coating: influence of the surface pre-treatment. Application to a potentiometric transducer as pH sensor*, *Electrochimica Acta* 47 (2002) 2597-2602.
- [143] A.C. Cruickshank, E.S.Q. Tan, P.A. Brooksby, A.J. Downard, *Are redox probes a useful indicator of film stability? An electrochemical, AFM and XPS study of electrografted amine films on carbon*, *Electrochemistry Communications* 9 (2007) 1456-1462.
- [144] M.A. Ghanem, J.-M. Chretien, A. Pinczewska, J.D. Kilburn, P.N. Bartlett, *Covalent modification of glassy carbon surface with organic redox probes through diamine linkers using electrochemical and solid-phase synthesis methodologies*, *Journal of Materials Chemistry* 18 (2008) 4917-4927.
- [145] M.M. Chehimi, G.r. Hallais, T. Matrab, J. Pinson, F.I. Podvorica, *Electro- and Photografting of Carbon or Metal Surfaces by Alkyl Groups*, *The Journal of Physical Chemistry C* 112 (2008) 18559-18565.
- [146] O. Buriez, E. Labbé, P. Pigeon, G. Jaouen, C. Amatore, *Electrochemical attachment of a conjugated amino-ferrocifen complex onto carbon and metal surfaces*, *Journal of Electroanalytical Chemistry* 619-620 (2008) 169-175.
- [147] T.H. Kim, H.S. Choi, B.R. Go, J. Kim, *Modification of a glassy carbon surface with amine-terminated dendrimers and its application to electrocatalytic hydrazine oxidation*, *Electrochemistry Communications* 12 (2010) 788-791.
- [148] M. Sandroni, G. Volpi, J. Fiedler, R. Buscaino, G. Viscardi, L. Milone, R. Gobetto, C. Nervi, *Iridium and ruthenium complexes covalently bonded to carbon surfaces by means of electrochemical oxidation of aromatic amines*, *Catalysis Today* 158 (2010) 22-28.

- [149] A. Aramata, S. Takahashi, G. Yin, Y. Gao, Y. Inose, H. Mihara, A. Tadjeddine, W.Q. Zheng, O. Pluchery, A. Bittner, A. Yamagishi, Ligand grafting method for immobilization of metal complexes on a carbon electrode, *Thin Solid Films* 424 (2003) 239-246.
- [150] G. Gao, D. Guo, C. Wang, H. Li, Electrocrystallized Ag nanoparticle on functional multi-walled carbon nanotube surfaces for hydrazine oxidation, *Electrochemistry Communications* 9 (2007) 1582-1586.
- [151] L. Yang, J. Chen, X. Wei, B. Liu, Y. Kuang, Ethylene diamine-grafted carbon nanotubes: A promising catalyst support for methanol electro-oxidation, *Electrochimica Acta* 53 (2007) 777-784.
- [152] C. Yin, L. Ying, P.-C. Zhang, R.-X. Zhuo, E.-T. Kang, K.W. Leong, H.-Q. Mao, High density of immobilized galactose ligand enhances hepatocyte attachment and function, *Journal of Biomedical Materials Research Part A* 67A (2003) 1093-1104.
- [153] A. Adenier, M.M. Chehimi, I. Gallardo, J. Pinson, N. Vilà, Electrochemical Oxidation of Aliphatic Amines and Their Attachment to Carbon and Metal Surfaces, *Langmuir* 20 (2004) 8243-8253.
- [154] X. Li, Y. Wan, C. Sun, Covalent modification of a glassy carbon surface by electrochemical oxidation of *r*-aminobenzene sulfonic acid in aqueous solution, *Journal of Electroanalytical Chemistry* 569 (2004) 79-87.
- [155] I. Gallardo, J. Pinson, N. Vilà, Spontaneous Attachment of Amines to Carbon and Metallic Surfaces, *The Journal of Physical Chemistry B* 110 (2006) 19521-19529.
- [156] M. Tanaka, T. Sawaguchi, Y. Sato, K. Yoshioka, O. Niwa, Surface Modification of GC and HOPG with Diazonium, Amine, Azide, and Olefin Derivatives, *Langmuir* 27 (2010) 170-178.
- [157] G. Liu, J. Liu, T. Böcking, P.K. Eggers, J.J. Gooding, The modification of glassy carbon and gold electrodes with aryl diazonium salt: The impact of the electrode materials on the rate of heterogeneous electron transfer, *Chemical Physics* 319 (2005) 136-146.
- [158] W.S. Knowles, R. Noyori, Pioneering Perspectives on Asymmetric Hydrogenation †, *Accounts of Chemical Research* 40 (2007) 1238-1239.
- [159] H.-U. Blaser, B. Pugin, F. Spindler, M. Thommen, From a Chiral Switch to a Ligand Portfolio for Asymmetric Catalysis, *Accounts of Chemical Research* 40 (2007) 1240-1250.
- [160] W. Zhang, Y. Chi, X. Zhang, Developing Chiral Ligands for Asymmetric Hydrogenation, *Accounts of Chemical Research* 40 (2007) 1278-1290.
- [161] H.U. Blaser, W. Brieden, B. Pugin, F. Spindler, M. Studer, A. Togni, Solvias Josiphos ligands: from discovery to technical applications, *Topics in Catalysis* 19 (2002) 3-16.
- [162] P. Barbaro, C. Bianchini, G. Giambastiani, S.L. Parisel, Progress in stereoselective catalysis by metal complexes with chiral ferrocenyl phosphines, *Coordination Chemistry Reviews* 248 (2004) 2131-2150.
- [163] T.J. Colacot, A concise update on the applications of chiral ferrocenyl phosphines in homogeneous catalysis leading to organic synthesis, *Chemical Reviews* 103 (2003) 3101-3118.

- [164] T. Hayashi, T. Mise, M. Fukushima, M. Kagotani, N. Nagashima, Y. Hamada, A. Matsumoto, S. Kawakami, M. Konishi, K. Yamamoto, M. Kumada, Asymmetric-Synthesis Catalyzed by Chiral Ferrocenylphosphine-Transition Metal-Complexes .1. Preparation of Chiral Ferrocenylphosphines, *Bulletin of the Chemical Society of Japan* 53 (1980) 1138-1151.
- [165] A. Togni, C. Breutel, A. Schnyder, F. Spindler, H. Landert, A. Tijani, A Novel Easily Accessible Chiral Ferrocenyldiphosphine for Highly Enantioselective Hydrogenation, Allylic Alkylation, and Hydroboration Reactions, *Journal of the American Chemical Society* 116 (1994) 4062-4066.
- [166] R. Gómez Arrayás, J. Adrio, J.C. Carretero, Recent Applications of Chiral Ferrocene Ligands in Asymmetric Catalysis, *Angewandte Chemie International Edition* 45 (2006) 7674-7715.
- [167] C. Bianchini, P. Barbaro, Recent aspects of asymmetric catalysis by immobilized chiral metal catalysts, *Topics in Catalysis* 19 (2002) 17-32.
- [168] P. McMorn, G.J. Hutchings, Heterogeneous enantioselective catalysts: strategies for the immobilisation of homogeneous catalysts, *Chemical Society Reviews* 33 (2004) 108-122.
- [169] B. Pugin, H.-U. Blaser, Immobilized Complexes for Enantioselective Catalysis: When Will They Be Used in Industry?, *Topics in Catalysis* 53 (2010) 953-962.
- [170] J.M. Thomas, R. Raja, Exploiting Nanospace for Asymmetric Catalysis: Confinement of Immobilized, Single-Site Chiral Catalysts Enhances Enantioselectivity, *Accounts of Chemical Research* 41 (2008) 708-720.
- [171] J.M. Fraile, J.I. García, C.I. Herrerías, J.A. Mayoral, E. Pires, Enantioselective catalysis with chiral complexes immobilized on nanostructured supports, *Chemical Society Reviews* 38 (2009) 695-706.
- [172] L. Xing, J.-H. Xie, Y.-S. Chen, L.-X. Wang, Q.-L. Zhou, Simply Modified Chiral Diphosphine: Catalyst Recycling via Non-covalent Absorption on Carbon Nanotubes, *Advanced Synthesis & Catalysis* 350 (2008) 1013-1016.
- [173] K. Tappe, P. Knochel, New efficient synthesis of Taniaphos ligands: application in ruthenium- and rhodium-catalyzed enantioselective hydrogenations, *Tetrahedron: Asymmetry* 15 (2004) 91-102.
- [174] B.P.a.H. Landert, *Solvias*, 1998.
- [175] D. Marquarding, H. Klusacek, G. Gokel, P. Hoffmann, I. Ugi, Stereoselective syntheses. VI. Correlation of central and planar chirality in ferrocene derivatives, *Journal of the American Chemical Society* 92 (1970) 5389-5393.
- [176] W.-S. Lam, S.H.L. Kok, T.T.L. Au-Yeung, J. Wu, H.-Y. Cheung, F.-L. Lam, C.-H. Yeung, A.S.C. Chan, An Efficient Approach to Chiral Ferrocene-Based Secondary Alcohols via Asymmetric Hydrogenation of Ferrocenyl Ketones, *Advanced Synthesis & Catalysis* 348 (2006) 370-374.
- [177] B. Pugin, H.-U. Blaser, Immobilized Complexes for Enantioselective Catalysis: the Industrial Perspective Heterogenized Homogeneous Catalysts for Fine Chemicals Production, in: P. Barbaro, F. Liguori (Eds.), Springer Netherlands, 2010, pp. 231-245.
- [178] L. Zhang, S. Luo, J.-P. Cheng, Non-covalent immobilization of asymmetric organocatalysts, *Catalysis Science & Technology* 1 (2011) 507-516.

- [179] R. Augustine, S. Tanielyan, S. Anderson, H. Yang, A new technique for anchoring homogeneous catalysts, *Chemical Communications* (1999) 1257-1258.
- [180] R.L. Augustine, S.K. Tanielyan, N. Mahata, Y. Gao, A. Zsigmond, H. Yang, Anchored homogeneous catalysts: the role of the heteropoly acid anchoring agent, *Applied Catalysis A: General* 256 (2003) 69-76.
- [181] R.L. Augustine, P. Goel, N. Mahata, C. Reyes, S.K. Tanielyan, Anchored homogeneous catalysts: high turnover number applications, *Journal of Molecular Catalysis A: Chemical* 216 (2004) 189-197.
- [182] B. Fei, H.F. Lu, Z.G. Hu, J.H. Xin, Solubilization, purification and functionalization of carbon nanotubes using polyoxometalate, *Nanotechnology* 17 (2006) 1589-1593.
- [183] B. Fei, H. Lu, W. Chen, J.H. Xin, Ionic peapods from carbon nanotubes and phosphotungstic acid, *Carbon* 44 (2006) 2261-2264.
- [184] V. Georgakilas, M. Otyepka, A.B. Bourlinos, V. Chandra, N. Kim, K.C. Kemp, P. Hobza, R. Zboril, K.S. Kim, Functionalization of Graphene: Covalent and Non-Covalent Approaches, Derivatives and Applications, *Chemical Reviews* 112 (2012) 6156-6214.

VITA

XIN ZHAN

Born in Chongqing, PR China

EDUATION

Aug. 2004 - Dec. 2012: Ph.D. candidate in Chemistry Department, Univerisity of Kentucky, Lexington, USA

Aug. 2002 - July. 2004: M.S.in Chemistry at Texas A&M University-Commerce, Commerce, USA

Sept. 1998 - Jul. 2001: M.S. in Physical Chemistry, Chongqing University, Chongqing, P.R. China

Sept. 1993 - Jul. 1997: B.S. in Analytical Chemistry, Yuzhou University, Chongqing, PR China

RESEARCH EXPERIENCES

Sept. 2005 - Dec. 2012: Graduate student in Dr. Bruce J. Hinds lab in Chemistry Department, University of Kentucky.

Aug. 2002 - Jul. 2004: Graduate research, Texas A&M University-Commerce.

Sept. 1998 - Jul. 2001: Graduate research, Chongqing University.

AWARDS

2012 Travel Award, University of Kentucky, Lexington, Kentucky

2002 Welch Scholarship, Texas A&M University-Commerce, Commerce, Texas

PUBLICATIONS

1. **Xin Zhan**, Ji Wu, Bruce. J. Hinds, 'Near monolayer functionality produced by electrochemical diazonium grafting on carbon nanotubes', *Applied Surface Science*, **2013** (submitted).
2. **Xin Zhan**, Ji Wu and Bruce J Hinds, 'Single-step electrochemical functionalization of double walled carbon nanotube membranes', *Nanoscale Research Letters*, **2013** (submitted).
3. **Xin Zhan**, Bruce J Hinds, 'Covalent and non-covalent immobilization of chiral ligand on carbon nanotubes for asymmetric hydrogenation', **2013**(In preparation).

4. Ji Wu, **Xin Zhan**, Bruce J. Hinds, 'Ionic rectification using voltage-gated single walled carbon nanotubes membranes', *Chemical Communications*, **2012**, **48**, 7979-7981.
5. Xin Su, **Xin Zhan**, Bruce J. Hinds, 'Pt monolayer deposition onto carbon nanotube mattes with high electrochemical activity', *Journal of Materials Chemistry*, **2012**, **22**, 7979-7984.
6. Xin Su, QingLiu Wu, **Xin Zhan**, Ji Wu and John Zhanhu Guo, 'Advanced titania nanostructures and composites for lithium ion battery', *Journal of Materials Science*, **47**, **6**, 2519-2534.
7. Xin Su, **Xin Zhan**, Fang Tang, Jingyuan Yao, Ji Wu, 'Magnetic nanoparticles in brain disease diagnosis and targeting drug delivery', *Current Nanoscience*, **2011**, **7**, 37
8. Ji Wu, Karen Gerstandt, Mainak Majumder, **Xin Zhan** and Bruce J. Hinds, 'Highly efficient electroosmotic flow through functionalized carbon nanotube membranes', *Nanoscale*, **2011**, **3**, 3321-3328.
9. Chunxia Zhao, Lance M. Hellman, **Xin Zhan**, Willis S. Bowman, Sidney W. Whiteheart, and Michael G. Fried, 'Hexahistidine-tag-specific optical probes for analyses of proteins and their interactions', *Analytical Biochemistry*, **2010**, **399**, 237-245.
10. Mainak Majumder, Karin Keis, **Xin Zhan**, Corey Meadows, Jeggan Cole, Bruce J. Hinds, 'Enhanced electrostatic modulation of ionic diffusion through carbon nanotube membranes by diazonium grafting chemistry', *Journal of Membrane Science*, **2008**, **316**, 89-96.
11. Mainak Majumder, **Xin Zhan**, Rodney Andrews, and Bruce J. Hinds, 'Voltage gated carbon nanotube membranes', *Langmuir*, **2007**, **23**, 8624-8631.
12. Changguo Chen, **Xin Zhan**, 'The application of statistics methods in X-ray diffraction phase analysis', *Computers and Applied Chemistry*, **2003**, **20**.
13. Changguo Chen, **Xin Zhan**, 'The phase analysis of airborne particle in Chongqing city areas', *Environmental Chemistry*, **2002**, **21**.
14. Changguo Chen, **Xin Zhan**, 'Study on the element, ion and phase composition of airborne dust in Chongqing city, Chongqing', *Environmental Science*, **2002**, **24**.

ABSTRACTS AND PRESENTATIONS

1. Oral presentation, 243rd ACS national meeting, 'Quantification of near monolayer functionality by electrochemical diazonium grafting for carbon nanotube membranes', San Diego, CA, **2012**
2. Naff symposium, 'Diazonium grafting and quantification of functional density for monolayer modification', Lexington, KY, **2011**

3. KY Nanoscience, 'Chiral catalysis on carbon nanotubes for membrane reactors', Louisville, KY **2008**
4. **Jason Zhan**, Monyka Macias, Dustin Knight and Ben W.-L. Jang, 'Study of RF plasma effect on metal dispersion and sintering resistance of alumina supported metal catalysts', *Am. Chem. Soc. Div. of Petrol. Chem.*, **2004**, 49, 32
5. **Jason Zhan**, Praveen Boopalachandran, Ben W.-L. Jang, Jai Cho and Richard B. Timmons, 'RF plasma modification of supported Pt catalysts for CO₂-CH₄ reforming', *Am. Chem. Soc. Div. of Fuel Chem*, **2004**, 49
6. Oral presentation, 37th annual ACS Dallas-Fort Worth section meeting-in-miniature, Dallas, TX, **2004**
7. 59th ACS southwest regional meeting of Oklahoma City, Oklahoma City, OK, **2003**
8. Texas A&M system 1ST annual pathway research symposium, Galveston, TX, **2003**
9. Hongmin Zhang, **Xin Zhan**, 'The edge of carbon cathode embed with Li of Li Ion cell', The tenth national electrochemistry society meeting, Hangzhou, China, **1999**